STUDIES ON PHYSICAL, CHEMICAL AND MECHANICAL PROPERTIES OF LIME ACTIVATED SLAG CEMENT

A THESIS SUBMITTED IN FULFILLMENT OF
THE REQUIREMENT FOR THE AWARD OF THE DEGREE
OF

DOCTOR OF PHILOSOPHY

IN

CIVIL ENGINEERING

BY

MEENA MURMU

(ROLL NO.- 509CE103)

NATIONAL INSTITUTE OF TECHNOLOGY
ROURKELA - 769008, INDIA
JULY – 2014

NATIONAL INSTITUTE OF TECHNOLOGY
ROURKELA - 769008, INDIA

CERTIFICATE

This to certify that the thesis entitled **"Studies on Physical, Chemical and Mechanical Properties of Lime Activated Slag Cement"** being submitted by **Meena Murmu** for the award of the degree of **Doctor of Philosophy** (Civil Engineering) of NIT, Rourkela is a record of bonafide research work carried out by her under my supervision and guidance. She has worked for more than four years on the above problem at the Department of Civil Engineering, National Institute of Technology, Rourkela and this has reached the standard fulfilling the requirements and the regulation relating to the degree. The contents of this thesis, in full or part, have not been submitted to any other university or institution for the award of any degree or diploma.

Place: Rourkela
Date:

Dr. Suresh Prasad Singh
Professor
Department of Civil Engineering
NIT, Rourkela

Dedicated To

My Parents

ACKNOWLEDGEMENT

This thesis is a result of research that has been carried out at National Institute of Technology, Rourkela. During this period, I came across with a great number of people whose contributions in various ways helped my field of research and they deserve special thanks. It is a pleasure to convey my gratitude to all of them.

First and foremost, I would like to express my deep sense of gratitude and indebtedness to my supervisor Prof. S.P. Singh for his advice and guidance from the early stage of this research and providing me extraordinary experiences throughout the work. Above all, he provided me unflinching encouragement and support in various ways which exceptionally inspire and enrich my growth as a student, a researcher, and a scientist.

I am grateful to Prof. S.K. Sarangi, Director, Prof. S.K. Sahu, Head of Civil Engineering Department, Prof. N. Roy and Prof. M. Panda, former Head of Civil Engineering Department, NIT, Rourkela, for their kind support and concern regarding my academic requirements.

I express my sincere gratitude to Prof. J. Bera, Ceramic Engineering Department, Prof. D. Bag, School of Management, NIT Rourkela for their guidance, valuable advice and inspiration during the Ph.D programme.

I would also like to thank faculty of Civil Engineering Department Prof. M.R. Barik, Prof. K.C. Biswal, Prof. K. K. Paul, Prof. C.R. Patra, Prof. K.C. Patra, Prof. S. K. Das, Prof. A.V. Asha and Prof. K.K. Khatua for their wholehearted suggestions at various stages of the work.

I express my thankfulness to the staff members of the civil Engineering Department for their continuous encouragement and suggestions. Among them, Mr S.C. Xess, Mr. A.K. Nanda, Mr. S. Sethi, Mr. H.M. Garnaik, Mr. C. Suniani and Mr. R. Lugun deserves special thanks for his kind cooperation in non-academic matters during the research work.

I acknowledge with thanks the help rendered to me by the staff members of the Ceramic Engineering, Mining engineering, Metallurgy & Material Engineering

department Laboratory and other staffs of Civil Engineering department for their continuous encouragement during the progress of my work.

Thanks are also due to my co-scholars at N I T, Rourkela, for their whole hearted support and cooperation during the duration of this work.

My parents deserve special mention for their inseparable support and prayers. They are the persons who show me the joy of intellectual pursuit ever since I was a child. I thank them for sincerely bringing up me with care and love.

The completion of this work came at the expense of my long hours of absence from home. Words fail me to express my appreciation to my brother Ram Chandra Murmu and my sister in law for their understanding, patience, and active cooperation throughout the course of my doctoral dissertation. I thank them for being supportive and caring.

Last, but not the least, I thank the one above all of us, the omnipresent God, for giving me the strength during the course of this research work.

Meena Murmu

Declaration

I declare that this thesis is my own work and has not been submitted in any form for another degree or diploma at any university or other institution of tertiary education. Information derived from the published or unpublished work of others has been acknowledged in the text and a list of references given.

Date: **Meena Murmu**

ABSTRACT

Concrete is the most versatile, indispensable and widely used building material, of which cement is an integral constituent. From the time immemorial Portland cement has been used as binder in concrete construction. However, the production of the cement is not eco-friendly and consumes enormous amount of energy which ultimately leads to the depletion of the fossil fuel reserve. In addition to this, it emits noxious greenhouse gases which are harmful for the biosphere. An attractive alternative to Portland cement is the binder obtained by alkaline activation of materials; rich in reactive amorphous silica and alumina. In order to enhance its physical and mechanical properties, slag is activated by different activators along with admixtures. Activated slag cement is a sustainable building material, and this cement product is carbon neutral. The use of slag as a cementious material results in a reduction of greenhouse gases. It also helps in preserving the natural raw materials, which would otherwise have been used in making ordinary Portland cement (OPC).

Cementing materials are produced from ground granulated blast furnace slag by activating it with alkali activators like NaOH, $Na_2SiO_35H_2O$ or by activating it using compounds of alkaline earth metals such as lime. A good number of literatures are available on slag activated by alkali activators but a few researches have been done on activation of slag by activators involving compounds of alkaline earth metals. The physical properties like setting characteristics of alkali activated slag were investigated by many researchers, Wang *et al.* (1995), Collins *et al.* (2000) and Puertas*et al.* (2004) and it was found that alkali activated slag cement (AASC) posed rapid setting and high drying shrinkage. Further, the setting characteristics of slag-lime mixes were determined

by using granulated slag and high calcium lime by Feret (1939) as well as Jolibois and Nicol (1952). Brough *et al.* (2000) used phosphate and malic acid as retarders in slag and sodium silicate base mixes in order to increase the setting time of the alkali activated slag cement. The mechanical property of slag activated by hard-burnt gypsum (anhydrite), plaster of Paris, and little amount of lime or OPC was investigated by Bijen and Niel (1981), Mehrotra *et al.* (1982) and Dutta and Borthakur (1990). Douglas and Brandstetr (1990) studied the influence of mineral admixture on mechanical strength of alkali activated slag cement taking different proportions of sodium silicate solution, lime, OPC, silica fume and fly ash. Yazic s*et al.* (2008) studied the effect of mineral admixtures on compressive strength of ternary blended cement. Bellman and Strak (2009) studied the effect of different accelerators such as calcium formate, calcium acetate, calcium chloride, sodium chloride, calcium nitrate, calcium bromide on strength. Aitcin(1958),Aldea*et al*. (2000), Kim *et al.* (2002), Ezzian*et al.* (2007), and Tanyildizi (2009) reported that a higher curing temperature improves the strength at early ages. The effect of type and amount of activators used, structure and composition of the slag and curing conditions on the formation of hydration products was investigated by Glukhovsky *et al.* (1983), Talling *et al.* (1981), Puertas (2000), and Shi and Li (1989).Scanning through the above literatures, it is perceived that researches based on alkali or alkaline activation of slag cement is not so profound and incoherent. The optimization of raw material proportions has been done randomly on the basis of limited experimental data. Keeping in view of all these aspects, an extensive laboratory testing program has been undertaken to investigate the physical, mechanical and chemical properties of slag activated with lime and plaster of Paris. Especially, optimization of raw

material based on compressive strength was made by using generalized reduced gradient method. The influence of mineral admixture, chemical admixture, and curing conditions on formation of hydration products, morphology, microstructure, and drying shrinkage was investigated from the optimized mix-proportion of raw materials, which was determined by using response surface plot.

The granulated blast furnace slag used in this work was collected from Rourkela Steel Plant (RSP). It was sun dried and mixed thoroughly to bring homogeneity in the sample. The same was ground in a ball mill to a Blaineôs fineness of 410m^2kg^{-1}. The plaster of Paris (POP) and hydrated lime used were procured from the local market. The mineral admixtures such as silica fume, fly ash, glass powder, and OPC as well as the chemical admixtures like calcium formate, calcium acetate, calcium nitrate, sodium carbonate, and sodium meta-silicate were used in this study.

The experiments were performed in two phases. In first phase, the physical properties of different mixes of slag-lime-plaster of Paris were evaluated. In addition to this, the optimization of raw material proportions was done on the basis of mechanical strength of different mixes of slag-lime-plaster of Paris adopting the generalized reduced gradient (GRG) technique and response surface plot. In second phase, the influence of mineral admixtures, chemical admixtures and curing conditions on mechanical strength, hydration product, microstructure, morphology, porosity, and drying shrinkage behavior were studied. A correlation has been established between the developed mechanical strength and hydration products, microstructure as well as the morphology of cured specimens.

The physical properties such as consistency, initial setting time (IS), final setting time (FS) and soundness of 42 different mixes of slag-lime-plaster of Paris were determined. The proportions of blast furnace slag in the slag-lime mixes were varied from 95 to 60% while the lime content from 5 to 40%. The amount of plaster of Paris in the slag-lime-plaster of Paris mixes was varied from 0 to 10%, which is taken on the combined mass of slag plus lime. The hydration products and formation of bonds in the paste were studied by using several techniques like X-ray diffraction (XRD), scanning electron microscope (SEM), thermo gravimetric analysis (TGA), differential scanning calorimeter (DSC), Fourier transform infrared (FTIR) and mercury intrusion porosimetry tests. The compressive strength of mortar specimens was determined for the above mix proportions after different curing periods. The optimization of mix-proportion based on compressive strength was done by adopting generalized reduced gradient technique and response surface plot. The effects of curing conditions on strength of slag activated with lime and plaster of Paris were investigated. This includes curing of specimens in water at different temperatures and periods. Accelerated curing of mortar specimens was also done at high pressure and temperature in an autoclave. Further, the effects of mineral admixtures such as silica fume, fly ash, glass powder, OPC as well as chemical admixtures like calcium acetate, calcium formate, calcium nitrate, sodium meta-silicate, and sodium hydroxide on mechanical strength, hydration products, morphology, and microstructure were determined. Finally, the compressive strength of specimens was correlated with hydration products, microstructure, morphology, and pore structure; obtained from several analyses like XRD, SEM, TGA, DSC and FTIR tests.

The test results indicate that the normal consistency values of slag-lime-plaster of Paris mixes increase with increase in the content of either lime or plaster of Paris. The initial and final setting times of the mixes decrease with either increase in lime or plaster of Paris content or both. Setting times of the mixes are lesser than that of the value prescribed for ordinary Portland cement. Further, addition of borax retards the setting time and a borax content of 0.4% by mass gives the setting time that is normally prescribed for OPC

The compressive strength results of mortar specimens containing slag-lime-POP in different proportions show that no appreciable increase in strength is incurred beyond 5% POP content. Depending on the slag and POP content, an optimum dose of lime exists and no further significant increase in strength is achieved beyond this dose. A higher dosage of lime reduces the strength. The strength of slag cement increases up to 90 days of curing and even beyond that. Microstructure and hydration product studies show the presence of compounds of ettringite and C-S-H gel, which mainly enhances the strength. An addition of lime beyond an optimum value results in the formation of hillebrandite and reduction in compressive strength. The optimum value of the response function that is the compressive strength is obtained using fitted response surface models by GRG method. The optimum lime and POP content for 90 days cured mortar specimen is found to be 19.12% and 4.26% respectively. However, for other curing periods the optimum values of lime and POP are found to vary from 15.75 to 19.12% and 3.95 to 4.57% respectively.

The strength of mortar specimens mainly depends on the curing period as well as the type, amount, and the fineness of the mineral admixtures. It indicates that the silica

fume added samples give the highest compressive strength than other mixes at similar test conditions. Silica fume added mortars specimens show the lowest porosity and exhibits uniformly distributed pores over the measured pore size range. This indicates that silica fume acts as a filler material and it also participates in the pozzolanic reactions. X-ray diffraction analysis shows a series of compounds such as calcium silicate hydrate, gypsum, quartz, and calcite. SEM analysis also confirms the existence of these components in the hydrated specimens as calcium silicate hydrated gel. FTIR spectrum shows a shift of Si-O, O-H, and Al-O bonds with wave number indicating that the hydration process continues with curing time and confirms the formation of calcium silicate hydrated gel during the reaction.

The addition of calcium based chemicals like calcium acetate, calcium formate and calcium nitrate up to 2% to the reference binder (D5) improves the compressive strength and after that it decreases. However, an addition of sodium based admixtures results no appreciable change in strength over the reference sample. The SEM image of specimens containing calcium based chemicals such as calcium acetate and calcium formate shows abundance of needle shaped Aft phase of calcium aluminate tri-sulphate and gel like calcium silicate hydrate. The presence of these hydration products result in enhancing the strength of the mortar specimens. However, in sodium based specimen these phases are found in lesser quantity.

Compressive strength results of mortar specimens cured under different temperatures revealed that higher curing temperature favors an early strength gain but the strength at a later age is found to be lower than the samples cured at moderate temperatures. Samples cured at low temperature show a rising trend of strength even after

90 days of curing whereas the strength of high temperature cured specimens gets stabilized much earlier. A crossover effect of strength is noticed between low and high temperature cured specimens. X-ray diffraction analysis shows a series of compounds such as calcium silicate hydrated and wollastonite in the hydrated specimens. Usually needle like crystals of ettringite are observed during the early periods of hydration whereas in the later curing period common fibrous type of irregular grains forming a reticular network of calcium silicate hydrate gel is found. The gradual shifting of v4-SiO_4 bond towards lower frequency with increase in temperature indicates the formation of more amounts of C-S-H with increased curing period. The optimum dose of raw materials is found to vary marginally based on curing temperature and curing period. X-ray diffraction analysis shows a series of hydration compounds such as calcium silicate hydrate, gismondine, xonotlite, and tobermorite in samples cured in autoclave whereas absence of gismondine, xonotlite and tobermorite is observed in samples cured in water at normal temperature of 27 ^{o}C. Furthermore, tobermorite structures having different morphology such as foiled and semi-transparent are observed in the spherical pores in autoclaved samples. A high temperature and pressure curing favors quick formation of hydration products and it results much faster gain of strength. The samples cured in an autoclave for 2 hours give almost equal strength to specimens cured in water at normal temperature for 28 days. No appreciable gain in strength is observed in specimens cured in autoclave beyond 2 hours whereas samples cured in water at normal temperature show a continuous increase in strength up to 90 days. The specimens cured in water for 90 days show a low porosity, higher mass density and more homogeneous distribution of

hydration products than the specimens cured in autoclave for 4 hours. This contributes to higher strength of the samples.

The objective of the present investigation is to understand the properties of lime activate slag cement through an extensive experimental program. Therefore, the test results obtained from present investigation builds a high level confidence that alkaline activated slag can be used as an alternate binding material to OPC.

TABLE OF CONTENTS

LIST OF TABLES

LIST OF FIGURES

LIST OF ABBREVIATIONS AND SYMBOLS

Abbreviations

AASC- Alkali activated slag cement

OPC- Ordinary Portland cement

POP- Plaster of Paris

FA- Fly ash

SF- Silica fume

GP- Glass powder

RSM- Response surface method

ANOVA- Analysis of variance

GRG- Generalized reduced gradient

XRD- X-ray Diffraction

SEM- Scanning Electron microscope

EDS- Energy Dispersive Spectrometer

FTIR- Fourier Transform Infrared

TGA- Thermo-gravimetric analysis

DSC- Differential scanning calorimeter

Symbols

fc- Compressive strength

x_1- Lime content

x_2- Plaster of Paris content

R- Regression coefficients

F- Factorial value

CHAPTER I
INTRODUCTION

1. INTRODUCTION

1.1 AN OVERVIEW ON CEMENT PRODUCTION AND UTILIZATION

In this present scenario, the economic development of a country majorly depends upon the development of infrastructures and industries. For construction of these infrastructures, concrete is adjudged to be an indispensable building material and cement is an integral constituent of this material. It is used universally for all construction works such as housing and industrial construction as well as for construction of infrastructures like ports, roads, power plants, etc. From the time immemorial, Portland cement has been used as binder in concrete construction. It is basically made up of a mixture of chemical compounds such as calcium oxide, silica, aluminium oxide, and iron oxide. Generally, the ordinary Portland cement is prepared by mixing clinker with some additives whereas the clinker is produced by calcinations of limestone (calcium carbonate) and siliceous material. During the clinker production process, de-carbonation occur which causes emission of huge amount of carbon dioxide to the atmosphere. The global cement production is likely to reach 5000 million tonnes in the year 2050 (Figure 1.1). Though today there is skyrocketing rise in demand for cement in construction field, its production is not adjudged to be eco-friendly due to emission of CO_2 which accounts for around 5%. The total emission of CO_2 per kg of cement clinker produced is 0.53 kg from the decarbonation of calcite, plus 0.33 kg from the burning process plus 0.12 kg from the generation of electrical power required, making a total of 0.98 kg. Therefore, for every

ton of cement clinker produced, an approximately equal amount of carbon dioxide is released into the atmosphere (Davidovits, 1991). The world cement industry contributes an approximate of 7% to the total man made CO_2 emission (Malhotra, 1999).

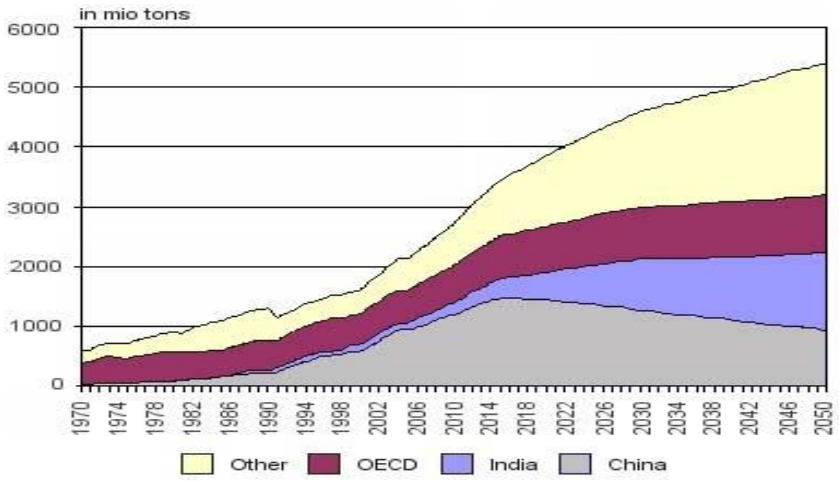

Figure1.1Global cement productions (1970-2050)
[Source: International Energy Agency (IEA)]

Figure 1.2 represents the total amount of CO_2 emitted to the atmosphere during last three years in different regions and from this it is observed that Asian region ranks second position in carbon dioxide emission. In the year 2011, the production of world cement has reached to 3.6 billion tones and emitted 2 billion tons of CO_2 to the environment which being produced both from calcinations of limestone and fossils fuel/gas used during the entire process. As per global cement sector, the emission of CO_2 for cement production can be reduced by three main parameters and those are:

- Energy efficiency,
- Alternative fuels or biofuels, and
- Clinker substitution.

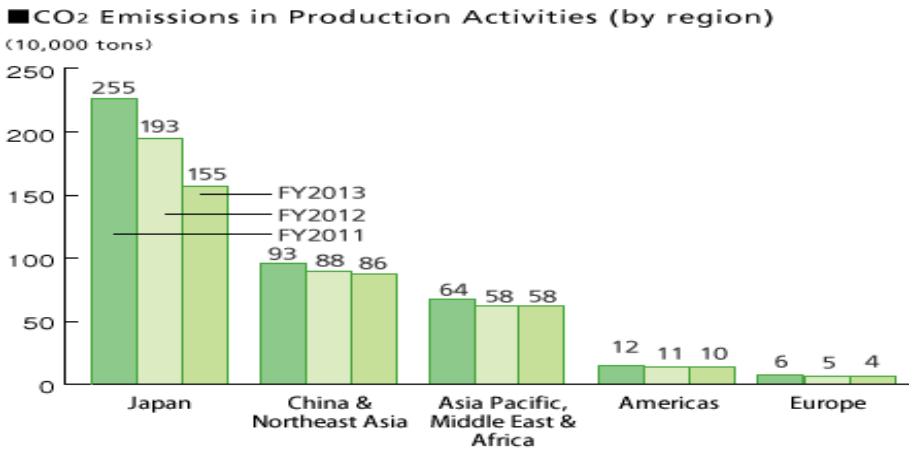

Figure1.2 CO_2 emission during last three years (2011-13)
[Source: International Energy Agency (IEA)]

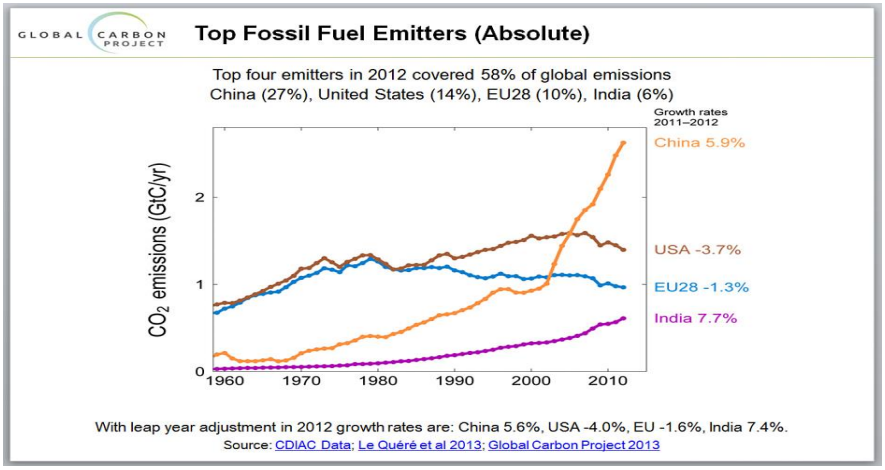

Figure 1.3 CO_2 emission in different countries (1960-2010)

Through the combination of these efforts, the emissions of CO_2 have been reduced by 16 percent from the 1990 levels of 750 kg CO_2 per tonne of cement. Further, reductions can be achieved through continued action using these three parameters but there is a practical limit on the reductions that can be achieved. Hence deep cuts in CO_2 emissions from cement production can be achieved only through cement clinker substitution. In addition to this, another disadvantage of cement production is that it consumes huge amount of energy. A closer look at the economics of the production of

Portland cement shows that energy input accounts for 58% of the total cost of production (28% for power, 30% for fuel). The energy required to produce different types of cement in terms of fuel consumption (Kilos per metric ton of cement) is given in Table1.1.

Table 1.1 Energy required for different type of cement production

Cement type	% Slag	Clinker production	Drying slag with grinding at 15% moisture	Grinding at 3000 Blaine (m^2/kg)	Total energy requirement (kg/ton)
Pure cement	0	106.1	0	10.5	116.6
Compound Portland cement	35	68.9	5.6	13.1	87.6
Blast furnace slag cement	30	63.7	6.4	13.5	83.6
	40	53.1	8	14.2	75.3
	50	42.4	9.6	15.0	67.3
	60	26.5	12	16.1	54.6
Slag cement and clinker	85	15.9	13.6	16.9	46.4
Slag 15% moisture, dried and ground	100	0	16.0	18	34
Dry slag ground	100	0	0	18	18

(Source from www.nationalslagassoc.org)

Taking into account the disadvantages of conventional Portland cement production it has been a challenge for the cement industry to meet the growing demand for cement with the need to forge a more sustainable cement industry. Though the current cement production and cement industry has not completely reduced the carbon dioxide

emission and not fully saved the energy consumption, there is an indigence of an alternative technology to reduce and save the energy.

The development of alternative cements based on the alkali-activation of slag has a relatively long history. Feret (1939) first described the use of slag instead of cement in 1939, while in 1940 Purdon focuses on alkali activated slag, but this concept become widespread in 1950s by Glukhovsky. In 1960s, several apartments and other engineering structures were constructed using alkali activated slag cements in Ukraine. Although these structures subjected to severe weather, they still are in stable condition. The use of slag in cement is especially attractive for a number of environmental reasons. Alternate alkali activated slag cement can be used by adding some activators such as lime and plaster of Paris in slag which also gives the same properties as alkali activated slag cement (AASC).

Literally, alkaline activated slag cement is a sustainable, eco-friendly binding material as well as a superior alternative to OPC as it possesses some major positive features that it emits negligible amount of carbon dioxide and consumes less amount of energy. Although the development of alternative cements based on the alkali-activation of slag has a relatively long history, still its implementation in the construction industry has never been overhyped and the commoners are unaware of its application so far. So a proper and comprehensive study need to be done in order to evaluate itôs physical, chemical and mechanical properties so that a high level confidence can be built up for itôs safe and extensive application in the construction field as an alternate to OPC.

1.2 ORGANIZATION OF THE THESIS

The work presented in this thesis involves fundamental knowledge on cement properties like physical, chemical, and mechanical properties of lime activated slag cement. The observations reported in literature and experimental procedure described in Indian Standard code was used as reference for the experimental and computational work. The research framework of this thesis is presented in Figure 1.4. It is composed of 8 chapters, which are described in details below.

Chapter 1of this thesis introduces some background knowledge on the importance of cement production, effects of cement production on the environment as well as its remedies and a brief description about different types of cement and substitution of cement.

A critical review of relevant literature is given in Chapter 2. This includes activation of pozzolanic materials by different activators and their effects on physical, chemical, and mechanical properties. The effects of curing conditions and admixtures on the strength and hydration products are also reviewed in this chapter. A few computer models for optimization of raw materials of cement are introduced with special emphasis on the computer model called generalized reduced gradient (GRG) algorithm and response surface method.

Chapter 3 of this thesis deals with the experimental procedure for material characterization, details of the experimental studies undertaken and the experimental procedure adopted.

Chapter 4 of this thesis deals with the physical properties of slag-lime-POP mixes. The reaction mechanism along with the formation of hydration products, their characteristics, compositions, and accompanying properties are investigated. A correlation is established between physical properties and developed hydration products and microstructure.

Chapter 5 of this thesis emphasizes on the mechanical properties of slag-lime-POP mixes. The compressive strengths of slag-lime-POP mixes after different curing periods are evaluated and are correlated with hydration products, chemical bonds, and microstructure. The optimization of raw material proportions was made based on the experimental values of compressive strength by adopting response surface plot and the generalized reduced gradient technique.

Chapter 6 of this thesis focuses on the effects of admixtures (mineral and chemical admixtures) on strength of lime activated slag cement. The mineral admixtures used are silica fume, fly ash, glass powder and OPC. Similarly, chemical admixtures used in this work are calcium acetate, calcium formate, calcium nitrate, sodium hydroxide, and sodium-meta-silicate. The effects of these admixtures on compressive strength, hydration products, microstructure and porosity are investigated and reported.

Chapter 7 of this thesis describes the effects of curing conditions on strength of lime activated slag cement. The curing is done in different curing temperatures in water bath and with high temperature and pressure for different curing periods in autoclave. The results of strength obtained in different curing conditions are compared and correlated with hydration products and chemical bonds formed after curing.

Chapter 8 of this thesis gives the detailed summary, conclusions, and future scope of the work.

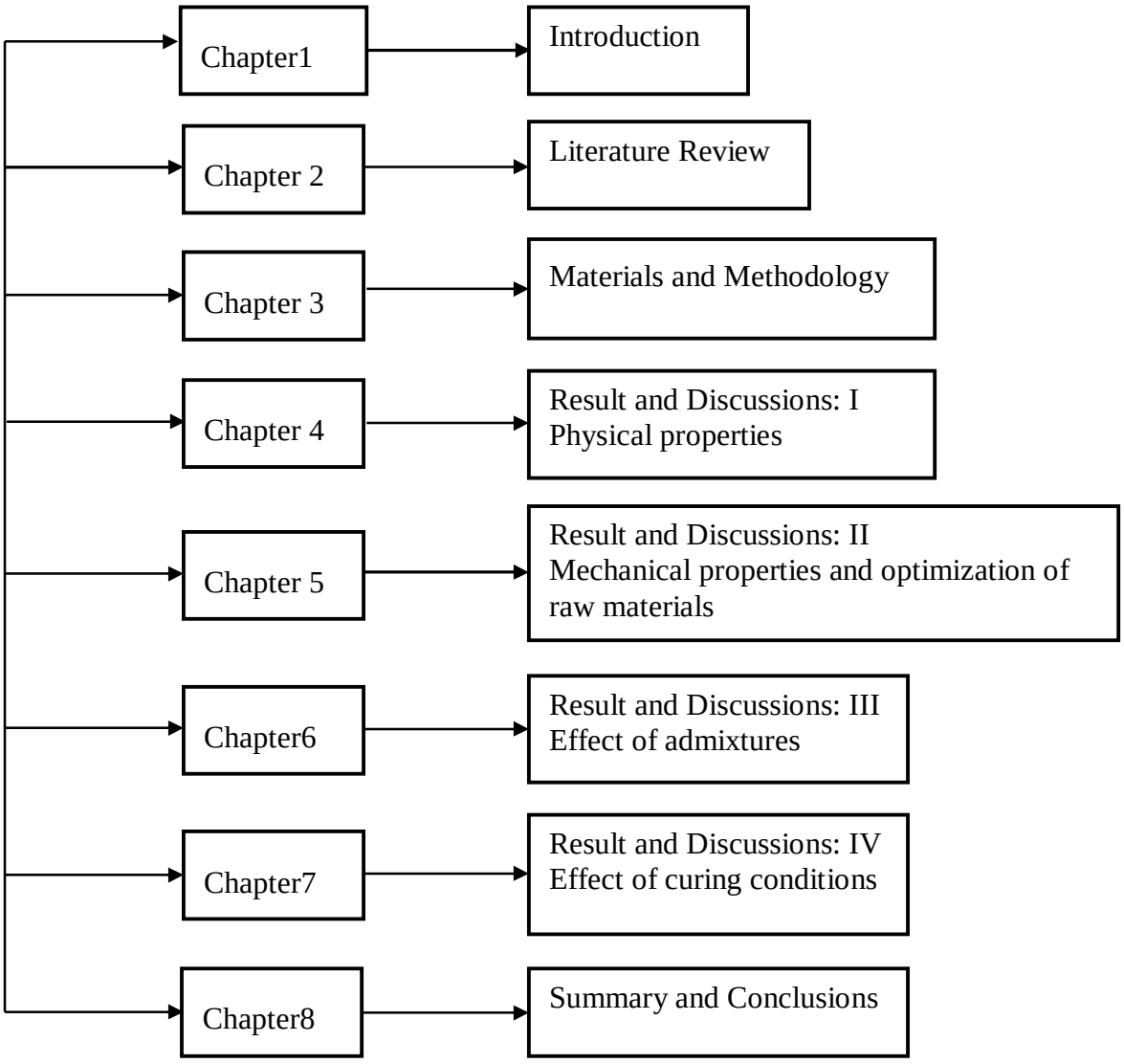

Figure 1.4 Structure of the thesis

CHAPTER II
LITERATURE REVIEW

2. LITERATURE REVIEW

2.1 INTRODUCTION

An extensive literature review pertaining to the activation of pozzolanic materials is conducted. A wealth of information were found in the literature and studied with respect to different properties of alkali activated slag, such as mix proportions, curing conditions, admixtures, hydration products and hydration mechanism, microstructure and morphology. The area of further research is to be looked into to open new avenues to enhance the knowledge on this alternate construction material. A brief review or summary of reports, papers and articles is given in below.

2.2 POZZOLANIC MATERIAL

Pozzolana, also known as pozzolanic ash, is a siliceous or siliceous and aluminous material in the form of amorphous or glassy materials. When it reacts with calcium hydroxide in the presence of water at room temperature, calcium silicate hydrate and calcium aluminate hydrate compounds are formed possessing cementitious properties. The term 'pozzolana' has two different meanings. The first one specifies the pyroclastic rocks, essentially glassy and sometimes zeolitised, which occur either in the neighbourhood of Pozzuoli (the ancient Puteoli of the Roman times) or around Rome. The second meaning includes all those inorganic materials, either natural or artificial, when these pozzolana materials mixed with calcium hydroxide (lime) and water which formed a harden material or that can release cementious properties. The use of pozzolanas has been mostly restricted to Italy, where considerable reserves of natural

pozzolanas are found and in Greece (Santorin earth) for a long day. In other countries the interest in these pozzolana materials is of relatively recent date and has arisen from the need for reusing some waste materials such as blast furnace slag, fly ash and silica fume. This historical background can help to explain why so many countries have long distrusted pozzolana containing cements, despite the millenary use of lime-pozzolana mortars and almost 100-year experience in pozzolanic cements. In any case, the results of a variety of studies have substantially confirmed that pozzolanic cements can yield concrete showing a higher ultimate strength and greater resistance to the attack of aggressive agents. Now-a-days the most pozzolanic cementing material is the activated of slag cement; which is an attractive, cost effective and environment friendly cementing material.

2.2.1 Activation of pozzolanic materials

The natural pozzolanic materials and the artificial pozzolana like industrial byproducts such as ground granulated blast furnace slag, fly ash, silica fume and rice husk can be used as cementious material. These pozzolanic materials are activated due to its latent hydraulic properties and become the most suitable cementing material alternate to OPC. The activation of pozzolanic materials can be achieved by three different activation methods such as:

1. Alkaline activation
2. Sulphate activation
3. Combined alkaline and sulphate activation

2.2.1.1 Alkaline activation

In alkaline activation alkalis or alkaline earth ions are used to stimulate the pozzolanic reaction or release the latent cementious properties of finely divided inorganic materials. In this process the solubility of the pozzolanic materials are influenced and solubility of the alumina, silica becomes greater with the increase in pH value of the aggressive solution. Figure 2.1 shows the solubility of amorphous silica and alumina in different pH ranges. The increase in solubility is particularly strong in the relevant pH value range of more than 10.

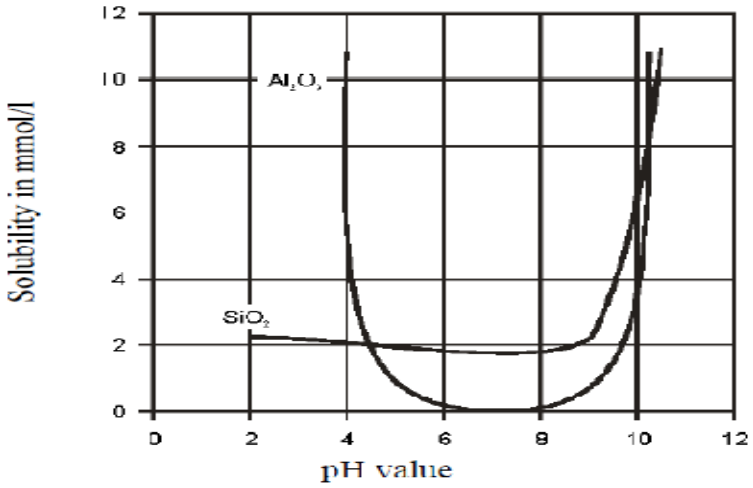

Figure 2.1 Solubility of Al_2O_3 and amorphous SiO_2 related to pH value (source Fra90)

The application of alkaline reacting material aggravates an increased solubility of the pozzolana silicates and improves the reaction capability of these materials. The alkaline compounds that are suitable as activators can be classified into three classes:

i. Alkaline salts of weak acids (except for silicates) e.g., sodium carbonate, sodium fluoride
ii. Alkaline silicate, e.g., sodium silicate, sodium silicate in a compound with sodium fluorosilicate
iii. Alkali hydroxide, e.g., $Ca(OH)_2$ is also included amongst the alkaline activators

The function of $Ca(OH)_2$ is different from that of the alkaline salts. It not only acts as a catalyst for the pozzolanic reaction, but also it takes part in reaction activity. During the reaction it produces C-S-H phases and calcium-alumina hydrate such as C_4AH_{13}. Jiang (1997) classified the activation of different pozzolanic materials as (1) alkali activated slag cement; (2) alkali activated portland-slag cement; (3) alkali activated fly ash-slag cement; (4) alkali activated pozzolana-lime cement; and (5) alkali activated pozzolana cement. The activators used are NaOH, KOH; Na_2SO_4; Na_2CO_3; $CaSO_4$, and soluble silicate of sodium and potassium. These alkali activate cementing materials have great potential and generate very early, high strength, greater durability and high performance. Krivenko (1994) classified the alkali activated cementious material based on the composition of hydration products. The alkaline alumino-silicate systems (R-A-S-H, where R= Na or K) were called ñgeocementsò, emphasizing the similarity of the formation process of these materials to the geological process of the natural zeolites. The alkalineï alkaline earth systems (R-C-A-S-H) where the hydration products are low basic calcium silicate hydrates (C-S-H gel with low Ca/Si ratio). This includes the alkali-activated slag and alkaline Portland cements.

2.2.1.2 Sulphate activation

The reaction of the pozzolana materials can also be stimulated by the addition of sulphate-containing compounds such as calcium sulphate. The effectiveness of this activator is based upon the reaction of these with the sulphate ions subject to the formation of etringitte, C-S-H phases and aluminium hydroxide. The reaction speed of the pozzolana materials are, however comparatively low when exclusively stimulated with sulphates. The effectiveness of the sulphate activation can only be improved to any

significant degree with the addition of alkaline reacting materials. With simultaneous alkaline activation an increase in the sulphate content has a positive effect on the reaction speed of these materials. The sulphate activation is used particularly in sulphate slag cements, which containsat least 75% and mostly between 80 and 85% GGBS. As activators, these cements contain between 10 to 15% anhydrite and about 5% Portland cement clinker or lime. The Al_2O_3 content in the raw material should be at least 14 % or higher to achieve high quality sulphate cement. In recent years, sulphate slag cements have been redeveloped using the present day GGBS qualities and the optimum dose of activators are to be finalized depending on the quality of slag.

2.2.1.3 Combined alkaline and sulphate activation

Pozzolanic materials can be activated by combined sulphate and alkaline activation. In this activation, in the early stage of the reaction the sulphate activation is predominant; leading for solidification and after termination of the solidification reactions the reaction of the pozzolana materials continues by alkaline activator. The pore solution in the hardened cement paste is characterized by the ever-present calcium hydroxide in the surplus due to very high pH values of at least 12.5. In addition, in the early hydration stage, it contains high concentration of sulphate ions, which originate from the calcium sulphate added as a solidification actuator and from the alkaline sulphates of the clinker. Sulphate is bound during the solidification process and forms calcium-aluminate-sulphate-hydrates which leads to the reduction of sulphate concentrations. At the same time the sulphate ions are replaced by hydroxide ions and the pH value increases. After the end of the solidification reactions, the pore solution contains mostly alkali and hydroxide ions and the pH value is between 13 and 14. The

solubility of the calcium in highly alkaline pore solution is still only minimal. The predominant part is present in the hardened cement paste in the form of solid $Ca(OH)_2$.

2.3 ALKALINE ACTIVATION OF SLAG

In the present study an extensive literature review is made on the activation of ground granulated blast furnace slag (GGBFS) by using different activators. The physical properties, mechanical properties, hydration products, microstructure, and morphology of slag activated by different activators have been reviewed and presented in the following sub-sections. The effects of curing conditions and admixtures on strength and hydration products are also reviewed.

2.3.1 Physical properties

The physical properties of the binding material are as important as the mechanical properties. The physical properties mainly consist of the consistency, setting time and soundness of the cementing material. A detailed review on physical properties of the activated slag is presented here.

Shi and Li (1989) studied extensively on the formation of hydration products of the alkali activation of slag activated by water glass. The properties of alkali-phosphorus slag cement were influenced by the modulus of water glass ($Na_2O:nSiO_2$), soluble phosphates, water to solid ratio and the fineness of the slag when water glass and granulated phosphorus slag (GPS) were used to make alkali-GPS cement. The anions of water glass react with Ca^{2+} dissolving from the surface of GPS grains and primarily calcium silicate hydrate forms at the initial stage of hydration. The main hydration product is reported to be hydrated calciumï aluminaï silicate, like C-Aï Sï H gel. This phase is different from

that formed in the Portland cement in the early period of hydration and has a lower C/S ratio. Wang *et al.* (1995) reported that the slag activated with sodium hydroxide poses quick setting and high shrinkage with micro crack formation. Brough *et al.* (2000) used phosphate and malic acid as retarders in slag and sodium silicate base mixes to increase the setting time of the alkali activated slag cement. Gong and Yang (2000) studied the effect of phosphate on the hydration mechanism of alkali activated red mud slag through micro calorimeter, X-ray diffraction, and energy dispersive spectroscopy. The setting time was found to be retarded due to the production of a new phase of (CaNa) O(SiAl)O_2y(CaNa) SO_4xH_2O.

2.3.2 Mechanical properties

The strength of cement mortar is the most important parameter which gives the overall measure of quality of cement and concrete. An attractive alternative with equal or more strength to Portland cement is the binders obtained by activation of pozzolanic materials, rich in reactive amorphous silica and alumina. In order to enhance its mechanical properties, slag is activated by different activators. This section summarizes the works regarding the development of compressive strength in alkali activated slag cement. Malolepszy and Nocun-Wczelik (1988) found that both compressive and flexural strengths of sodium silicate-activated slag cement mortars decreased with increase in molarity of sodium silicate solution. Shi and Li (1989) activated granulated phosphorus slag by water glass (Na_2O:nSiO_2) and determined the effect of modulus of water glass (Na_2O:nSiO_2), soluble phosphates, water to solid ratio and the fineness of the slag on hydration mechanism and the mechanical strength of the cement. The results indicate that the modulus of water glass and fineness of slag have pronounced effect on the strength of

the cement and the increase in water to solid ratio is not helpful both to the early hydration and strength of the cement. Douglas *et al.* (1991) activated the ground granulated blast-furnace slag mortars and concrete with alkaline reagents (NaOH, $Ca(OH)_2$, sodium or potassium silicates). The results indicate that the activation of sodium silicate can be used to make slag concrete with satisfactory workability and strength properties. Wang *et al.* (1994) investigated on the activation of acidic, neutral, and basic slag with water glass having different moduli. The results indicate that the optimum modulus for the acidic, neutral and basic slag was around 0.75-1.25, 0.9-1 and 1.0-1.5 respectively. Bakharev *et al.* (1999) activated the slag by sodium silicate, sodium hydroxide, sodium carbonate, sodium phosphate, and combinations of these activators. The result indicates that the compressive strengths are in the range from 20 to 40 MPa and most effective activator is found to be liquid sodium silicate. Sodium silicate solution with a low Na content and modulus equal to 0.75 is recommended for formulation of AAS concrete. Puertas *et al.* (2000) studied the strength behavior of alkali-activated slag/ fly ash pastes activated with either 2 M or 10 M of NaOH solutions. The slag to fly ash ratios were 100/0, 70/30, 50/50, 30/70 and 0/100. The results indicated that as slag content in the pastes increased, compressive strength increased. The higher strengths were obtained when 10 M NaOH was used. Glukhovsky *et al*. (1983), Bakharev *et al.* (2001) reported that the alkali activated slag cement (AASC) had lower resistance to alkali aggregate attack than that of the OPC concrete of similar grade. Escalante-Garcia *et al.* (2002)studied the strength properties of blended slag mortars with replacement levels of 0, 5, 10, 15 and 20% geothermal silica waste, and slag was activated with 6% Na_2O equivalent of NaOH and water glass. The lime was added as an activating agent to

promote pozzolanic reaction with the silica. It was found that the presence of silica waste increased the reactivity of the cementitious materials, and compressive strength increased with increase in silica content up to 15% replacement; thereafter, the strength was reduced. Ben Haha *et al.* (2011) reported the strength of slag cement that was activated by NaOH and $Na_2SiO_35H_2O$. The slag activated by $Na_2SiO_35H_2O$ gave higher strength compared to slag activated by NaOH.

2.3.3 Effect of admixtures

Mineral admixtures mainly used in concrete works in order to make the cement more economical, reduce permeability, increase strength, and influence other properties of hardened concrete. The industrial by-products like fly ash (FA), silica fume (SF), and glass powder (GP) can be used as mineral admixtures. Silica fume,fly ash, and glass powder generally has been used as an admixture in slag based alkali-activated systems.Phillips and Cahn (1973) commented that glass cullet up to 35% could be used in concrete in combination with low-alkali cement. Samtur (1974) reported that the fine glass powder of size less than 75 μm acts like a pozzolana material and it reduced the tendency of reactive aggregate to undergo alkali silica reaction. Douglas and Brandstetr (1990) studied the mechanical strength of alkali activated slag cement taking different proportions of sodium silicate solution, lime, OPC, silica fume and fly ash. It has been found that silica fume activator (SFA), a product prepared from silica fume and water solution of alkali compound, is more active than NaOH and water glass Zivica (1993). Rousekova (1997) reported that the SFA is a highly effective substance for the alkali activation of the combinations of Portland cement, silica fume and blast furnace slag as well as slag alone. The positive effect of silica fume is based on the intensiýcation of the

production of calcium silicate hydrates. Shi and Day (1999) studied the early strength development and hydration of alkali activated blast furnace slag/fly ash blend cements by activating with sodium hydroxide and water glass. The authors found a decrease in strength with increase in the amount of OPC, but in the case of fly ash it is reversed.Shao *et al.* (2000) reported that the finer particle size of 75 εm or less of glass powder is favorable for pozzolanic reaction. Zivica (2004) investigated the effectiveness of silica fume natrium hydroxide, natrium carbonate, and water glass, on the strength of activated slag. They prepared fresh mortar mixtures of activated slag by adding SFA (a product prepared from silica fume and water solution of alkali compound), natrium hydroxide and water glass and result shows that improvement of strength is due to activation of SFA.Shi (2005) found that the fine glass powder possesses high pozzolana reactivity. The effect of silica fume activator (SFA) on strength is more active than natrium hydroxide, natrium carbonate, and water glass. Zivica (2006) activated blast furnace slag by SFA, the author found an increase in compressive strength and the resistance to permeability of water. Yazic *et al.* (2008) studied on the effect of mineral admixtures on compressive strength of ternary blended cement. The results indicated that the reactive powder concrete containing high volume binary (SF-FA or BFS) or ternary (SF-FA-BFS) blends have satisfactory mechanical performance.

2.3.4 Effects of curing temperature

For cement based materials, the curing conditions are the main key variables, because these influence both the early hydration kinetics and the properties of the hardened cement paste and concrete. Curing conditions and curing temperature influence the properties of hardened concrete. Aitcin (1958) opined that if curing is neglected in the

early period of hydration, the mechanical properties of concrete will decrease at later ages and suffer some irreparable loss. Bakharev *et al.* (1999) studied the effect of elevated curing temperature on the properties of alkali-activated slag concrete and concluded that the heat treatment signiýcantly accelerated the strength development but in later ages the compressive strength was reduced as compared to the concrete cured at room temperature. Puertas *et al.* (2000) studied the strength behavior and hydration of alkali activated fly ash slag cement on different curing conditions. The results indicated that increased curing temperature has a positive effect on early strength gain and the strength increased up to a fly ash content of 30%. However, increase in fly ash content beyond this lowers the strength for a variety of activators and curing regime. Talling (1989) reported that an increase in strength of alkali activated slag cement occurred when the curing temperature was raised from 50 ^{o}C to 60 ^{o}C, and then no obvious temperature effect was observed up to 90 ^{o}C regardless of activator dosage.Shi *et al*.(1991) examined the strength developed in alkali-activated phosphorus slag cement and pointed out that the curing temperature had a very significant effect on the strength development in slag cement. Carino (1991) and Carino, and Tank (1992) reported that the crossover effect did not occur in hot cured high strength concrete prepared using OPC as the binding material. Fernandez and Puertas (1997) reported that the activation energy of alkali-activated slag cement is higher than that of Portland cement and it is expected that high temperature curing may be very helpful in improving the strength of alkali-activated slag cement. Zain and Radin (2000) studied the compressive strength and modulus of elasticity of high-performance concrete made with four types of concrete mixes exposed to temperatures within the range of 20 ^{o}C to 50 ^{o}C under three different types of curing

methods. The results showed that the compressive strength of concrete incorporating mineral admixtures practically reached above 100MPa from the age of 7 days. Puertas *et al.* (2000) studied the strength behaviour and hydration of alkali activated fly ash slag cement on different curing conditions. The fly ash / slag (100/0, 70/30, 50/50, 30/70 and 0/100) are activated with NaOH solution with concentration of 2 and 10 molality at curing temperature 25^{o}C & 65^{o}C. Their results indicated that the curing temperature has positive effect in the strength increase at first days of reaction. But at longer ages the effect is the inverse. The strengths are higher when curing temperature is 25^{o}C. Escalante Garcia (2001) and Sharp, (2001) reported on the crossover effects in mortar specimens made from OPC blended with fly ash/ground granulated blast furnace slag. The degree of hydration of the cement phases has been reported to be higher at increased temperatures in the early stages, but at later period the situation was reversed. A higher curing temperature at early ages increases the rate of hydration. However, it does not allow the reaction products to become uniformly distributed within the pores of hardening paste. Jin-Keun *et al*. (2002) reported the results of curing temperature and curing period on the strength and elastic modulus. They prepared the concrete with binders of cement and fly ash concrete, cured in isothermal conditions of 10, 23, 35, and 50^{o}C and determined the strength and elastic modulus at the ages of 1, 3, 7, and 28 days. The results indicate that the concretes subjected to high temperatures at early ages attain higher early-age compressive and splitting tensile strengths, but lower later-age compressive and splitting tensile strengths than concrete subjected to normal temperature. Shi *et al.* (2006) opined that an increase of 10^{o}C curing temperature doubled the rate of chemical reaction. According to a study conducted by Shi *et al.* (2006) on alkali activated slag cement the

compressive strength was found to be the highest at curing temperature of around 80 to 90 ^{o}C, but the strength decreased as the temperature was further increased to 100 ^{o}C. Ezzian *et al*. (2007) prepared mortar specimens with 0, 10, 20, 30 and 40% of natural pozzolana replacement and cured under constant curing temperature of 20, 40 and 60 ^{o}C with saturated humidity. The results indicate that pozzolana enhances the ultimate compressive strengths and increases the activation energy which indicates the slow reactivity. The effect of the temperature on the ultimate strength is reduced with increase in temperature. Tanyildizi (2009) reported that a higher curing temperature improves strength at early ages. At a later age, the important hydrates formed have no time to arrange suitably and this causes a loss of ultimate strength.

2.3.5 Autoclave curing

The compressive strength is the main factor considered in the design and construction of concrete structures. The compressive strength of the samples is known to depend on the curing conditions adopted. Curing conditions and curing temperature influence the properties of hardened mortar and concrete also. Neville (1995) reported that the 28 days strength of normal curing can be achieved in about 24 hour with autoclave curing. Furthermore, studies showed that the incorporation of fine silica also enhances the mechanical properties. Aldea *et al*. (2000) studied the effects of curing conditions on properties of slag cement concrete. Autoclaving (175 ^{o}C, 0.5 MPa) and steam curing (80 ^{o}C) were compared to normal curing (28 days, 20 ^{o}C, and 100% RH). Four different concrete mix designs with the same mix proportions and different cement replacements were used: 0% slag (control), 25% slag, 50% slag, and 75% slag. The effects of slag replacement and curing conditions upon concrete properties were

examined. Shi and Hu (2003) studied the effect of autoclave curing on hydration product and microstructures of alkali activated slag cement with and without silica fume as an admixture. Sugma and Brothers (2004) investigated on the effects of curing temperature on strength properties of sodium silicate activated slag cement. It was found that sodium silicate activated cement autoclaved at temperature up to 200 ^{o}C displayed an outstanding compressive strength of more than 80 MPa. Hong and Glasser (2004) studied the hydration products of alkali activated slag cement and reported that C-S-H gel of appropriate compositions normally gets converted rapidly to crystalline phases of tobermorite and xonotlite in 12 to 18 hour at autoclaving temperature of 160 ^{o}C to190 ^{o}C. Yazici (2007) studied the effect of curing conditions on the mechanical properties of ultra-high strength concrete mixes manufactured using OPC and mineral admixtures like class-C fly ash and pulverized slag (PS). The specimens were cured in water, steam cured (90 ^{o}C) at atmospheric pressure and autoclave cured (210 ^{o}C) at pressure of 2MPa. The test results showed that high strength concrete can be obtained with high volume mineral admixtures. Yazici *et al.* (2009) prepared and studied the strength of alkali activated slag cement cured in water, steam, and autoclave (210 ^{o}C) under 2 MPa pressure for 8 hour. The result indicated that the steam and autoclave curing caused some reduction in þexural strength as compared to the standard water curing for 28 days. However, an addition of ground granulated blast furnace slag (GGBFS) and /or fly ash (FA) decreased the negative effect on strength of specimen cured in both steam and autoclave. Rashad *et al.* (2012) activated ground granulated blast furnace slag with quartz powder at various replacement levels ranging from 0 to 30% with sodium silicate as alkali activator. These were cured in autoclaved at a pressure of 8 bars and a temperature of 170 ^{o}C with

autoclaving times varying from 0 to 10 hour. An improvement in compressive strength is reported up to 30% replacement of slag by quartz powder.

2.4 SULPHATE ACTIVATION OF SLAG

2.4.1 Physical properties

Bijen and Niel (1981) prepared the super-sulphated cement consisting of a mixture of 83% of Dutch blast furnace slag, 15% of fluoro-gypsum (anhydrite) and 2% of Portland clinker, and mixture is ground to a specific surface of 500 m^2/kg. The results indicate that fineness of mixture reduces the setting time. Mehrotra *et al.* (1982) opined that plaster of Paris is a better activator than the conventional hard burnt gypsum (anhydrite) for activation of slag but, this cement has shorter setting time. Dutta and Borthakur (1990) reported the physical properties like setting time of super sulphated slag cement, prepared the blended cement by using slag, anhydrite/gypsum and clinker. They found the initial and final setting times of different compositions are in the range of 50-80 min and 105-170 min respectively. The optimum amount of anhydrite to activate the slag was varying from 15 and 20%.

2.4.2 Mechanical properties

The mechanical property like compressive strength of activated slag cement is studied by many authors. Weast (1979) reported that the solubility of gypsum is lower as compared to plaster of Paris and the slag activated by gypsum gains strength at a slower rate than treated with plaster of Paris. Bijen and Niel (1981) reported on the mechanical strength of super-sulphated cement, which was prepared with a mixture of 83% blast furnace slag, 15% flour gypsum (anhydrite) and 2% clinker (Portland cement). Mehrotra *et al.* (1982) reported that plaster of Paris (POP) is a better activator than the conventional hard-burnt gypsum (anhydrite) at least for a class of blast furnace slag, which ordinarily

considered less ideal for this purpose. The early strength of sulphate activated cement was reported to be lower than the OPC, but the strength exceeds than that of OPC with prolonged curing. Dutta and Borthakur (1990) reported the mechanical properties of super sulphated slag cement prepared by using (70-85)% slag, (10-25)% anhydrite and 5% clinker. The results indicated that the compressive strengthincreases with hydration time and optimum amount of anhydrite required to activate the slag is in the range of 15-20%. The 3 and 7 days strength of these compositions are about 50-60% of the 28 days. Li Dongxua *et al*. (2000) studied the influences of compound admixture like sodium sulphate on slag activated with gypsum and anhydrite. The results indicate that the compound admixtures not only speed up the breakage of slag structure, but also accelerate the hydration of clinker and the solution of anhydrite and lead to production of more hydrates and improvement in all properties of high-content slag. Savastaro *et al*. (2001) prepared the blended cement using blast furnace slag, lime and gypsum with 80, 8, and 12 % respectively. Their results indicate that the compressive strength is 24.5 MPa with this mix proportion. Jhon *et al.* (2005) studied on the durability of slag mortar reinforced with coconut fibre and prepared the binder with blast-furnace slag activated by 10% of gypsum and 2% of lime with acidic solution (chloridric acid, 10%) in an ultrasonic bath. They found that the fibers remained undamaged, as it was observed by scanning electron microscopy (SEM) analysis after 12 years.

2.5 COMBINED ALKALINE AND SULPHATE ACTIVATION

2.5.1 Physical properties

The setting characteristics of slag-lime mixes were studied by Feret (1939) and Jolibois and Nicol (1952) by using granulated slag and high calcium lime. The slow setting of the mixes was improved by adding sodium sulphate to the extent of 1 %, but it

suffered from producing efflorescence. An addition of gypsum is recommended in their work instead of sodium sulphate. Naceri *et al.* (2009) activated the slag cement by hydrated lime with 0, 2, 4, 6, 8, and 10% (by addition and substitution method) and observed a reduction in setting time with an increase of lime content. The setting and hardening of cement paste could be correlated with the formation of chemical compounds, phases, and hydration products.

2.5.2 Mechanical properties

Douglas *et al.* (1991) found that the strength of slag cement activated by lime and silica fume is higher than that obtained from activating with lime alone. Shi and Day (1993) reported that 6% hemihydrate gypsum is sufficient to activate the lime pozzolana cement. Cheng and Sarkar (1994) obtained a compressive strength of 75 MPa, when the slag was activated by 10% lime and 5% Na_2O by weight of slag. Singh and Garg (1995) produced blended cement by mixing anhydrite with granulated blast furnace slag, $Ca(OH)_2$, and small amounts of $Na_2SO_4.10H_2O$ and $FeSO_47H_2O$ as activators. The results indicate that the activation of granulated slag with the gypsum anhydrite and $Ca(OH)_2$ forms ettringite and tobermorite. Melo Neto *et al*. (2010)reportedthe compressive strength, shrinkage (autogenous and drying) and microstructure (porosity, hydrated products) of blast furnace slag (BFS) pastes activated with hydrated lime (5%) and hydrated lime (2%) plus gypsum (6%). Theycharacterized the paste mixture using powder X-ray diffraction (XRD), mercury intrusion porosimetry (MIP) and thermo-gravimetric analysis (TG/DTG). The results indicate that BFS activated with lime and gypsum (LG) larger amounts of ettringite when compared with BFS activated with lime (L). The presence of ettringite

and the higher volumes of macro-pores cause the compressive strength of BSF activated with hydrated lime plus gypsum to be smaller than that of BFS activated with lime.

2.5.3 Effects of admixtures

Douglas *et al.* (1991) found that the strength of slag cement activated by lime and silica fume is higher than that obtained from activating with lime alone. Bellman and Strak (2009) activated the blast furnace slag and prepared super-sulphate cement by mixing of 80-85% slag, $Ca(OH)_2$ and $CaCO_3$ instead of calcium sulphate. They accelerated the cement and studied the effect of accelerators such as calcium formate $Ca(COOH)_2$, calcium acetate $CaCH_2(COOH)_2$, calcium chloride ($CaCl_2$), sodium chloride (NaCl), calcium nitrate, calcium bromide with the range of (0.5-5)% by weight of cement on the compressive strength. The result indicates that the early strength of slag cement is increased from 6 to 16 MPa after the two days of addition of admixture and the final strength is increased from 36 to 53 MPa after 28 days.

2.6 HYDRATION PRODUCT AND MICROSTRUCTURE

Talling *et al*. (1981) and Shi and Day (1989) studied extensively on the alkaline activation of slag and the hydration products. The main hydration product was found to be C-S-H and hydrated calcium-alumina-silicate like C-A-S-H gel. This phase is different from that formed in the Portland cement in the early period of hydration and has a lower C/S ratio. The formation of other phases or hydrated compounds depends on the type and amount of the activator used, structure, and composition of the slag and curing conditions of hardening cement and concrete. Mehrotra (1982) analyzed the unhydrated and hydrated compound of mortar specimen of plaster of Paris activated slag cement by differential thermal analysis (DTA). DTA curve shows that unhydrated composition is

obtained as endothermal peak at 165 ^{o}C due to dehydration of plaster of Paris. After one week hydration, another small endothermic peakis obtained at 140 ^{o}C which may attribute to C-S-H. Stade (1989) reported that if the sodium amount is higher enough than the gel is named as sodium calcium silicate hydrate (NCSH). Shi *et al*. (1991) studied the hydration products of alkali activation of blast furnace slag, having detected the formation of CSH and xonotlite under autoclaving. Wang *et al.* (1994) activated the slag by NaOH and water-glass solution and hydration peak measured by DTA analysis. The endothermic peak at 90-110 is due to C-S-H (I) and at 130-170 ^{o}C,indicated the presence of Afm-type phase. These phases are obtained only when the slag was activated by NaOH. Singh and Garg (1995) produced blended cement, a mixtures of anhydrite with granulated blast furnace slag, Ca(OH), and small amounts of $Na_2SO_4.10H_2O$ and $FeSO_47H_2O$ as activators. Their results indicate that the activation of granulated slag with the gypsum anhydrite and $Ca(OH)_2$ to form ettringite and tobermorite. Wang and Scrivener (1995) examined the hydration products using XRD, DTA andmicrostructural development; they confirmed that CSH gel is the main reaction product of alkali activation of blast furnace slag, with low C/S ratio. That is conceivably due to the high pH solutions, which favors low Ca concentrations and high Si concentrations. The authors reported that formation of crystalline phase of hydrotalcite type when slag is activated with either NaOH or water-glass; and crystalline phase of AFm type in slag activated with NaOH. Hong and Glasser (1999, 2000) reported that the amount of sodium inside the C-S-H phase increases with the decrease of C/S ratio. Song *et al.*(1999, 2000) reported that the main reaction product of blast furnace slag during hydration is C-S-H

gel with minor amounts of hydrotalcite, which was detected by XRD analysis. These are formed only when the slag attains a high level of hydration.

Puertas *et al.*(2000) studied the hydration products in the mixtures of fly ash and blast furnace slag activated by alkali.They reported that CSH gel was the main reaction product, they also identified the formation of hydrotalcite ($Mg_6Al_2CO_3(OH)_{16}\cdot 4H_2O$), pirssonite ($Na_2Ca(CO_3)\cdot 2H_2O$), as well as calcite, however, they did not find any alkaline alumino-silicate phase. Kim and Hong (2001) observed that the ion concentration change of liquid phase during hydration was different depending on the activator and the hydration time. Zhihua *et al*. (2000, 2003) studied the alkali activation of blast furnace slag mixed with red mud.They have investigated on the hydration products of this cement at ambient temperature by means of XRD, IR, TG-DTA, TEM, and EDXA. They detected the hydration product C-S-H gel with low Ca/Si ratio, neither $Ca(OH)_2$ and AFt, which are usually present in the hardened Portland cement paste, nor zeolite-like products. Brough and Atkinson (2002) studied the hydration products of activated blast furnace slag, and reported that XRD analysis shows no crystalline products, however, the SEM analysis reveal the formation of hydrotalcite after one month and these phases are distinctly visible after one year.Escalante-Garcēa *et al.*(2003) studied hydration products of blast furnace slag mortars with 10% replacement by silica wastes. Silicaand the binder were activated by 6%Na_2O by weight, equivalent of NaOH and water glass. They obtained CSH gel and hydrotalcite as reaction products by SEM and X-ray element analysis. Puertas and Fernandez-Jimenez (2003) analyzed the hydration products of alkali-activated mixtures of blast furnace slag and fly ash. They reported two types of CSH gel, calcium silicate hydrate aluminium with sodium in its structure and also an

alkaline alumino silicate hydrate with a three-dimensional structure due to the fly ash activation. Puertas *et al*. (2003) analyzed the phases formed in blast furnace slag activated with NaOH, by XRD analysis and they reported the presence of hydrotalcite ($Mg_6Al_2CO_3(OH)_{16}\cdot 4H_2O$), calcite ($CaCO_3$) and CSH. The authors have observed that activator NaOH leads to reaction products with the molar ratio Al/Si higher than that obtained with the activator NaOH mixed with waterglass. Gruskovnjak *et al.* (2008) activated the two different slag with 15% natural anhydrite and 0.5% KOH by weight and also $Al_2(SO_4)_3.16H_2O$ and Ca(OH). The hydration products formed during the hydration inactivated slag is determined by XRD and TGA. They observed supplementary ettringite in addition to $Al_2(SO_4)_3.16H_2O$ and $Ca(OH)_2$in the hydration product. Bezerra *et al* .(2012) reported that the addition of crystalline silica, in the form of silica flour or silica sand modifies the trajectory of this natural conversion process and transforms C-S-H, at 120 ^oC, into tobermorite, which shows low permeability and high resistance to compression. At the increased temperature, new transformations occur at 150 ^oC, with the conversion of tobermorite into xonotlite ($Ca_6Si_6O_{17}(OH)_2$).

2.7 OPTIMIZATION OF RAW MATERIALS

Kunhanandan Nambiar *et al.* (2006) developed the empirical model for compressive strength and density of foam concrete through statistically designed experiments and response surface plots which helped in visually analyzing the influence of factors on the responses. The relative influence of fly ash replacement on the strength and density of foam concrete is studied by comparing it with mixes without fly ash and brought out that replacement of fine aggregate with fly ash will help in increase the strength of foam concrete at lower densities allowing high strength to density ratio.

Confirmatory tests have shown that the relation developed by statistical treatment of experimental results can act as a guideline in deciding the mix proportion of foam concrete. Many researchers have used the response surface methodology in optimizing various parameters in their investigations. Maghsoud *et al.* (2008) used techniques response surface method and genetic algorithm for optimization of cement clinkering process. The result indicates that both techniques are capable, but the response surface is better than the genetic algorithm. Timur Cihana *et al.* (2013) used various methods for process improvement, development, and optimization. They reduced the number and the variations of effect-parameters by using response surface methodology. They determined the influence levels of the main and interaction terms of effect variables using 27^3 fractional factorial designs in order to reduce the number of simultaneously controllable variables. They determined the quadratic terms using D-Optimal design, and response surface graphics were plotted. Serdar (2013) studied the effects of binary and ternary combination of ground granulated blast furnace slag (GGBFS), fly ash, and silica fume on compressive strength, flexural strength of OPC mortars. They have determined optimum replacement ratios of fly ash and silica fume in order to increase the quality of alkali activated slag mortars by Response Surface Method (RSM). The optimization of these admixtures was done using response surface method.

2.8 POROSITY AND PORE SIZE DISTRIBUTION STUDY

Shi and Day (1996) observed the relationships between compressive strength and the mercury intrusion porosity of alkali-activated slag and Portland cement mortars. The distribution of pore size of alkali-activated slag mortars is significantly different from that which Portland cement mortars. This may be due to the difference in the nature of their

main hydration products. Raymond and Cook (1999) performed porosity and pore size distribution on 92 hardened cement paste specimens of water/cement mercury porosimetry, they observed that longer curing times and lower w/c ratios resulted in smaller total porosities. Sharath *et al.* (2012) studied the porosity and pore size distribution by mercury intrusion porosimetry (MIP) of concrete specimens under the elevated curing regime.The result observed that there is an increase in the number of pores in the microstructureof concrete with an increase in curing temperature.

2.9 CRITICAL OBSERVATIONS

Based on the extensive literature review, it is observed that most of the studies are concentrated on the activation of slag by alkalis or sulphates. The available literature on slag activated by combination of alkaline and sulphate activation or lime and plaster of Paris is very limited and no attempt has been made to optimize the raw material compositions by using computational algorithm. Further, it shows that a limited attention has been paid to establish the influence of admixtures on the strength and microstructure. Again, it shows that several attempts have already been made to study the effect of high temperature curing on the strength only for alkali activated slag cement and ordinary Portland cement not in lime activated slag cement nor in combination of sulphate and alkaline activation of slag cement.Almost no literature is available on the effects of high temperature and pressure curing on strength of lime (alkaline earth metal) activated slag cement. Limited attempt has been made to establish a correlation between the mechanical strength and the hydration products, microstructure as well as morphology of the cured specimens.

2.10 OBJECTIVES AND SCOPE

The objective of the present research is to prepare and characterize a sustainable binding material using primarily the industrial byproducts as an alternate to Portland cement.

The scope of the research is as follows:

- To prepare and characterize a cementing material by activation of industrial by-products like granulated blast furnace slag using activators such as lime and plaster of Paris to have comparable physical, chemical and mechanical properties like that of OPC.
- To optimize the raw material proportions of lime activated slag cement using response surface plot and generalized reduced gradient technique.
- To study the effect of mineral and chemical admixtures as well as curing conditions on hydration products, morphology, microstructure and strength of lime activated slag cement.
- To correlate the mechanical strength of specimens with the hydration products, morphology and microstructure of specimens.

CHAPTER III
EXPERIMENTAL WORK AND METHODOLOGY

3. EXPERIMENTAL WORKAND METHODOLOGY

3.1INTRODUCTION

The main objective of the present study is to assess the suitability of a cementing material prepared by activating the ground granulated slag with lime and plaster of Paris as an alternate cementing material to ordinary Portland cement. This will also avert the exhaustion of natural resources, enhancement of the usage of waste materials, safe guarding global environment, and overall a change over from the mass-production, mass-consumption, mass waste society to a zero-emission society. This chapter introduces the details of raw material used, their characterization, parameters investigated, detail procedure of experimental works and the methodologies adopted.

3.2 DETAILS OF TESTS CONDUCTED

An extensive laboratory testing program was undertaken to investigate the physical, chemical, and mechanical properties of lime-slag-plaster of Paris mixes. The total work can be broadly divided into two phases. In the first phase of investigation the physical properties such as consistency, setting timeand soundness for different mixes of lime-slag-plaster of Paris were determined. This also includes the study on hydration products and microstructure using several techniques like XRD, SEM,and FTIRtestscorresponding to initial and final setting time of different mixes. In the second phase of tests the mechanical property, microstructure, porosity, and drying shrinkage of mixes were determined. This is achieved in three series of tests. In the first series of tests, the compressive strength of 36 mixes of slag-lime-plaster of Paris was determined. Based

on which, the optimization of raw materials was done for different curing periods adopting the response surface plot and generalized reduced gradient technique. The optimum composition of raw materials is termed as reference sample (D5), which contains slag and lime in ratio of 80:20 and plaster of Paris of 5% over the combined mass of slag and lime. In the second series of tests, the effects of admixtures (mineral and chemical admixtures) on the compressive strength, microstructure, porosity, and drying shrinkage of reference sample were studied. In the third series of tests, the effects of curing temperature and curing condition on the compressive strengthand microstructure of reference sample with mineral admixtures were studied. After that correlation has been established between chemical bonds, hydration products, microstructure and morphology with strength of the mix. The details of tests conducted in this experimental program are summarized in Table 3.1.

Table 3.1 Details of experimental program

i	**Aim**	**Evaluation of physical and chemical properties of slag-lime-POP mixes**
	Apparatus used and parameters evaluated	Vicat apparatus (Consistency and setting time) Le-Chatelier apparatus (Soundness) XRD (Chemical compounds) FTIR (Chemical bonds) SEM (Microstructure and morphology)
	Raw materials and its mix proportions	Slag (95, 90, 85, 80, 70 and 60%) Lime (5, 10, 15, 20, 30, and 40%) POP (0%, 1%, 1.5%, 2%, 2.5%, 5%, and 10%) *Note: *POP is taken over the combined mass of lime and slag*
	Number of tests conducted and repeatability	Consistency (42 mix proportions, 3observations each) Initial setting time (42 mix proportions, 3 observations each) Final setting time (42 mix proportions, 3 observations each) Soundness (42 mix proportions, 2 observations each)
	Results presented in Chapter	Chapter: 4

ii	**Aim**	**Study of mechanical property, microstructure, porosity and drying shrinkage of slag-lime-POP mixes and optimization of raw material proportions**
	Apparatus used and parameters evaluated	Compression testing equipment (Compressive strength) XRD (Chemical compounds) FTIR (Chemical bonds) SEM (Microstructure and morphology) TGA (Mass loss in terms of chemical compounds) DSC (Chemical compounds) Mercury Intrusion porosimeter (Porosity and pore size distribution) Length comparator (Drying shrinkage)
	Mix proportions	Slag (95, 90, 85, 80, 70 and 60%) Lime (5, 10, 15, 20, 30, and 40%) POP (1%, 1.5%, 2%, 2.5%, 5%, and 10%) Note: *POP is taken over the combined mass of lime and slag
	Number of mixes and number of samples tested	Compressive strength (36 mix proportions, 540 samples) Porosity and Pore size distribution (1 mix proportion, 3 samples) Drying shrinkage (1 mix proportion, 6 samples)
	Curing condition	Curing temperature: 27 ^{o}C (water curing) Curing period: 3, 7, 28, 56 and 90 days
	Results presented in chapter	Chapter: 5
iii	**Aim**	**Study the effects of mineral admixtures on compressive strength, microstructure, hydration products, porosity and drying shrinkage behaviour**
	Apparatus used and parameters evaluated	Compression testing equipment (Compressive strength) XRD (Chemical compounds) FTIR (Chemical bonds) SEM (Microstructure and morphology) TGA (Mass loss in terms of chemical compounds) DSC (Chemical compounds) Mercury Intrusion porosimeter (Porosity and pore size distribution) Length comparator (Drying shrinkage)
	Mix proportion	Reference specimen (D5) with admixtures in different proportions (as listed) Flyash: 0, 10, 20, 30, 40% Silica fume: 0, 5, 10 and 15% Glass powder: 0, 5, 10 and 15% OPC: 0, 5 and 10%

	Curing condition	Curing temperature: 27 ^{o}C (water curing) Curing period: 3, 7, 28, 56 and 90 days
	Number of samples tested	Compressive strength (198 samples) Porosity and Pore size distribution (6 samples) Drying shrinkage (6 samples)
	Results presented in chapter	Chapter: 6
iv	**Aim**	**Study the effects of chemical admixtures on compressive strength, microstructure, and hydration products**
	Apparatus Used and Parameters evaluated	Compression testing equipment (Compressive strength) XRD (Chemical compounds) FTIR (Chemical bonds) SEM (Microstructure and morphology) TGA (Mass loss in terms of chemical compounds) DSC (Chemical compounds)
	Chemical admixture used and mix proportion	Calcium formate, calcium acetate, calcium nitrate, sodium hydroxide, and sodium meta silicate (0, 0.5, 1, 2 and 4%)
	Curing condition	Curing temperature: 27 ^{o}C (water curing) Curing period: 3, 7, 28, 56 and 90 days
	Number of samples tested	Compressive strength (780 samples)
	Results presented in chapter	Chapter: 6
v	**Aim**	**Study the effects of curing temperature on compressive strength and microstructure for slag-lime-POP mixes**
	Apparatus used and parameters evaluated	Compression testing equipment (Compressive strength) XRD (Chemical compounds) FTIR (Chemical bonds) SEM (Microstructure and morphology) TGA (Mass loss in terms of chemical compounds) DSC (Chemical compounds)
	Mix proportion	Slag (80%) Lime (20%) POP (1%, 1.5%, 2%, 2.5%, 5%, and 10%) Note: *POP is taken over the combined mass of lime and slag
	Curing Condition	Curing temperature: 27, 45, 60 and 75^{o}C Water curing) Curing period: 3, 7, 28, 56 and 90 days
	Number of samples tested	Compressive strength (270 samples)
	Results presented in chapter	Chapter: 7

vi	**Aim**	**Study the effects of autoclave curing conditions on compressive strength and microstructure for slag-lime-POP mixes**
	Apparatus used and parameters evaluated	Cement autoclave (Curing of specimens) Compression test (Compressive strength) XRD (Chemical compounds) FTIR (Chemical bonds) SEM (Microstructure and morphology) TGA (Mass loss in terms of chemical compounds) DSC (Chemical compounds)
	Mix proportion	Reference specimen (D5) with flyash or silica fume Fly ash: 0, 10, 20, 30,and 40% Silica fume: 0, 5, 10 and 15%
	Curing condition	Water curing: Curing temperature: 27 ^{o}C Curing period: 3, 7, 28, 56 and 90 days Autoclave curing: Curing temperature: 210 ^{o}C Pressure: 2MPa Curing time: 1, 2, 3 and 4h
	Number of samples tested	Compressive strength (84 samples)
	Results presented in chapter	Chapter: 7

3.3 MATERIALS USED

For this work, raw materials like ground granulated blast furnace slag; lime and plaster of Paris were used to prepare the binding material. Sand is used for the preparation of mortar specimens. Fly ash, silica fume, glass powder are used as mineral admixtures and ordinary Portland cement as additives. Calcium acetate, calcium formate, sodium meta-silicate, sodium hydroxide, and calcium nitrate were used as chemical admixtures. The physical properties and chemical compositions for all the materials are given in Table 3.2 and Table 3.3 respectively.

3.3.1Ground Granulated Blast Furnace Slag (GGBFS)

The blast furnace slag used in this work was collected from Rourkela Steel Plant (RSP). The slag was sun dried and mixed thoroughly to bring homogeneity in the sample.

The same was ground in a ball mill to a Blaineôs fineness of 410 m^2/kg. The surface morphology of slag is rough and angular-shaped as shown in Figure 3.1(a). The characterization of blast furnace slag was done by XRD analysis; from this test result it is observed that the slag is purely glassy material. The XRD pattern of slag sample is shown in Figure 3.2(a).

3.3.2 Lime

Lime was procured from the local market. It was air dried, passed through 150 micron sieve and mixed thoroughly in dry condition. Then lime was stored in air tight container for subsequent use. From the SEM image as shown in Figure 3.1(b), it is observed that the particles of lime are irregular in shape. The XRD test result of lime sample is shown in Figure 3.2(b). From the figure it is observed that the predominantconstituents are calcium oxide and calcium carbonate.

3.3.3 Plaster of Paris

Plaster of Paris was procured from the local market. It was air dried and mixed thoroughly in dry condition. It was passed through 150 micron sieve and stored in airtight container for subsequent use. The microstructure of Plaster of Paris is irregular in shape as shown in Figure 3.1(c). The XRD analysis result for plaster of Paris sample is shown in Figure 3.2(c). From the figure it is observed that calcium oxide, calcium sulphate, silicon oxide, and aluminum oxide are mainly present in plaster of Paris.

3.3.4 Mineral admixtures

Mineral admixtures such as fly ash, silica fume, glass powder and OPC are used in the present study.

3.3.4.1 Fly ash

The fly ash used in the present investigation was collected from the Rourkela Steel Plant, Sundargarh, Odisha. The fly ash had grayish white colour. The tests on fly ash were carried out as per IS: 1727-1967. The specific gravity of fly ash was found to be 2.3. The SEM image for fly ash as shown in Figure 3.1(d) reveals that most of the particles are spherical structure with few irregular particles. The XRD analysis result for fly ash is shown in Figure 3.2(d) from which it is observed that the predominant constituents are silicon oxide, aluminum oxide, and iron oxide.

3.3.4.2 Silica fume

The silica fume was collected from the Corniche India Ferro Silicon Alloy Mumbai. The specific gravity of silica fume was 2.21. The value of Blaineôs specific surface area of this material was 17256 m^2/kg. The physical, chemical, morphological, and mineralogical data for the silica fume is presented in the following sections. From the SEM image as shown in Figure 3.1(e), it is observed that the particles of silica fume are spherical in shape. The crystalline peaks of SiO_2 are prominent in the XRD images shown in Figure 3.2(e).

3.3.4.3 Glass powder

The glass powder used in the present investigation was prepared from broken shards of waste glass. The specific gravity of glass powder was 2.65. The Blaineôs specific surface area value of these materials was 210 m^2/kg. The physical, chemical,morphological, and mineralogical data for the glass power is presented.

3.3.4.4 Ordinary Portland cement (OPC)

In this study ordinary Portland cement is used as an additive with the raw materials. The ordinary Portland cement used in this experiment was collected from UltraTech Company, Kolkata. The specific gravity of ordinary Portland cement was 3.17. The Blaineôs specific surface area value of this material was 257 m^2/kg.

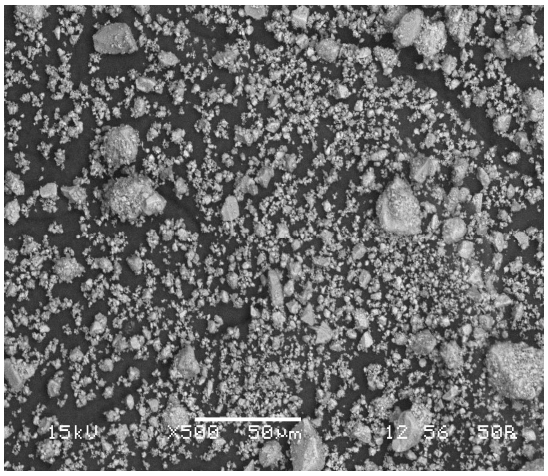

(a)GGBFS

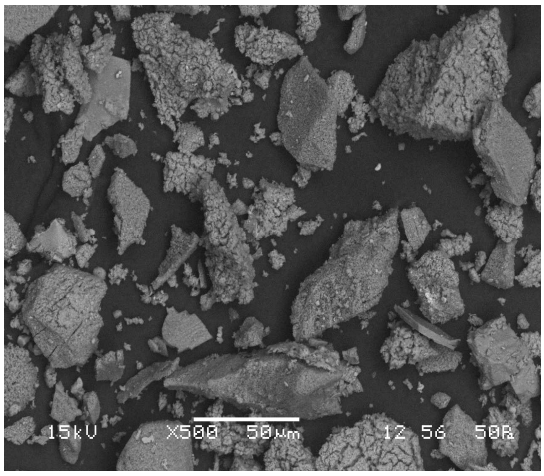

(b) Lime

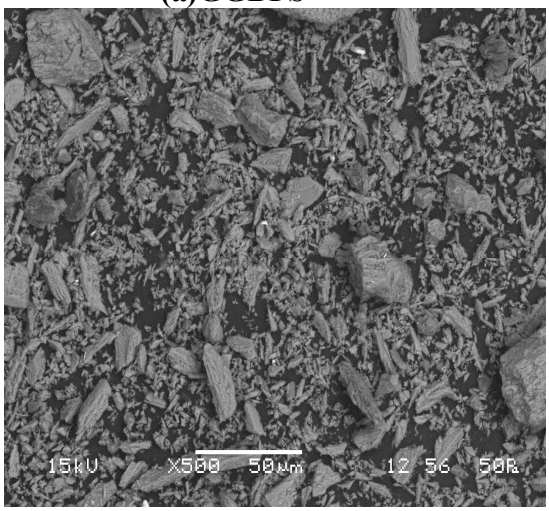

(c) Plaster of Paris

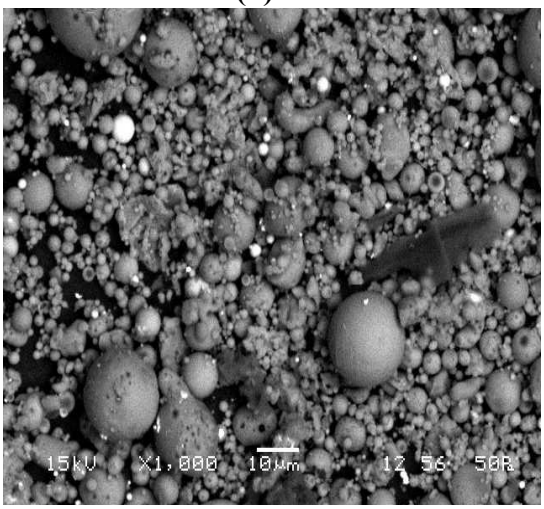

(d) Fly ash

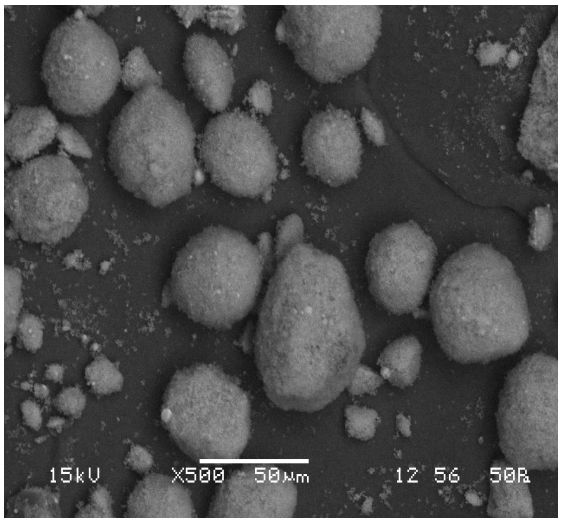

(e) Silica fume

Figure 3.1 Scanning Electron Micrograph (SEM) images of the raw materials

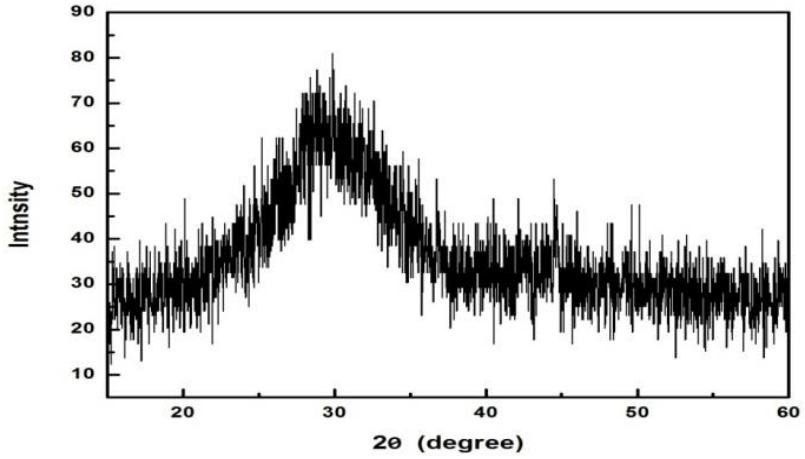

(a) GGBFS

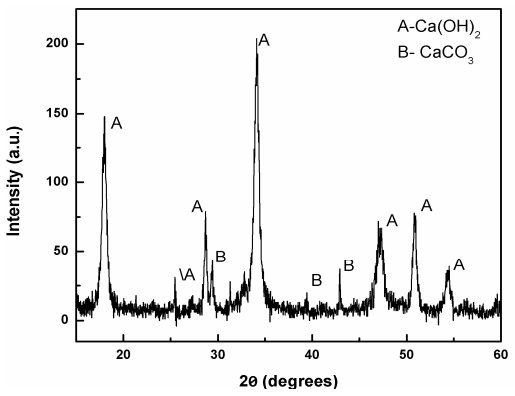

(b) Lime

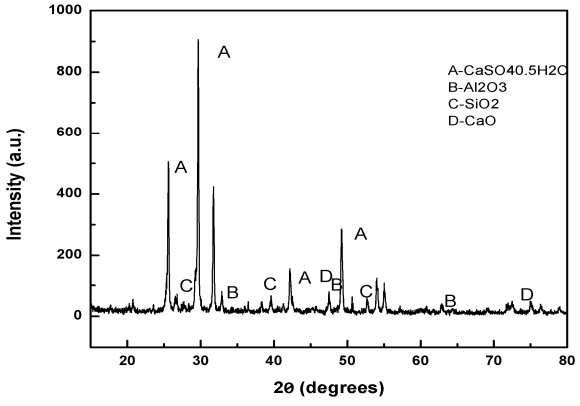

(c) Plaster of Paris

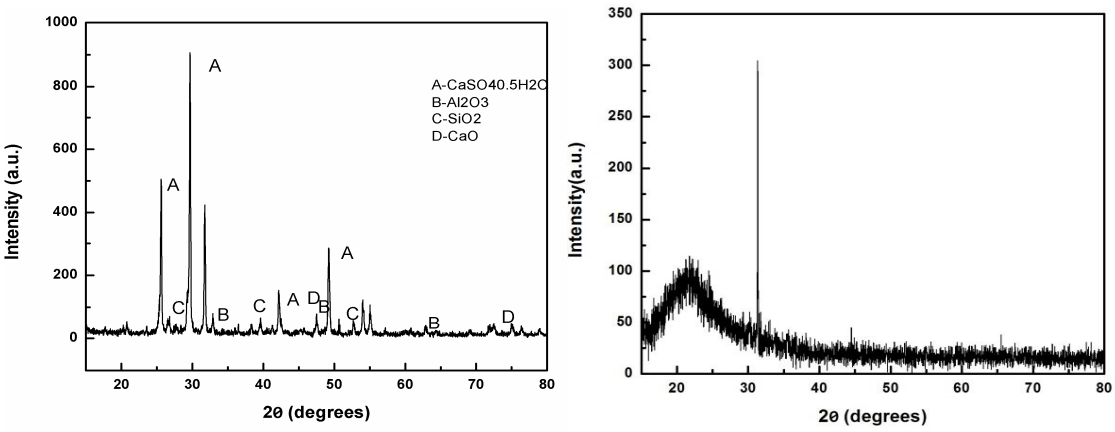

(d) Fly ash **(e) Silica fume**

Figure 3.2 X-ray diffraction (XRD) patterns of the raw materials

Table 3.2 Physical Properties of raw materials

Sample	Fineness (m^2/kg)	Specific gravity
Ground granulated Blast furnace Slag	410	2.94
Lime	-	2.49
Plaster of Paris	-	-
Silica fume	17256	2.21
Fly ash	334	2.30
OPC	257	3.17
Glass Powder	210	2.65

3.3.5 Chemical admixtures

Different types of chemical admixtures such as calcium acetate, calcium formate, sodium meta-silicate, sodium hydroxide and calcium nitrate were used in the experimental program. These were collected from local chemical shop.

Table 3.3 Chemical compositions of raw materials

Composition (%)	Slag	Plaster of Paris	Lime	Fly ash	Silica fume	OPC
MgO	9.52	1.92	2.47	1.7	1.04	0.86
Al_2O_3	21.06	1.13	0.98	28.1	1.48	5.57
SiO_2	30.82	0.916	2.75	53.6	88.2	19.3
K_2O	1.04	0.661	0.9	1.97	3.95	0.76

P_2O_5	-	0.58	-	1.72		-
CaO	32.02	41.45	90.26	2.65	1.92	63.54
Fe_2O_3	1.37	0.852	0.381	1.8	0.98	3.46
Na_2O	0.088	1.55	0.52	0.5	-	0.13
MnO	0.14	-	-	0.3	-	-
TiO_2	1.04	-	-	0.85	-	-
SO_3	0.66	39.88	-	-	-	2.91
Loss on Ignition	1.81	6.25	0.84	6.5	1.18	3.59

3.3.6 Sand

Ennore sand confirming to Indian Standard IS 650-1991 was used for preparing the mortar specimens for compressive strength test.

3.4 EXPERIMENTAL PROCEDURE

The experimental procedures undertaken in the present study involves several experiments, conducted to obtain various properties. The physical properties tests such as consistency test, setting time test and soundness test of the mixes were determined. The mechanical property that is compressive strength was obtained by conducting uniaxial compression test. The raw material optimization was done on the basis of compressive strength of different mix proportion on hit and trial basis following response surface plot by adopting generalized reduced gradient method. The hydration products and formation of chemical bonds were studied using several techniques like XRD, SEM, FTIR, TGA and DSC analysis. Also, porosity and drying shrinkage were found out. The detailed experimental procedures adopted in this study are presented in the following sections.

3.4.1 Determination of physical properties

The physical properties such as consistency, setting time and soundness of the mixes were determined following Indian standard codes of practice and the detailed experimental procedure is discussed in the following sections.

3.4.1.1 Determination of normal consistency

The normal consistency of 42 mixes of slag-lime-POP was determined following IS code 4031 -1988 (part 4). The lime content in the mix was varied as 5, 10, 15, 20, 30 and 40%; and the POP content as 0, 1, 1.5, 2, 2.5, 5 and 10%. The plaster of Paris content is taken over the combined mass of lime and slag. The test results are presented in Table 3.4.

Table 3.4 Consistency of slag-lime-POP mixes

Lime content (%)	Consistency (%)						
	Plaster of Paris content (%)						
	0	1	1.5	2	2.5	5	10
5	28.89	28.89	29.24	29.24	29.25	29.25	29.42
10	29.24	29.24	29.60	29.60	29.62	29.78	29.90
15	29.60	29.96	29.96	29.96	29.96	30.32	30.5
20	29.60	30.32	30.32	30.32	30.32	30.74	31.42
30	33.17	34.24	34.24	34.24	34.24	34.24	34.42
40	36.20	36.90	37.10	37.10	37.20	37.20	37.4

3.4.1.2 Determination of initial and final setting time

In order to place mortar and concrete in position conveniently, it is necessary that the initial setting time of the binder should not be too quick and after it has been laid the hardening should be rapid so that the structure can be made as possible. To determine the setting time of slag-lime-POP mixes, pastes were prepared by adding water equal to 85% of normal consistency of cementing powder. The paste was filled in Vicat mould immediately after 3 minutes of through mixing and surface was made smooth within 5 minutes as shown in Figure 3.3. The initial setting time was determined as the period elapsed between the time when water was added to cement and time at which the square needle fail to pierce the test sample about 5 mm from bottom and the final setting time

was the time period elapsed between the time when water was added to the mix and time at which the annular attachment of needle fails to pierce the test sample. All these tests were conducted as per IS: 4031 (Part 5)-1988.

The proportions of lime and POP in the slag-lime-POP mixes were varied as 5, 10, 15, 20, 30 & 40% and 0, 1, 1.5, 2, 2.5, 5, 10% respectively. Thus 42 different mixes were prepared and tested. Initial and final setting times for different mixes are presented in Tables 3.5 and 3.6 respectively. In addition to this, the effect of borax on setting time was studied by adding 0.2, 0.4, 0.6, 0.8, and 1% borax to the mixes containing 20% lime and different percentages of plaster of Paris as mentioned above. The test results are presented in Tables 3.7 and 3.8.

Figure 3.3Vicat apparatus

Table 3.5 Initial setting time of slag-lime-POP mixes

Lime content (%)	Initial setting time (min)						
	Plaster of Paris content (%)						
	0	1	1.5	2	2.5	5	10
5	271	269	47	47	24	18	13

10	270	236	30	29	20	17	12
15	239	150	26	24	16	16	12
20	235	109	21	21	14	14	11
30	214	35	20	20	14	13	11
40	163	19	19	18	12	12	10

Table 3.6 Final setting time of slag-lime-POP mixes

Lime content (%)	Final setting time (min)						
	Plaster of Paris content (%)						
	0	1	1.5	2	2.5	5	10
5	540	495	480	470	310	270	79
10	533	470	450	430	290	266	74
15	493	441	424	410	251	236	72
20	478	370	350	320	219	230	72
30	442	361	320	310	218	181	71
40	375	275	230	280	205	170	55

Table 3.7 Initial setting time of slag-lime-POP mixes with borax

Borax content (%)	Initial setting time (min)					
	Plaster of Paris content (%)					
	1	1.5	2	2.5	5	10
0	109	21	21	14	13	11
0.2	119	54	37	30	21	19
0.4	155	106	100	96	27	23
0.6	160	130	121	109	89	63
0.8	171	164	153	150	100	67
1.0	291	199	187	185	118	99

Table 3.8 Final setting time of slag-lime-POP mixes with borax

Borax content (%)	Final setting time (min)					
	Plaster of Paris content (%)					
	1	1.5	2	2.5	5	10
0	370	350	320	230	219	71
0.2	376	370	361	345	262	209
0.4	382	375	367	354	279	245
0.6	398	379	372	366	289	279
0.8	406	393	388	370	307	287
1.0	415	398	390	375	314	295

3.4.1.3 Determination of soundness

To measure the excess of free lime and magnesia present in the binder, soundness test was conducted for different mixes as per IS 4031-1988 (part-3) using Le-chatelier apparatus (Figure 3.4). The mix proportions taken for these tests are the same as mentioned for setting time tests. The lightly oiled mould was placed on a lightly oiled glass sheet and it was filled with cement paste formed by gauging cement with 0.78 times the water required to give a paste of standard consistency following IS: 4031 (Part 4)-1988. The mould was covered with another piece of lightly oiled glass sheet, a small weight was placed on this covering glass sheet, and immediately the whole assembly was submerged in water at a temperature of 27 ± 2 ^{o}C and kept for 24 hours. The distance separating the indicator points to the nearest 0.5 mm was measured. Again the mould was submerged in water at the temperature prescribed above. The water was brought to boiling, with the mould kept submerged, in 25 to 30 minutes, and kept it boiling for three hours. The mould was then removed from the water, allowed to cool and the distance between theindicator points was measured. The difference between thesetwo measurements indicates the expansion ofthe cement. For each mix 2numbers of observations were taken and the average of these values is presented in Table 3.9.

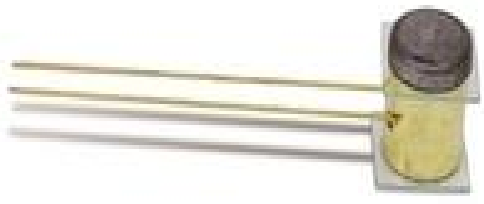

Figure 3.4 Le-chatelier apparatus

Table 3.9 Soundness of slag-lime-POP mixes

Lime content (%)	Soundness (mm)						
	Plaster of Paris content (%)						
	0	1	1.5	2	2.5	5	10
5	2	2	2	1.5	1	1	1
10	2	2	2	1.5	1	1	1
15	2	2	2	1.5	1	1	1
20	2	2	2	1.5	1	1	1
30	2	2	2	2	1	1	1
40	2	2	2	2	2	2.5	3

3.4.2 Determination of mechanical properties

The mechanical property that is compressive strength of slag-lime-plaster of Paris mixes was determined following IS: 4031 (Part 6&7)-1988. The detailed test procedure is given below.

3.4.2.1 Compressive strength

To determine the compressive strength, 1 part of the binder was mixed with 2.5 parts of standard sand. The binder and sand were mixed for one minute in dry state and then required amount of water was added and the mixing continued for another 3 minutes in mechanical mixture machine. The cubical test specimens of 50 x50 x 50 mm size were prepared and these specimens were cured in water at an average temperature of 27 ^{o}C. The compressive strength of the samples was determined in uniaxial compression testing machine after 3, 7, 28, 56 and 90 days of curing. For each mix proportion and each curing period, three identical specimens were prepared and the average of the strengths was reported as the compressive strength of the mix. The apparatus used for the preparation of test specimens and testing the mortar cubes are shown in Figure 3.5.

(a) Cubical specimen

(b) Cubical specimen

(c) Mixture machine

(d) Vibrating table

(e) Compression testing machine

Figure 3.5 Detailed arrangements for mortar specimen preparation with testing facilities

Table 3.10 Mix proportions and compressive strength of mixes

Mix designation	Mix proportions (%)			Compressive strength (MPa)				
	Slag	Lime	POP	3 Days	7 Days	28 Days	56 Days	90 Days
A1	95	5	1	9.24	15.38	18.78	22.19	23.67
B1	90	10	1	12.03	16.56	22.36	24.65	26.53
C1	85	15	1	16.35	18.96	22.98	26.76	28.45
D1	80	20	1	17.96	20.12	24.23	31.03	33.62
E1	70	30	1	17.34	17.91	21.81	29.92	33.26
F1	60	40	1	16.22	16.78	20.14	27.75	27.99
A1.5	95	5	1.5	13.38	18.95	22.76	24.78	26.35
B1.5	90	10	1.5	13.23	17.69	23.75	26.65	28.52
C1.5	85	15	1.5	18.74	20.69	25.67	28.64	30.68
D1.5	80	20	1.5	20.14	21.81	27.36	33.23	35.65
E1.5	70	30	1.5	18.08	19.67	24.33	32.08	34.32
F1.5	60	40	1.5	17.62	18.18	22.75	29.68	31.23
A2	95	5	2	18.18	22.65	26.58	30.35	32.86
B2	90	10	2	18.64	21.65	26.89	33.86	35.68
C2	85	15	2	20.42	23.64	28.65	33.67	35.98
D2	80	20	2	21.54	24.12	29.65	34.8	37.86
E2	70	30	2	19.02	20.67	26.57	33.85	36.84
F2	60	40	2	17.99	19.86	24.98	31.68	32.98
A2.5	95	5	2.5	19.52	23.56	27.5	31.78	34.56
B2.5	90	10	2.5	19.58	23.82	28.13	34.87	36.44
C2.5	85	15	2.5	20.97	24.65	29.98	35.64	37.86
D2.5	80	20	2.5	21.81	24.96	30.98	37.15	40.14
E2.5	70	30	2.5	19.86	22.13	27.21	34.65	37.32
F2.5	60	40	2.5	18.86	21.36	25.98	32.86	34.32
A5	95	5	5	20.32	24.33	30.13	35.19	37.69
B5	90	10	5	20.54	24.62	31.12	37.89	39.67
C5	85	15	5	22.37	26.48	32.86	39.77	41.71
D5	80	20	5	23.77	27.14	33.67	39.97	42.21
E5	70	30	5	20.14	23.98	28.96	35.67	37.68
F5	60	40	5	19.58	22.98	27.98	34.69	35.86
A10	95	5	10	21.15	24.82	31.23	36.17	38.67
B10	90	10	10	21.36	25.18	31.94	39.18	41.36
C10	85	15	10	22.93	26.58	33.69	40.62	42.68
D10	80	20	10	24.62	27.69	34.59	40.95	43.95
E10	70	30	10	21.17	24.67	29.89	36.68	37.94
F10	60	40	10	20.56	23.68	28.89	35.78	36.31

3.4.3 Optimization of raw material proportions

The optimum composition of the raw materials was determined by mixing the raw materials in different proportions and evaluating the compressive strength of mortar in accordance with IS: 4031 (Part 6) 1988. In this series 36 different mixes of slag-lime-plaster of Paris were taken and 540 numbers of samples were tested.Based on the experimental values obtained from compressive strength tests, optimization of raw material proportions was done using response surface plot and the generalized reduced gradient technique. Table 3.10 presents the compressive strength of different mixes at different curing period.

3.4.3.1 Response surface method (RSM)

Response Surface Methodology (RSM) is a collection of statistical and mathematical technique used for developing response models and optimizing process [Myers Raymond H, Montgomery D C, 2002]. This method was originally developed to model experimental responses (Box and Draper, 1987), and then shifted to model numerical analysis also. The approximation of the response function in relation with inputs in the form of polynomials with optional transformation of inputs and/or response is called response surface methodology. Due to the existence of a complex interaction of inputs (x_1=lime % and x_2=POP %) with the response such as compressive strength, a response surface model of third degree polynomial is considered. The general third-degree polynomial response surface model for two predictive variables is represented as:

$$F(x_1, x_2) = p_{00} + p_{10}.x_1 + p_{01}.x_2 + p_{20}.x_1^2 + p_{11}.x_1.x_2 + p_{02}.x_2^2 + p_{30}.x_1^3 + p_{21}.x_1^2.x_2 + p_{12}.x_1.x_2^2 + p_{03}.x_2^3 \quad \text{é .é .(3.1)}$$

Where, p_{00}, p_{10}, p_{01}, p_{20},é ,p_{03} are the regression coefficients to be estimated from the data and $F(x_1, x_2)$ is the dependent variable for given independent variables x_1 and x_2. A statistical RSM has been used to obtain the optimum values of lime and plaster of Paris by maximizing the response function such as compressive strength by adopting nonlinear generalized reduced gradient (GRG) method in excel solver. This method was developed by Leon Lasdon and the details of which are presented by Leon Lasdon *et al.* (1973).

3.4.4 Chemical bonds, hydration products, micro structure and morphology

The chemical bonds, hydration products, microstructure and morphology of few selected samples were studied using several techniques like XRD, SEM, FTIR, TGA and DSC analysis and the above mentioned analysis process are described in the following sections.

3.4.4.1 X-ray diffraction (XRD)

The X-ray diffraction (XRD) tests were used to determine the hydration peaks that appeared in the pastes at different curing periods. This is performed by using Philips X' PERT System X-Ray diffractometer and shown in Figure.3.6. After specified curing period, representative samples were collected and soaked in anhydrous ethanol to stop further hydration. After this, mortar pieces were ground in mortar pestle to sizes less than 75 micron before being used in XRD analysis. The XRD test was done to determine the phases that appeared in the hydrated paste and mortar. This was performed by using Philips X' PERT System X-Ray diffractometer. The powder sample was affixed to the sample holder and the upper surface of the sample was smeared by a glass slide to get a smooth and uniform surface. The specimen was then placed in the diffractometer and scanned in a continuous mode from 7^0-70^0 with a scanning rate of 0.05 degree/sec.

Figure 3.6 Philips X' PERT System X-Ray Diffractometer with sample holder

3.4.4.2 Scanning electron microscope (SEM)

The morphology and microstructure in the paste were studied with the help of SEM analysis. Microscopic studies were undertaken to examine the morphology and microstructure of hydrated specimens. These were done by a JEOL 6480LV SEM, equipped with an energy dispersive X-ray detector of Oxford data reference system as shown in Figure 3.7. The powdered as well as broken samples were loaded and fixed in the sample holder using a carbon tape which is further coated with a thin layer of electrically conductive platinum material. Micrographs were taken at accelerating voltage of 20 kV for the best possible resolution from the surface.

Figure 3.7 JEOL-JSM-6480 LV

3.4.4.3 Fourier transform infrared (FTIR)

The formation of different chemical bonds during the hydration process was studied in Fourier Transform Infrared (Perkin Elmer, USA/RX-I FTIR-TM series) equipment with a pellet-holding accessory. After a specified period of setting/hydration, representative samples were collected and are soaked in anhydrous ethanol to stop further hydration. These samples were ground to sizes less than 75 microns before being used in FTIR tests. Further, the specimens used in FTIR tests were prepared by mixing 1mg of the powdered sample in 300 mg of potassium bromide (KBr)in a mortar and pestle; the mixture was then compressed under 10 tons of force for 10 minutes to form a solid pellet. The spectral analysis was performed in the range 4000-400 cm^{-1} with spectral resolution of $1cm^{-1}$. When smoothing of data was required, a 5-point adjacent averaging filter was used in the plotting software. The detailed arrangement or setup of Fourier Transform Infrared with sample holder and hydraulic jack compressor is shown in Figure. 3.8.

Figure 3.8 FTIR with total set of pelletize

3.4.4.4 Thermo-gravimetric analysis/ Differential scanning calorimeter (TGA/DSC)

For thermal analysis test, the hydrated specimens were taken after different days of curing and soaked in anhydrous ethanol to stop the further hydration. After this, mortar pieces was ground in mortar pestle and passed through 75εm sieve. The powder sample was used to know the hydration of cement paste by using thermal analysis.The thermal analysis of cementing materials was carried out using NETZSCH STA 499C as shown in Figure 3.9. For this test, approximately 20 mg of powder sample was heated at the rate of 10 ^{o}C/min from room temperature to 1000 ^{o}C. Al_2O_3 was taken as a reference sample for

this test. Differential temperature and the mass loss corresponding to different temperature range were recorded.

Figure 3.9 NETZSCH STA 449 C

3.4.5 Porosity and pore size distribution

The porosity and pore size distribution study of cured mortar specimens were conducted in mercury intrusion porosimetry analyzer, Pore Master (PR-33-13) as shown in Figure 3.10. A constant size of broken samples were collected after the compressive strength test and the pressure was applied from zero to 240 MPa with a constant contact angle of 140^0 and with a constant surface tension of mercury of 480mN/m (miliNewton/meter). The pore diameter and pore size distribution were measured at ages of 7, 28 and 90 days for reference specimen and specimens containing silica fume. Forspecimens containing other mineral admixtures and additives (OPC), the porosity and pore size distribution was determined after 90 days curing only.

1.1.1.1.1.1.1 Figure3.10 Mercury intrusion porosimetry analyzer, Pore Master (PR-33-13)

3.4.6 Drying shrinkage

The drying shrinkage mortar specimen was measured by using beam mould with 25 mm x 25 mm size and 282 mm internal length. The materials for molding each batch of test specimens were mixed separately using required amount of dry materials and water. The amount of water added for this test was same as that required for preparation of mortar specimens for compressive strength test. Mixing was done mechanically immediately after that the test specimen was placed in the mold in two layers, each layer being compacted with the thumb and fore fingers by pressing the mortar into the corners, around the reference inserts and along the surfaces of the mould until a homogeneous specimen is obtained. The mortar was leveled off to flush with the top of the mould and the surface smoothened with few strokes of the trowel. After 24 hour, the specimens were demoulded and immersed in water at 27 ^{o}C for six days. At 7 and 28 days the specimens

were removed from the water and change in length was measured using a length comparator. The length comparator with beam mould is shown in Figure 3.11.

Figure 3.2 Length comparator with beam mould

3.5 PARAMETRIC INVESTIGATIONS AND SAMPLE DESIGNATIONS

Based on the compressive strength of 36 slag-lime-POP mixes, optimization was done and a reference mix was obtained. Various mineral and chemical admixtures were added to the reference mix. The sample identification along with the mechanical properties of these samples is given in the following sections. The effects of curing conditions on compressive strength, microstructure, and porosity of mortar specimens were also studied in this work. For this, specimens were cured at different temperatures in water and few specimens were also cured in autoclave. In addition to this, specimens were also prepared with different admixtures and cured in autoclave. The identification of these samples along with their compressive strengths is presented in subsequent sections.

3.5.1 Mineral admixtures

The effect of mineral admixtures on strength of lime activated slag cement was studied by adding different proportions of admixtures and then evaluating their compressive strength. Mineral admixtures used in this work are fly ash (FA), silica fume (SF), glass powder (GP), and OPC. The proportions of trial mixes are given in Table 3.11. The samples were cured in temperature controlled water tanks at an average temperature of 27 ^{o}C and to determine the compressive strength specimens were tested in a compression testing equipment after curing periods of 3, 7, 28, 56 and 90 days. The above four types of mineral admixtures were used with different percentages of reference sample by weight as described below:

- 5, 10 and 15% of powdered glass by weight were added to the reference sample
- silica fume was added to the reference sample in 5, 10 and 15% by weight
- fly ash was added to the reference sample in 10, 20, 30 and 40% by weight
- ordinary Portland cement was added to the reference mixture in 5 and 10% by weight

Table 3.11 Details of mix proportion and compressive strength of mortar specimens added with mineral admixtures

Sample ID	Mineral admixture	Amount of admixture in the mix (%)	Proportion of raw materials in the mix (%) (S+L+P)+ Admixture	Compressive strength (MPa)				
				3 Days	7 Days	28 Days	56 Days	90 Days
FA1	Fly ash (FA)	10	(76.2+19.0+ 4.8)+10	17.34	24.56	32.15	37.89	45.1
FA2		20	(76.2+19.0+ 4.8)+20	18.5	31	43.68	48.96	53.52

FA3		30	(76.2+19.0+ 4.8)+30	23	32.73	46.79	53.69	58.41
FA4		40	(76.2+19.0+ 4.8)+40	21.13	32.17	45.51	51.36	55.96
D5	Reference sample	0	(76.2+19.0+ 4.8)+0	23.78	27.13	33.67	39.77	42.21
C11	Ordinary Portland cement (OPC)	5	76.2+19.0+ 4.8)+0	17.35	23.5	32.35	43.65	53.13
C22		10	(76.2+19.0+ 4.8)+10	18.19	24.62	34.68	45.36	56.79
SF1	Silica fume (SF)	5	(76.2+19.0+ 4.8)+5	22.78	25.67	42.56	52.69	59.67
SF2		10	(76.2+19.0+ 4.8)+10	23.98	31.35	45.56	55.69	65.28
SF3		15	(76.2+19.0+ 4.8)+15	24.56	32.73	47.98	59.63	68.78
GP1	Glass powder (GP)	5	(76.2+19.0+ 4.8)+5	16.53	24.34	29.65	35.64	39.28
GP2		10	(76.2+19.0+ 4.8)+10	16.88	24.62	31.37	38.96	44.22
GP3		15	(76.2+19.0+ 4.8)+15	17.45	24.91	32.65	40.36	45.36

3.5.2 Chemical admixtures

The compressive strength of mortar specimens containing different chemical admixtures was determined as per IS: 4031 (Part 6).These results were compared with the reference specimen. The reference specimen is a mixture of finely ground blast furnace slag and hydrated lime, mixed in weight proportions of 80:20 along with 5% of plaster of Paris and water to binder ratio 30.74. The above optimum composition of the raw materials was obtained by mixing the raw materials in different proportions and evaluating their mechanical properties which was studied in previous experiment which was done to lime slag and plaster of Paris mix. The chemical admixtures such as calcium acetate, calcium formate, sodium meta-silicate, and sodium hydroxide were added with 0.5, 1, 2 and 4% of total reference mix (S+L+P). The binder and sand were mixed with

liquid of chemical admixture for one minute in dry state and then required amount of water was added while mixing in mechanical mixture for another three minutes. Seven hundred eighty numbers of specimens were cast for determining the compressive strength of mortar. The effect of chemical admixtures on the strength of slag cement was studied by adding above different proportions of admixtures and evaluating their compressive strength. The mix proportions of chemical admixture mixes are given in Table 3.12. The cubical test specimens were cured in a temperature controlled water tanks at an average temperature of 27 ^{o}C. These specimens were tested in a compression testing equipment after specified days of curing that is at 3, 7, 28, 56 and 90 days. After specified curing period the compressive strength was determined and crushed pieces of sample were collected for further tests like SEM, XRD, TGA, DSC and FTIR analysis.

Table 3.12Details of mix proportion and compressive strength of mortar specimens added with chemicals

Sample ID	Chemical admixtures	Proportion of admixtures in the mix (%)	Compressive strength(MPa)				
			3 Days	7Days	28Days	56Days	90Days
N1	Sodium meta silicate	0.5	20.58	23.2	32.2	38.9	44
N2		1	20.02	22.9	30.7	35.6	39.4
N3		2	20.02	22.9	32.2	35.2	39.4
N4		4	18.22	22.4	30.7	34.5	38.6
C1	Calcium acetate	0.5	20.38	24.1	35.1	48	54.8
C2		1	20.75	24.6	38.6	48.8	55.2
C3		2	21.3	25.7	39.7	51.2	58
C4		4	20.18	24.6	37.8	46.4	48.4
S1	Sodium hydroxide	0.5	23.22	24.3	33	36.9	44
S2		1	24.65	26.6	34.9	39.2	48.8
S3		2	24.05	25.2	34.2	38.6	47.2
S4		4	15.38	22.4	31.8	34.7	44
F1	Calcium formate	0.5	16.23	24.4	32.2	44.2	45.9
F2		1	16.51	24.4	31.3	44.7	48
F3		2	17.38	24.9	33.2	44.7	52
F4		4	15.86	21.25	30.2	41.9	43

CN1	Calcium Nitrate	0.5	16.24	23.78	30.8	46.4	48
CN2		1	16.23	23.78	29.1	44	49.6
CN3		2	15.94	23.78	27.4	40.8	48
CN4		4	15.38	22.37	25.2	40	41.6
D5	Reference sample	0	23.77	27.14	33	39.9	42.2

3.4.5 Curing temperatures

The effects of curing temperatures and curing periods on compressive strength of mortar specimens were studied. For determine the compressive strength same procedure was followed as mentioned in 3.4.2.1. The test specimens are cured under different curing temperatures in both water bath and autoclave are shown in Figure 3.12.

3.4.5.1 Water curing

The cubical test specimens were prepared and cured in separate water tanks and water bath at an average temperature of 27, 45, 60or 75 ^{o}C with an accuracy of ±1 ^{o}C. All the mortar specimens prepared for this test contain 20% lime as the binder, whereas the amount of plaster of Paris was varied from 1 to 10%.Table 3.13 presents the compressive strength of mixes cured in water bath under different temperatures.

3.4.5.2 Autoclave curing

The compressive strength of mortar specimens containing mineral admixtures and cured in autoclave for different periods was determined. These results were compared with the reference specimen. Mineral admixtures like silica fume (SF) and fly ash (FA) were added to reference sample (D5) in weight proportions of 5, 10, 15% and 10, 20, 30% respectively. These blended samples were designated as SF1, SF2, SF3 andFA1, FA2, FA3 respectively. For preparing the mortar specimens the amount of water added was based on the consistency of each mix and tests were carried out as per Indian standard

Table 3.13 Compressive strength of mortar specimen cured in water bath

Mix Code	Mix proportions (%)			Curing temperature (^{o}C)	Compressive strength (MPa)				
	Slag	Lime	POP*		3Days	7Days	28Days	56Days	90Days
D1	80	20	1.0	27	18	20.2	24.3	31.1	33.6
D1.5	80	20	1.5		20.2	21.8	27.4	33.2	35.7
D2	80	20	2.0		21.5	24.2	29.7	34.8	37.9
D2.5	80	20	2.5		21.8	25	31	37.2	40.2
D5	80	20	5.0		23.8	27.2	34	40	42.2
D10	80	20	10		24.6	27.7	34.6	41	44
D1	80	20	1.0	45	20.2	20.7	28.2	31.7	33.5
D1.5	80	20	1.5		21	22.3	29.2	34.2	36.2
D2	80	20	2.0		22	25.2	30.4	35.5	38
D2.5	80	20	2.5		23	25.6	34.4	38.3	40
D5	80	20	5.0		25	27.4	35.2	40.1	43
D10	80	20	10		26.6	28.6	37.1	43.4	44.5
D1	80	20	1.0	60	21.8	22.7	32.3	33.1	33.8
D1.5	80	20	1.5		22.4	24.2	35	35.2	36.6
D2	80	20	2.0		23	26.7	36.5	36.7	37.9
D2.5	80	20	2.5		24	27.2	40	40.1	41
D5	80	20	5.0		23	29	42.7	43.4	44.5
D10	80	20	10		28	31.8	45.2	47	47.6
D1	80	20	1.0	75	20.7	22.7	31	31.2	32.1
D1.5	80	20	1.5		22	24.2	33	33.5	34.5
D2	80	20	2.0		22.4	24.7	34.5	34.2	35.2
D2.5	80	20	2.5		23.3	25.2	39.3	39.2	39.2
D5	80	20	5.0		25.2	27	43.6	43.2	43.3
D10	80	20	10		27.2	31	44	44.2	44.3

*POP is taken over the combined mass of lime and slag

code of practice IS: 4031 (part 4) 1988. The cubical mortar specimens were kept in the mold for 24 hour at room temperature of about 27 ^{o}C. After demolding, the specimens were cured in autoclave at 215 ^{o}C temperature and under 2.0 MPa pressure for 1, 2, 3 or 4h. The temperature of the autoclave was raised gradually from room temperature that is from 27 ^{o}C to 215 ^{o}C at a rate of 1.5 ^{o}C /min. Thereafter, the temperature and pressure were maintained constant at 215 ^{o}C and 2 MPa for specified curing periods that is 1, 2, 3

or 4 hour and then it was gradually cooled to room temperature in 2 hour. The specimen is left over in autoclave until the temperature of the autoclave was reduced to room temperature. The compressive strength of each set of samples was determined under uniaxial compression testing condition. The compressive strength of mortar specimens cured in autoclave was compared with specimens cured at 27 ^{o}C in water for 7, 28 and 90 days. Table 3.14 presents the compressive strength of mixes cured under different conditions like autocalve and water curing.

(a) Water bath

(b) Autoclave

Figure 3.3 Curing of mortar specimens in water bath and autoclave

Table3.14Compressive strength of mortar specimens cured in autoclave and water

Sample ID	Mineral admixture	Admixture in the mix (%)	Compressive strength (MPa)						
			Autoclave curing time				Water curing time		
			1 hour	2hour	3hour	4hour	7days	28days	90days
SF1	Silica fume	5	39.1	43.3	48.9	49.3	25.7	42.6	59.7
SF2		10	41.9	44.7	50.4	50.9	31.6	45.6	65.3
SF3		15	43.4	53.2	55.9	56.0	32.7	47.9	68.8
FA1	Fly ash	10	27.4	43.4	46.2	46.4	24.6	32.2	45.1
FA2		20	31.9	43.1	47.6	48.0	31.0	43.7	53.6
FA3		30	35.8	43.9	48.2	48.8	32.7	46.9	58.4
D5	Reference sample	0	26.3	39.7	41.9	42.0	27.2	33.7	42.2

CHAPTER IV

RESULTS AND DISCUSSIONS I

4. PHYSICAL PROPERTIES

4.1 INTRODUCTION

An extensive laboratory testing program was undertaken to investigate the physical properties like normal consistency, setting time, and soundness of 42 different mixes of slag-lime-plaster of Paris. The lime content in the slag-lime mixes were varied as 5, 10, 15, 20, 30 and 40% by mass. Furthermore, the plaster of Paris was added to the above mixes of slag-lime and its proportion in the mix was taken as 0, 1, 1.5, 2, 2.5, 5 and 10% of the total weight of slag and lime. In order to examine the effect of borax on the setting time of a mix containing 20% lime, different amount of borax such as 0, 0.2, 0.4, 0.6, 0.8, and 1% were added as a retarder. The experimental findings and discussions on it are presented in the following sub-sections. This also includes the study on hydration products and microstructure of this binding mix corresponding to their respective initial and final setting periods.

4.2 PHYSICAL PROPERTIES

4.2.1 Normal consistency

The typical curves presenting normal consistency values with lime at a given plaster of Paris content is presented in Figure 4.1. It is seen that the normal consistency increases with either increase in lime or plaster of Paris contents. The consistency values of slag-lime-plaster of Paris mixes vary over a wide range from 28.89% to 37.4% whereas the same is about 30% for ordinary Portland cement. The increase of water

demand or consistency mainly depends on percentage of lime and plaster of Paris content in the mix. This is attributed to the increase in calcium ions in the mixture or (Ca/Si) ratio. Hence, an increase in lime and/or plaster of Paris content in the mixture results in an increase in consistency values. A similar trend was also observed by Benghazi *et al*. (2009).

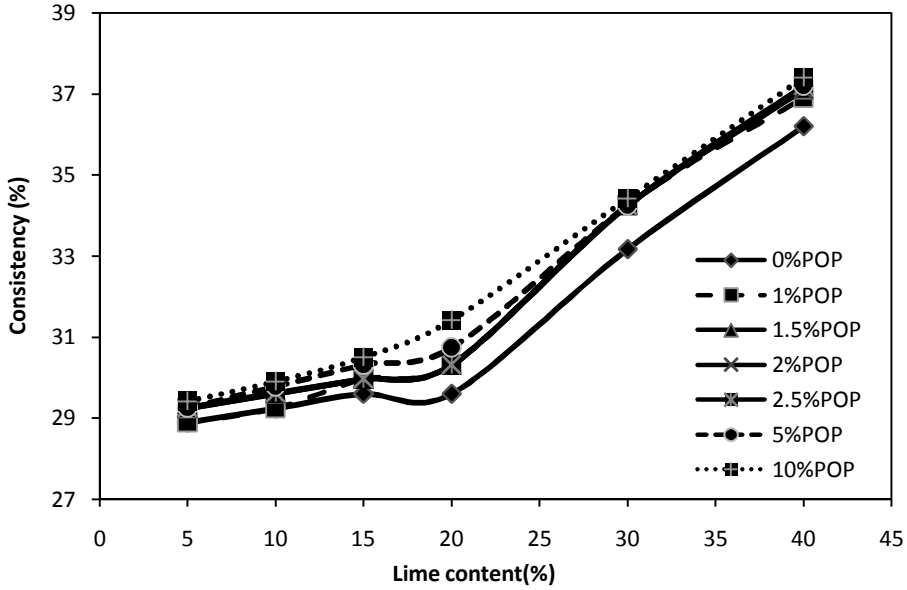

Figure 4.1Variation in consistency with lime content

4.2.2 Setting time

The effect of lime on initial and final setting time of slag-lime-plaster of Paris mixes are delineated in Figure 4.2 and Figure 4.3 respectively. The setting time of mixes containing no plaster of Paris is too long for cementing materials as prescribed in Bureau of Indian Standards. For a given plaster of Paris content, both the initial and final setting time of the mixes are observed to decrease with an increase in the lime content. Similar results were also obtained by Naceri *et al*. (2011). The reduction in setting time of the mix with addition of lime is due to the increase in cation concentration and increase in pH value of the mix. In alkaline activation, the introduction of calcium hydroxide, sodium

hydroxide, soda and others in an aqueous solution leads to formation of corresponding silica-hydrate. The calcium silicate is known to be structure forming phase whereas the sodium silicate is soluble. This results in a marginal decrease in setting time of the mix. Further, it is observed that at a given lime content, an increase in plaster of Paris greatly reduces the setting times. This quick setting action is attributed to the high concentration of sulphate ions in solution, which reacts quickly with aluminum rich slag forming hydrated products. It is reported by Chandra (1996) that when the calcium sulphate activator is mixed with slag, it interacts directly with the alumina, calcium-hydroxide, and water to form hydro-sulphate-aluminates ($3CaO\text{-}Al_2O_3\text{-}CaSO_4\text{-}12H_2O$) along with other new phase-formations during the hardening process.

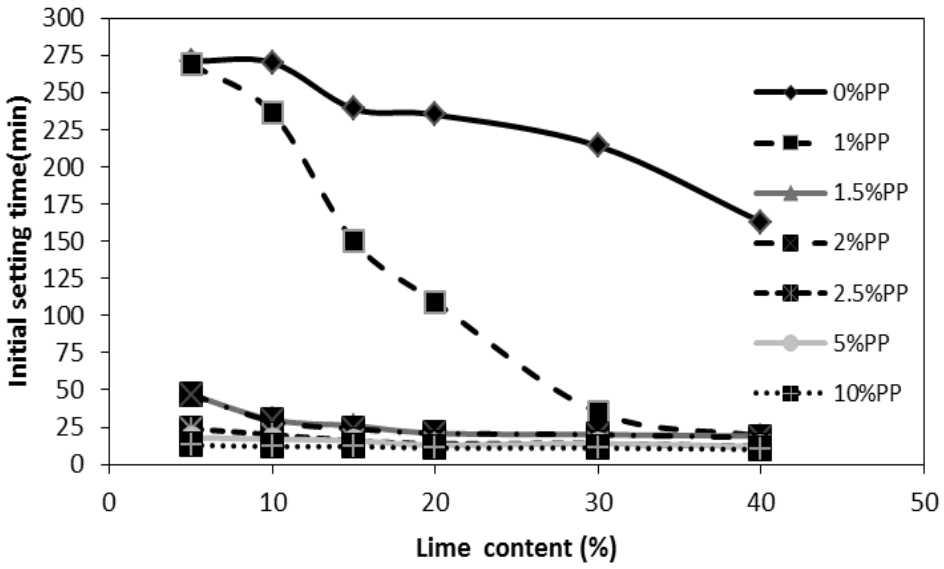

Figure 4.2 Variation in initial setting time with lime content

The formation of new phases retards in setting time of the mixes. In general, it is observed that the initial and final setting times of the mixes containing plaster of Paris are lesser than that of the value prescribed for ordinary Portland cement. In order to overcome this problem, borax was added in these mixes. The effect of borax on the initial

and final setting times of slag-plaster of Paris mixes at 20% lime content is highlighted in Figure 4.4 and Figure 4.5 respectively. From these figures, it is observed that the setting time increases when the borax is added to the mixture of slag-lime-plaster of Paris. Further, it is observed that the retarding effect is not significant before a critical amount of retarder is used; beyond this the setting time increases. This indicates the retarding effect is very sensitive to the amount of retarder. The excess amount of borax retards the setting time significantly. On the other hand, insufficient amount of retarder cannot retard the setting time to the required workability. Similar results were also obtained by Mehrotra *et al.* (1982) and Chang *et al*. (2003). It is well known that the anions and cations present in the activators play a major role in deciding the physical properties of fresh mixtures.

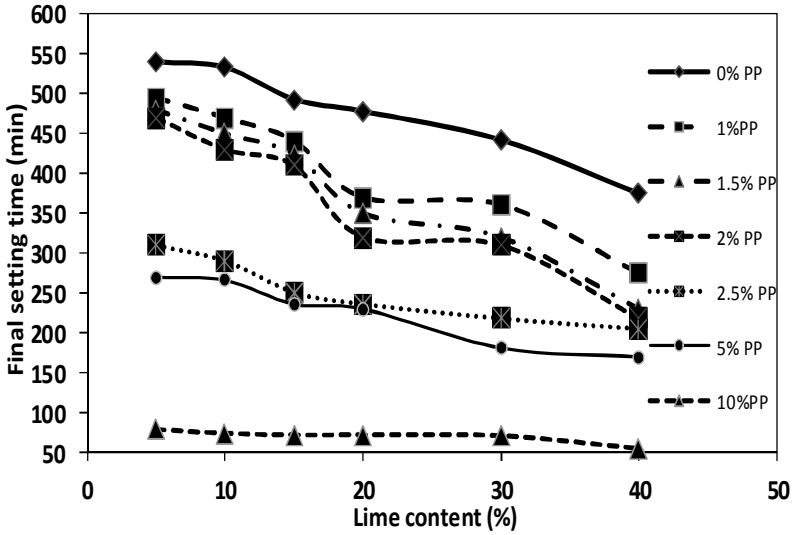

Figure 4.3 Variation in final setting time with lime content

The setting times mainly depend on types of activator and concentration of the activator. It is found that borax content of 0.4% is sufficient to increase the initial setting time from 11 min to a workable range of 23 minutes and final setting time from 72 to 245 min.

Higher borax content further delays the initial setting time than that prescribed for ordinary Portland cement.

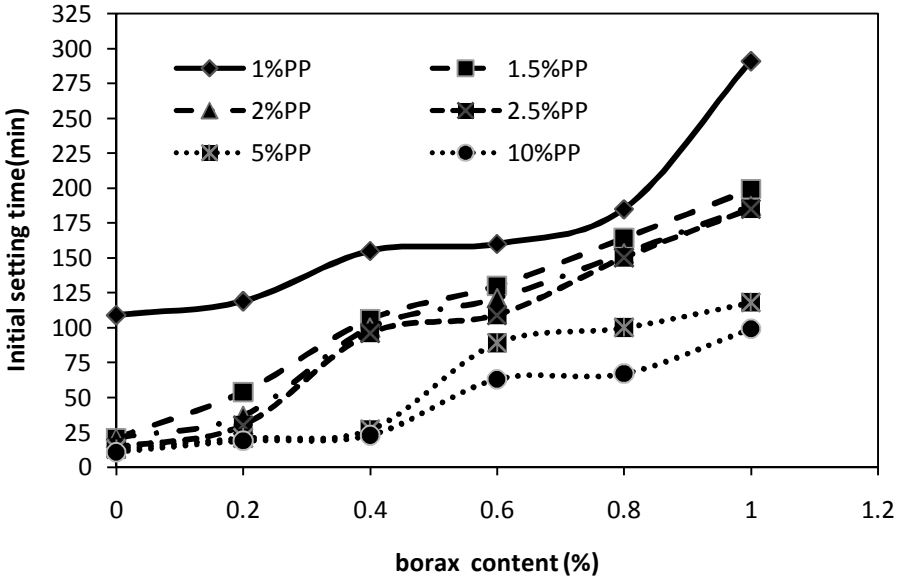

Figure 4.4 Effects of borax on initial setting time of mixes containing 20% lime

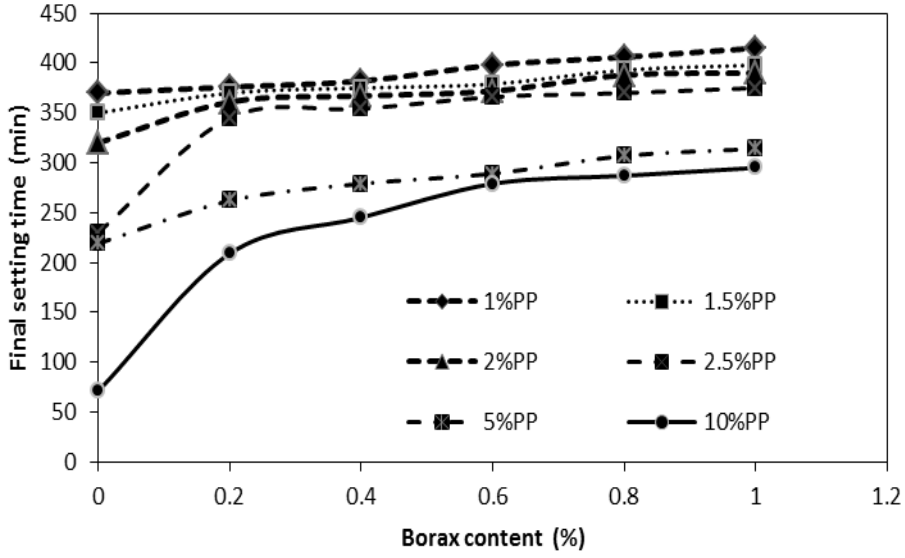

Figure 4.5 Effects of borax on final setting time of mixes containing 20% lime

4.2.3 Soundness

The soundness value of various mixes of slag-lime-plaster of Paris is presented in Figure 4. 6. It has been seen that the soundness of these mixes varies between 1 mm to 2.5 mm for all the mixes except for the mix containing 10% plaster of Paris and 40% lime. For the said composition, the soundness value is 3 mm. It may be due to the presence of an excess amount of free calcium and magnesia in the mix. According to Bureau of Indian Standards, the soundness of cement should not exceed 10 mm. Therefore, the above mixes are sound and can be used as building material.

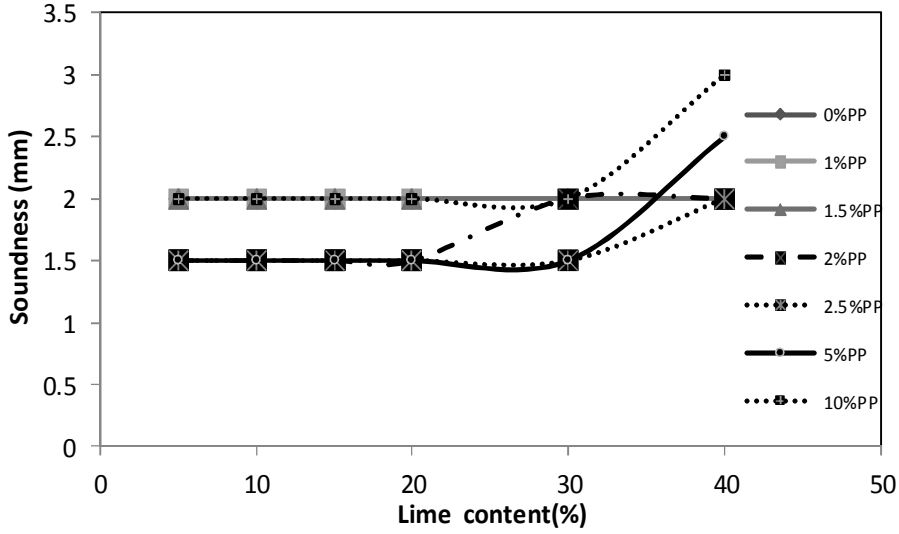

Figure 4.6 Soundness of slag-lime-plaster of Paris mixes

4.3 CHEMICAL BONDS AND HYDRATION PRODUCTS

The hydration products and microstructure of hydrated paste D10 sample (contains 80% slag, 20% lime and 10% plaster of Paris) during setting or hydration process were examined using XRD and SEM analysis. Also, the formation of chemical bonds was studied by using FTIR analysis. The XRD patterns of D10 specimens (with the testing condition: CuKŭ; 7-70°; 2ɗ; 2°/minutes) cured for different setting periods are shown in Figure 4.7. From the XRD analysis, a series of crystalline compounds such as

calcium-hydroxide, quartz, calcium-sulfate-hydrate, portlandite, calcium silicate hydrate, and gypsum were found. As the hydration time increases, the series of crystalline compounds or phases are intensified. The crystalline peaks of calcium-sulphate-hydrate, calcium carbonate, and portlandite appeared for 5 minutes of setting time. Thereafter, that is at 11 min (initial setting time) quartz and gypsum compounds appeared, and the peaks become more intensified. An increase in the hydration period, especially at 72 min (final setting time) the peaks become more intensified. However, after 24 hours of setting, abundance of calcium-silicate-hydrate was observed.

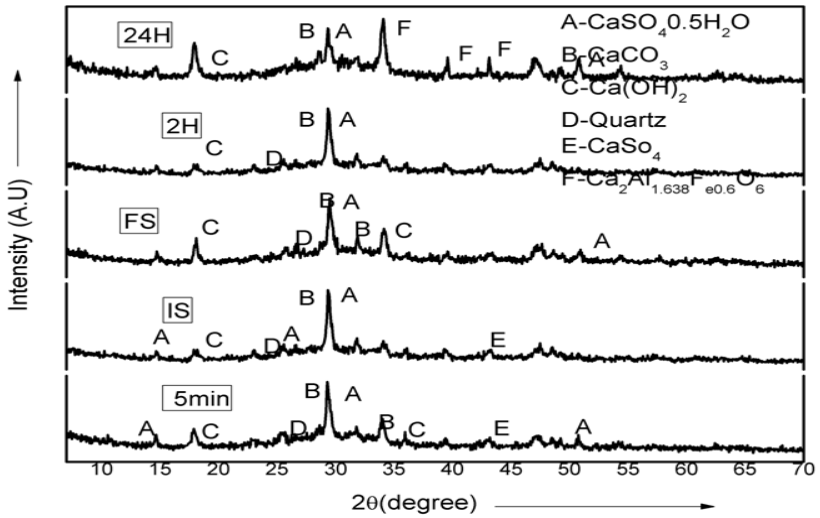

Figure 4.7 XRD patterns of D10 sample at different curing time

The microstructure and surface morphology of specimens cured for different periods have been studied using SEM and EDX analyzer respectively. Figure 4.8 shows the microstructure of specimens cured for different periods. Abundance of needle-like structure is found in specimens cured for 5 min; usually, needle-like crystals appeared during the early period of hydration. As curing period proceeds in, the needle shaped crystals change to hexagonal platy crystals and some gel-like substances appeared.

Further, increase in setting period (24 hour of curing) results in an increase of crystal concentration and more gel like phase of calcium-alumina-silicate-hydrate appeared. This results in an increase of strength and hardness of specimens. The elemental composition was analyzed using EDX. The EDX output for D10 sample after the curing period of 5 min, 11 min and 24 hour are shown in Figure 4.9, Figure 4.10 and Figure 4.11 respectively along with the corresponding surface morphology obtained from SEM analysis.

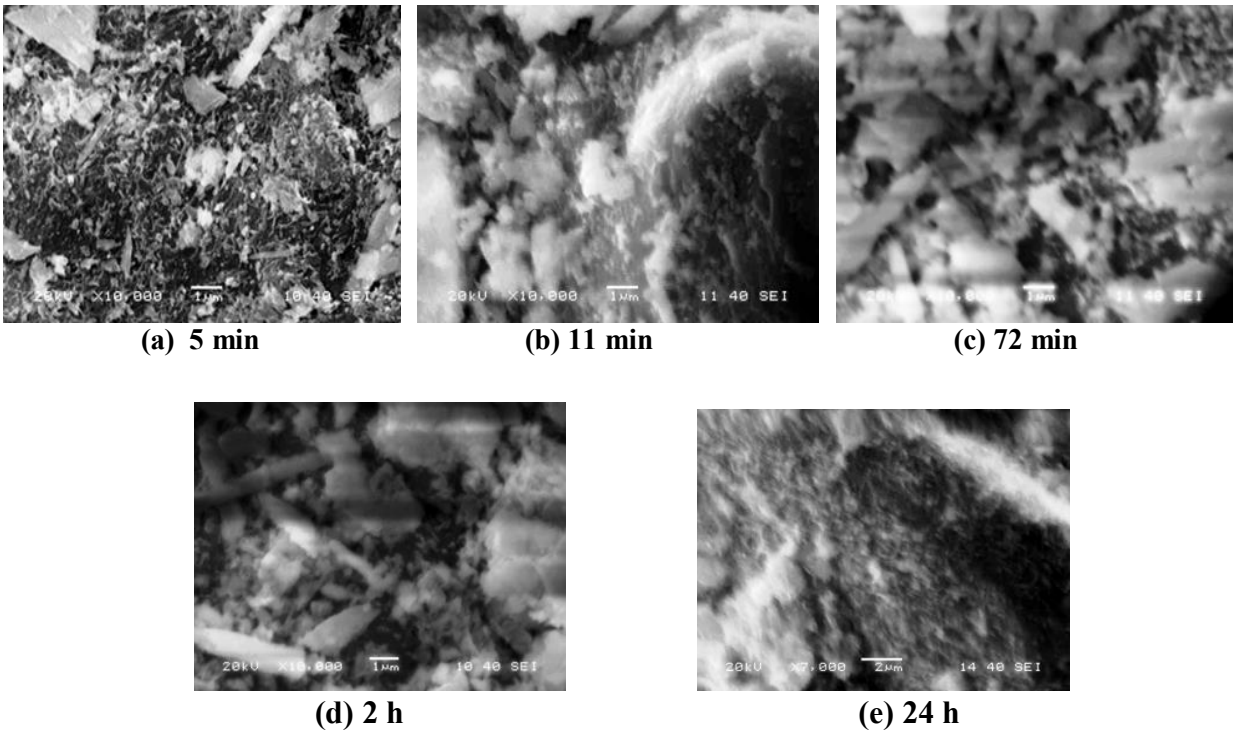

(a) 5 min **(b) 11 min** **(c) 72 min**

(d) 2 h **(e) 24 h**

Figure 4.8 Typical microstructure of D10 sample after different curing times

For D10 specimen at an early stage of setting (5min) as in Figure 4.9, hydrated oxides of Ca, Al, S, and Si are found indicating the presence of compounds of calcium-alumina-sulfate-hydrate that is the C-A-S-H gel. At 11 minutes setting, abundance of element sulfur is noticed in addition to other elements like Ca, Al, and Si, indicating intensification of calcium-alumina-sulphate-hydrate compounds shown in Figure 4.10.

The C-A-S-H gel is found to form in the early stages of curing in slag activated by alkali instead of C-S-H gel, as generally found in hydration-products of ordinary Portland cement. A similar observation was also reported by Puertas *et al.* (2011). Specimen cured for a longer period that is for 24 hours revealed the presence of Ca, Al, Si and S indicating the formation of both calcium-alumina sulphate-hydrate and calcium-silicate-hydrate compounds as shown in Figure 4.11.

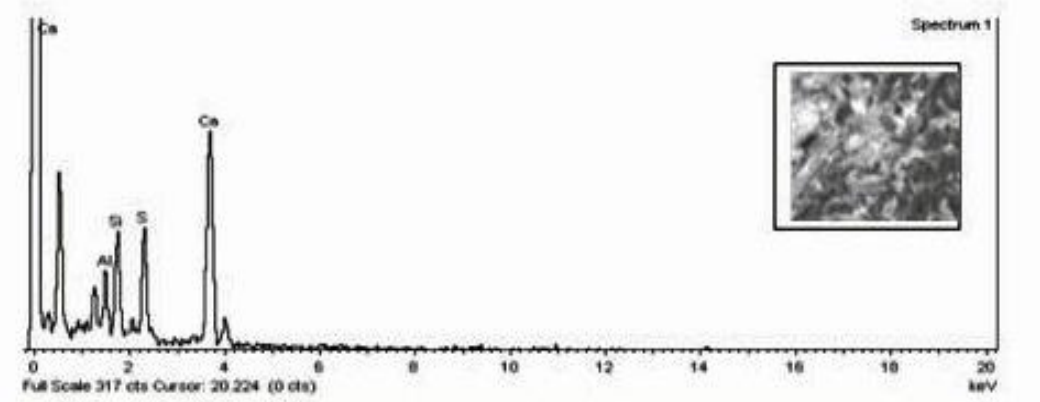

Element	App	Intensity	Weight%	Weight%	Atomic%	
	Conc.	Corrn.		Sigma		
Al K	9.74	1.0241	19.71	1.39	23.53	
Si K	11.47	0.8363	28.43	1.64	32.61	
S K	4.04	0.7733	10.81	1.42	10.86	
Ca K	19.06	0.9616	41.05	1.76	33.00	
Totals			100.00			

Figure 4.9 EDX analysis of D10 sample at 5min curing period

At this setting time the atomic percentage of sulphur is much lower than the earlier cases. This may be due to conversion of tri-sulphate alumina (AFt) to mono-sulphate alumina (AFm). The Si/Ca (% atomic ratio) is 1.02, 0.98, and 0.94 at 5 min, 11 min and 24 hour setting of the sample respectively. From this, it is concluded that more amount of calcium

reacted with un-reacted silicon ion of slag. The Al/Ca ratio (% atomic) is 0.54, 0.71 and 0.79 at 5 min, 11 min and 24 hour setting of the sample respectively and in all the cases the concentration of Al is lower as compared to Si. These parameters indicate the formation of C-S-H phase with an increase in curing period.

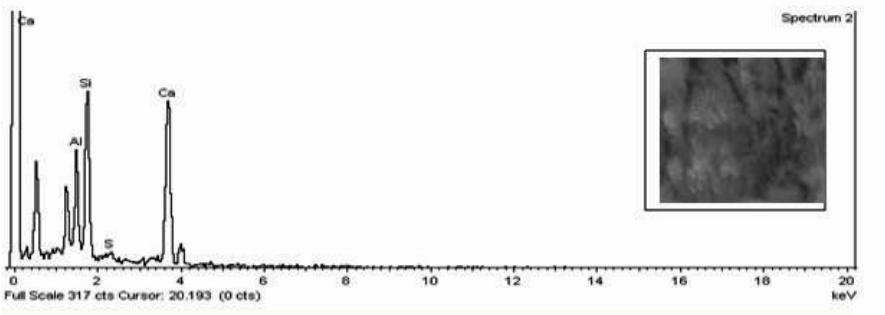

Element	App	Intensity	Weight%	Weight%	Atomic%
	Conc.	Corrn.		Sigma	
Al K	12.32	1.0507	24.25	1.45	28.29
Si K	13.72	0.8004	35.46	1.75	39.75
S K	0.57	0.7171	1.63	1.00	1.60
Ca K	18.07	0.9668	38.65	1.75	30.36
Totals			100.00		

Figure 4.10EDX analysis of D10 sample at 11min curing period

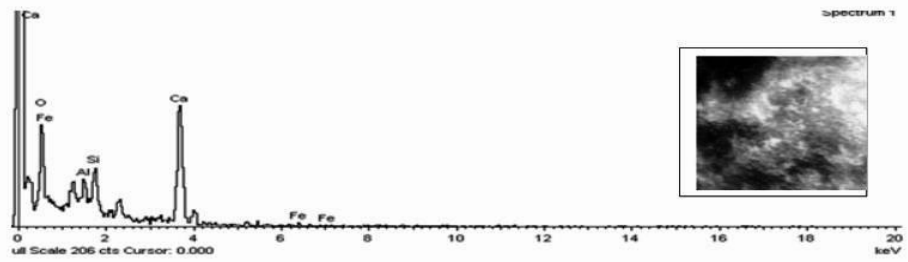

Element	App	Intensity	Weight%	Weight%	Atomic%
	Conc.	Corrn.		Sigma	
O K	33.85	0.6158	65.25	3.64	80.70
Al K	2.49	0.7632	3.87	1.27	2.84
Si K	4.52	0.8228	6.52	1.33	4.60
Ca K	19.68	1.0049	23.24	2.52	11.47
Fe K	0.77	0.8082	1.12	1.38	0.40
Totals			100.00		

Figure 4.11 EDX analysis of D10 sample at 24 h curing time

The presence of this phase results in imparting hardness and strength to the mass. The elemental analysis of samples, cured for different periods, shows compounds that are identified earlier from XRD analysis. Hence, the EDX analysis confirms the XRD results.

The FTIR spectra of the D10 specimen are given in Figure 4.12 for different curing periods. Analysis of the results showed the bond of O-H at wave numbers 1780 cm^{-1} and 3345-3500 cm^{-1}. The minor band range 570-715 cm^{-1} indicates the presence of small amounts of siliceous and alumina-silicate material. The stretching vibration band of O-H is banded at wave number of 3345-3500 cm^{-1} due to calcium hydroxide phase. The presence of peak at 1410 cm^{-1} is due to the bonding in CO_3^{2-} ions. This indicates the presence of carbonated minerals, possibly due to the absorption of CO_2 from the atmosphere.

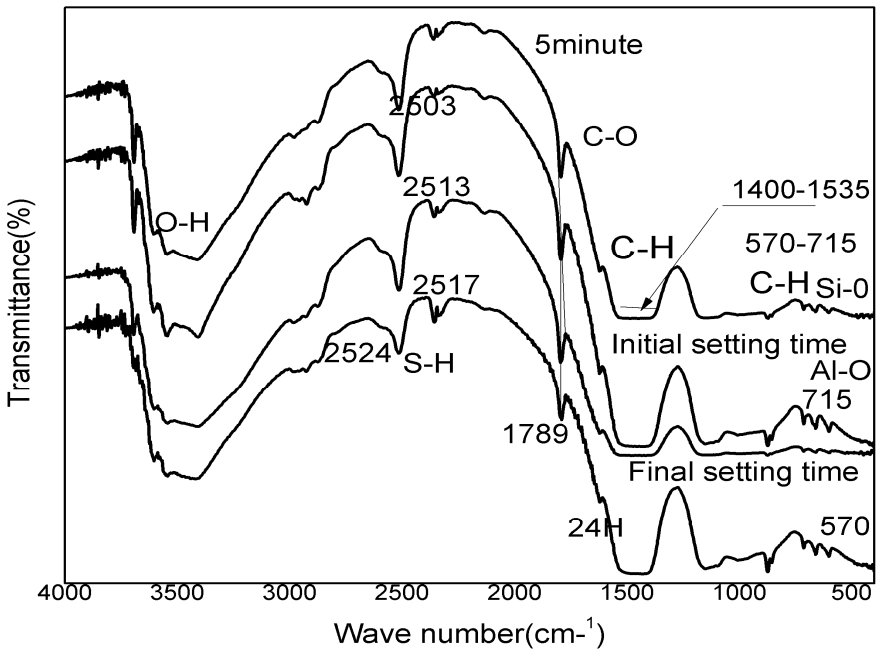

Figure 4.12 FTIR spectra of D10 sample for different curing times

The bending vibration band of O-H is observed at wave numbers 875 cm^{-1}. The quick setting of paste is due to S-rich compounds such as gypsum. Prominent peaks found at 1650 cm^{-1} indicate the formation of S-O bonds in the paste. The presence of this bond indicated the formation of calcium-sulphate-hydrate phase. The S-O and O-H groups are found to be shifted right with the increase in curing period. This indicates that the hydration process continues with setting time and more amount of calcium-sulfate-hydrate gel is formed during the hydration process.

4.4 SUMMARY

The physical properties of 42 mixes of slag-lime-POP are studied and presented in this chapter. It seems that the physical parameters of slag-lime-POP mixes very much depend on the mix proportions. In general, the setting times of the mixes are too low as compared to OPC. However, an addition of small amount borax brings the setting times that meets the specifications as stipulated in Indian code of practices for the cementing material.

CHAPTER V
RESULTS AND DISCUSSIONS II

5. MECHANICAL PROPERTIES AND OPTIMIZATION OF RAW MATERIAL PROPORTIONS

5.1 INTRODUCTION

This chapter presents the compressive strength test results of 36 different mixes of slag-lime-plaster of Paris after curing periods of 3, 7, 28, 56 and 90 days. The lime content in the binding mix was varied as 5, 10, 15, 20, 30 and 40% of the mass of slag and the plaster of Paris content as 1, 1.5, 2, 2.5, 5 and 10% of the combined dry mass of slag and lime. In total 514 numbers of mortar specimens were prepared and these specimens were cured in water at an average temperature of 27 ^{o}C and tested. The optimization of raw materials proportions of the binding mixture was achieved from the experimental results using response surface plot and generalized reduced gradient technique. Furthermore, the chemical analysis of hydration products, microstructure, morphology, chemical bonds formed for slag-lime-POP mixes were made using XRD, SEM, FTIR, and TGA. The mechanical strength of mortar specimens are correlated to the hydration products microstructure, and morphology of the specimens. Also, porosity and drying shrinkage were determined by mercury intrusion porosity tests and length comparator.

The results of these tests were presented in terms effects of lime, plaster of Paris, and curing period on compressive strength, hydration products, microstructure, morphology and pore structure. The hydration products observed under different testing

conditions were compared with the results reported by earlier researchers. Further, the optimization of raw material proportions for attaining maximum compressive strength at a given curing period is made. These are presented in the following sub-sections.

5.2 MECHANICAL PROPERTIES AND HYDRATION PRODUCTS

5.2.1 Effects of lime

The effect of lime on strength of activated slag for different mix proportion was evaluated. The typical variation of compressive strength with lime content for POP content of 2.5% is shown in Figure 5.1. It is seen that at a given POP content, an increase in lime results in an increase in compressive strength up to about 20% lime. However, a further increase in lime in the mix results in a decrease in strength. This trend is observed for samples containing all POP contents and for all curing periods.

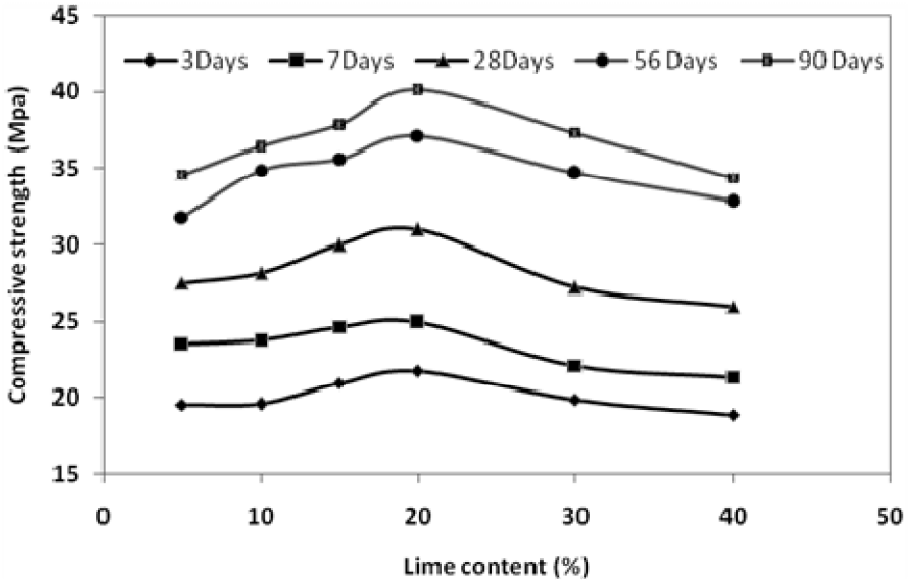

Figure 5.1 Variation in compressive strength with lime at POP content of 2.5%

It clearly indicates that depending on the proportion of slag, activators, and curing conditions, there exists an optimum dose of lime. No significant increase in strength can

be achieved beyond this dose. A further increase in lime content reduces the strength and other harmful properties such as efflorescence and brittleness may increase because of the effect of the free alkali in the product. A similar result was reported by Wu *et al*. (1990). It was reported that an excess addition of alkali activator results in degradation of strength. Cheng *et al*. (1994) reported that both the early and 28 days strength increased dramatically by adding 1.9-3.45% $Ca(OH)_2$. Glukhovsky *et al.* (1983) reported that OPC clinker was considered to have similar effects when added to alkali activated slag cement. The presence of gypsum neutralizes the alkaline component and produces expansive nonï binding substances, which is dangerous to strength. However, in the present study it is observed that a certain percentage of POP in the lime-slag mixture improves the strength.

The compressive strength of mortar was correlated with hydration of the sample and analyzed with SEM results. The SEM image of A2.5, C2.5, D2.5, and E2.5 sample at 28 days curing period is analyzed and presented in Figure 5.2. The hydration products like ettringite and C-S-H gel are not clearly visible in A2.5 specimens. This indicates that the lime added is not sufficient to trigger the pozzolanic reactions completely. On the other hand, E2.5 sample that contains more lime shows the formation of an excess coagulated matrix. However, images obtained for C2.5 and D2.5 samples show lots of hydration products of needle-like ettringite and fibrous C-S-H gel. These hydration products in D2.5 and C2.5 samples are responsible for imparting higher strength to these specimens.

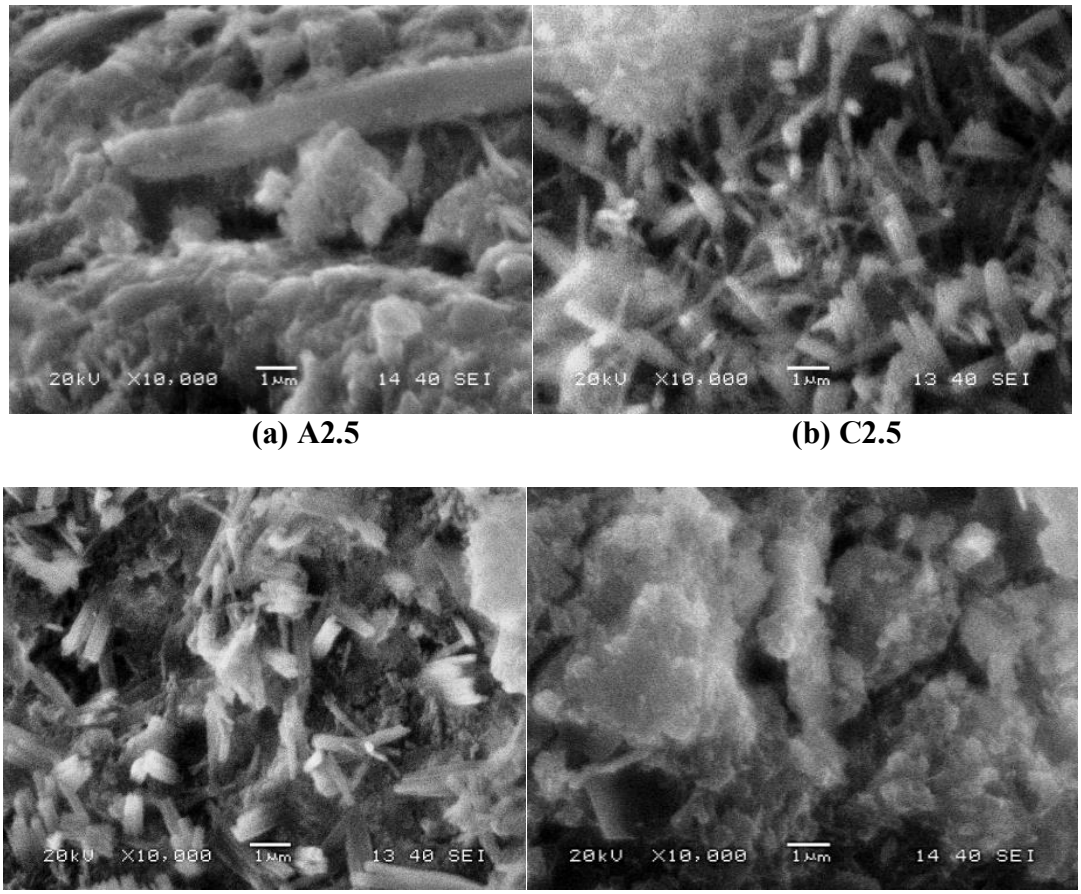

(a) A2.5 **(b) C2.5**

(c) D2.5 **(d) E2.5**

Figure 5.2 Microstructure of samples after 28 days curing

5.2.2 Effects of plaster of Paris

The effect of POP on the compressive strength of mortar specimens was studied by varying the POP contents as 1, 1.5, 2, 2.5, 5 and 10% of the total weight of the slag-lime mixture. The compressive strength test results are given in Table 3.10. Typical variation of compressive strength with POP content for specimens containing 20% lime is presented in Figure 5.3. The result shows that for a given lime content, the compressive strength of mortar cubes increases non-linearly with plaster of Paris content.

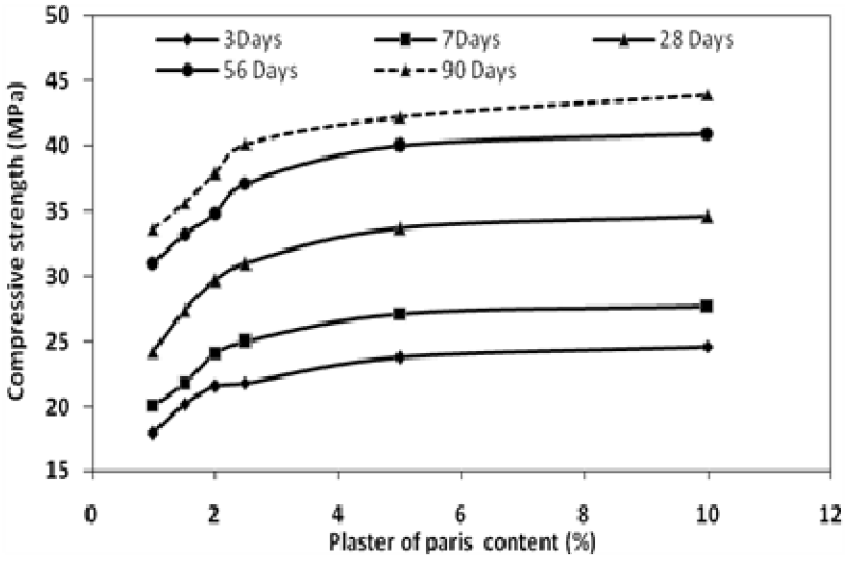

Figure 5.3 Variation in compressive strength with POP at lime content of 20%

Initially, the rate of increase of strength with plaster of Paris content is high, followed by a mild increase in strength. Further, it is observed that no appreciable increase in strength occurs beyond 5% plaster of Paris content. The test results show that the compressive strength of mortars containing 10% POP is about 3 to 4% higher than samples containing 5% POP. Excess amount of POP in the mix may cause efflorescence in future and neutralize the alkaline components. It may also produce non-binding substance that is harmful to long term strength of concrete. Keeping this in mind it is concluded that with the quality of raw materials used in the present testing program, the optimum amount of POP is about 5 percent.

The XRD pattern of D2.5 and D10 samples at 28 days is presented in Figure 5.4. Compounds like ettringite, gypsum, quartz, calcite and C-S-H gel are found in D10 samples, whereas a D2.5 sample contains compounds like quartz, calcite, and C-S-H gel. The amorphous calcium silicate hydrate hump with broader base is observed in D10

specimen compared to D2.5 specimen. The SEM images of D2.5 and D10 samples are presented in Figure 5.5. A lesser quantity of needle-like structures of ettringite is observed in D2.5 specimen as compared to D10 sample. Similarly, D10 sample contains more C-S-H gel as compared to D2.5 samples. The presence of more needle-shaped crystals of ettringite and C-S-H gel imparts higher strength to D10 specimens as compared to D2.5 specimens.

The crystalline peaks of calcite and secondary gypsum are more intensified in D10 sample as compared to D2.5 sample. It is found that ettringite is not formed in D2.5 sample and formations of C-S-H peaks are not that prominently intensified. This results in lesser compressive strength in D2.5 sample as compared to D10 sample. The formation of ettringite mainly depends upon the amount of POP and in D10 samples; the POP content is higher than D2.5 samples resulting the formation of more ettringite and higher compressive strength.

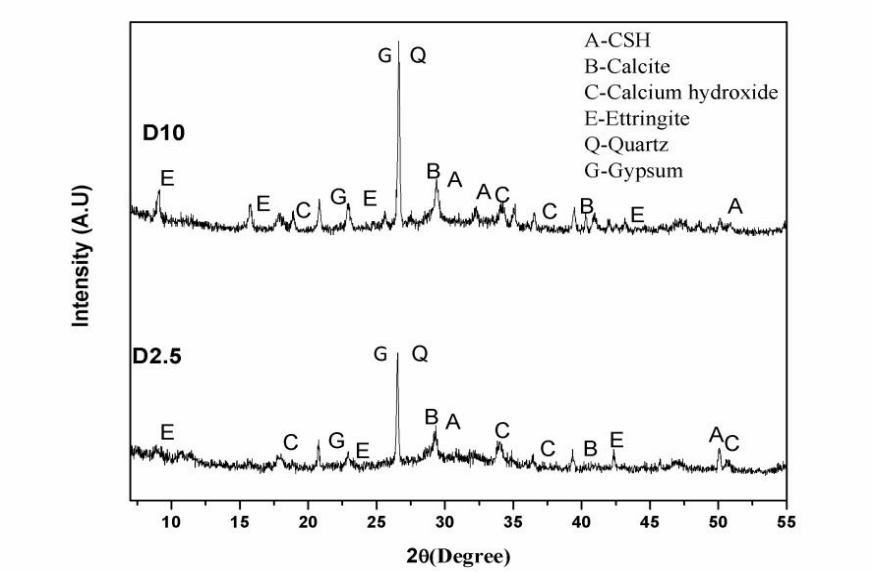

Figure 5.4 XRD patterns for samples after 28 days cured

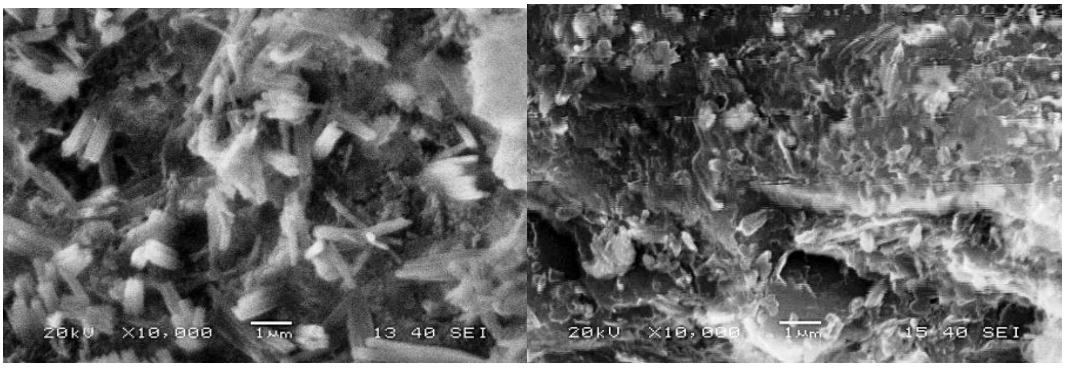

(a) D2.5 sample **(b) D10 sample**

Figure 5.5 Microstructure for samples after 28 days curing

5.2.3 Effects of curing period

The compressive strength of trial mixes was determined after different curing periods. The test results are presented in Table 3.10. The typical relationship between compressive strength and curing period for samples containing 20% lime with different POP content is presented in Figure 5.6.

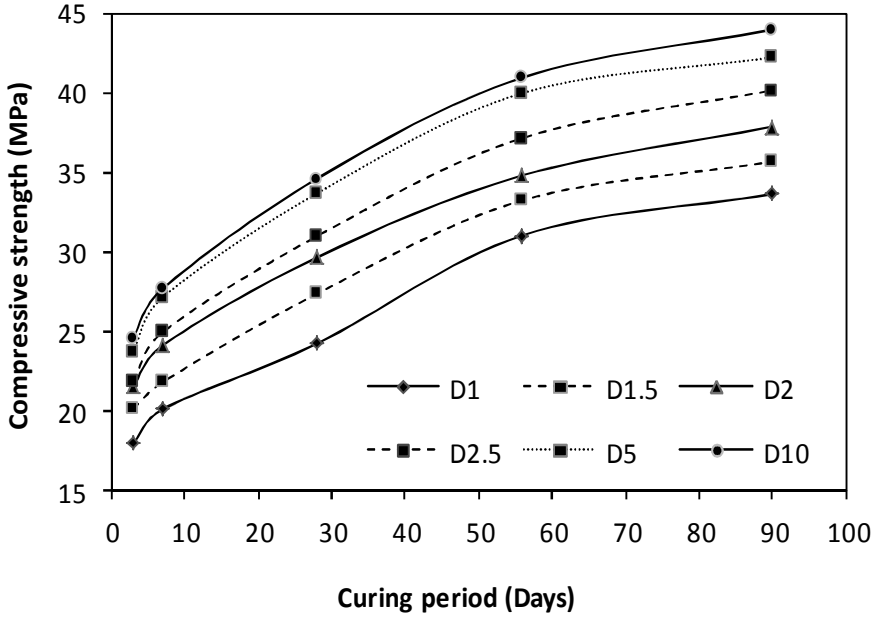

Figure 5.6 Variation in compressive strength with curing period for 20 % lime in mix

The result shows that for a given lime content with different plaster of Paris content, the compressive strength of mortar cubes increases non-linearly with curing period. Initially, the rate of increase in strength with time is high, followed by a mild increase in strength. Further, it is observed that for all mix proportions the strength continues to increase up to 90 days of curing, and the curves have an upward trend. This indicates that unlike OPC, the lime-slag cement continues to gain strength for a longer period. The specimens containing 20% lime and 10% plaster of Paris attain compressive strength of 34.59MPa and 43.56MPa at 28 and 90 days curing period respectively. Further, it is noticed that for all curing conditions, an increase in POP content results in an increase in strength. However, beyond a POP content of 5% no significance gain in strength is noticed.

5.2.4 Hydration products and Microstructure

The formations of hydration products, microstructure, surface morphology and chemical compounds during the hydration period were studied by using XRD, SEM, EDX, FTIR and TGA analysis for D10 sample. The XRD patterns for D10 sample after 3, 28, and 90 days of curing are shown in Figure 5.7. A series of chemical compounds or phases such as ettringite, quartz, calcium silicate hydrated, gypsum and calcite were found. The amorphous hump of calcium silicate hydrate appeared at 3 days of curing at about 300 scattering angle (2ẽ). These peaks become more boarder base for specimens cured for 28 days. However, additional peak representing calcium hydrogen silicate appeared at 500 scattering angles in specimens cured for 90 days. The appearance of additional amorphous humps of calcium hydrogen silicate at 500 scattering angle is responsible for imparting additional compressive strength to the specimens. The calcite

peak obtained at 290 is due to the occurrence of calcium carbonate in the waste lime, used in this work. The peaks corresponding scattering angle of 90, 150, and 230 is characteristics of ettringite and these phase is found to present in samples cured for 3, 28, and 90 days.The compressive strength of mortar and concrete mainly depends on the presences of C-S-H gel and ettringite. Ettringite gives the early strength and excess amount of ettringite causes expansion. An increase in lime content results in an increase of C-S-H gel and the compressive strength. However, addition of lime beyond an optimum value results in the formation of hillebrandite and reduction in compressive strength.

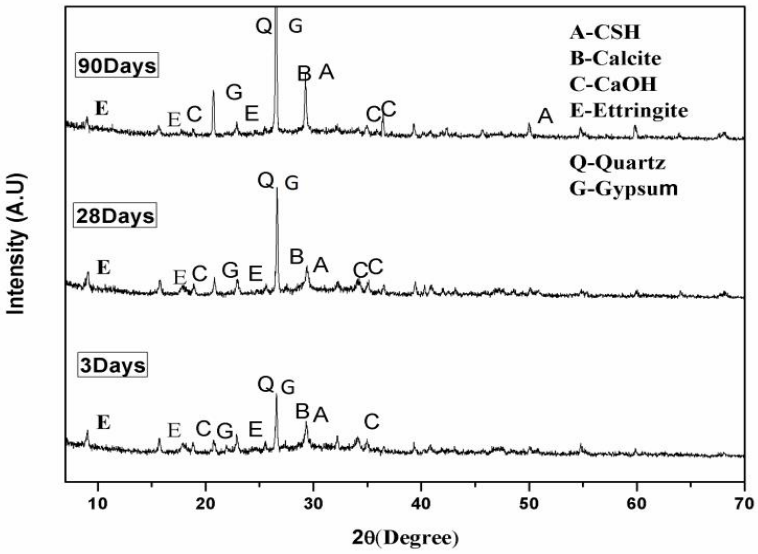

Figure 5.7 XRD patterns of D10 specimen for different curing periods

The hydrated specimens of D10 sample was analyzed by SEM after 3, 7, 28 and 90 days of curing. The SEM images are shown in Figure 5.8. The SEM images show that the needle-like crystals of ettringite exist in the hydration product. At earlier ages, that is at 3 days curing period, little ettringite was formed. After 7 days of curing, the amount of hydration products increased and more needle-shaped structures were formed. Especially

after 28 days, more ettringite and foil like material of C-S-H were appeared. In the later ages, that is at 90 days the hydration went steadily; more C-S-H gel is formed and the hydrated specimen is filled in between the rod-like crystals of ettringite. In addition to this, the calcium hydrated silicate gels ($CaH_4Si_2O_7$) are formed. At 90 days of hydration, much of the ettringite was wrapped in C-S-H gel and coated with slag particles. More and more C-S-H filled into the pores of hardened paste improving the compressive strength further.

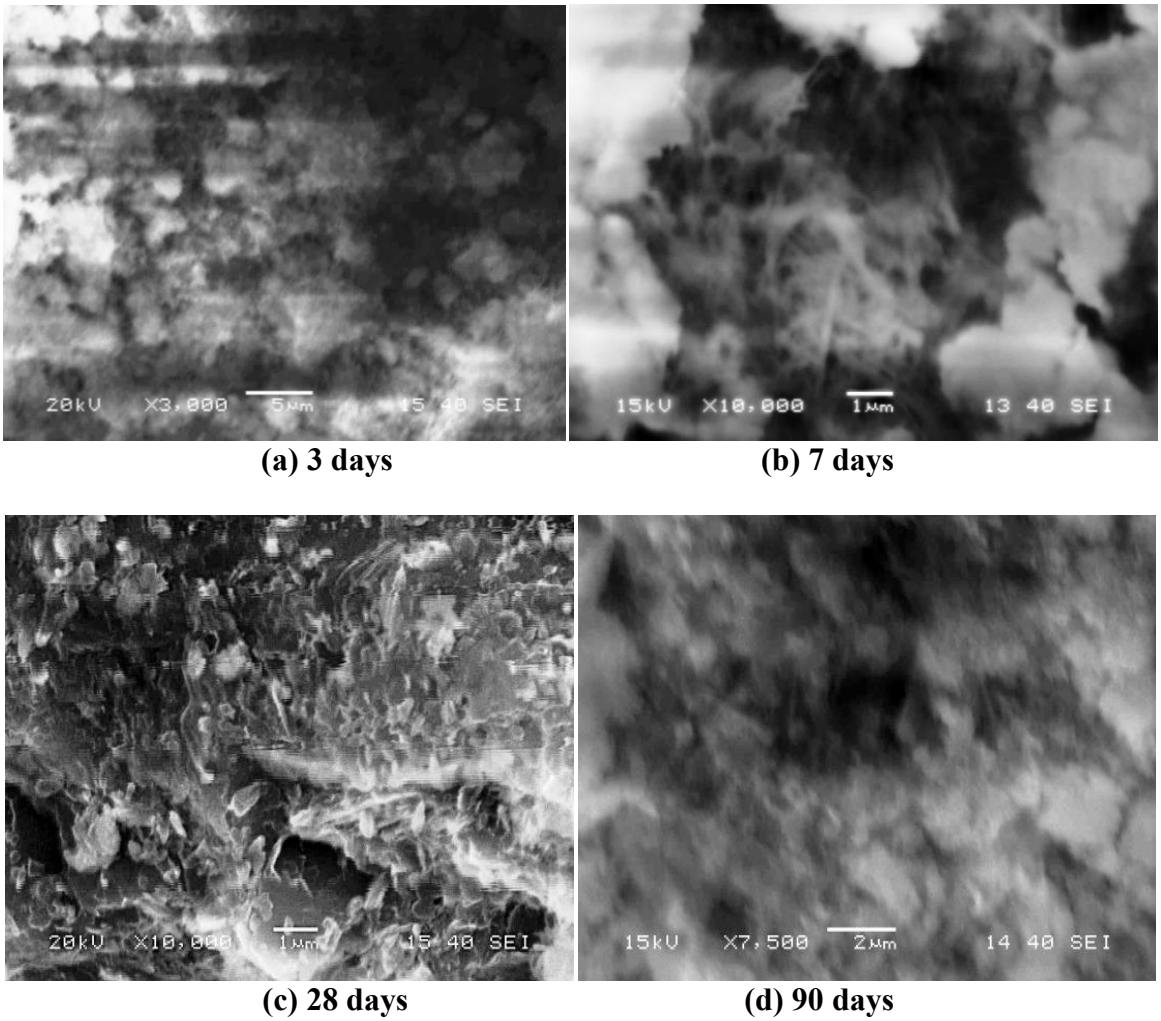

(a) 3 days **(b) 7 days**

(c) 28 days **(d) 90 days**

Figure 5.8 Microstructure of D10 sample for different curing periods

The EDX output for D10 sample after curing period of 90 days is shown in Figure 5.9, along with the corresponding surface morphology obtained from SEM analysis. The main elements present in EDX analysis of D10 sample are Ca, Si and lesser quantities of Al. These elements indicate the presence of compounds of calcium-silicate-hydrate. The main hydration peak of amorphous C-S-H is obtained at 30^o and 50^o scattering angles (2ẽ). With increased curing period the hydration products like ettringite is intensified up to 28 days after that the peak of ettringite is not obtained. As curing time increases the series of hydration products are intensified. The amorphous peaks of calcium silicate hydrate appeared at 3 days of curing at 30^o scattering angle (2ẽ). These humps become more boarder base for specimens cured for 7 days and 28 days. However, additional peak representing calcium hydrogen silicate appeared at 50^o scattering angles (2ẽ) in specimens cured for 90 days. The appearance of additional amorphous peaks of calcium hydrogen silicate at 50^o scattering angle is responsible for imparting additional compressive strength to the specimens. A similar result was also obtained by Cheng *et al*. (1994) and Bijen ss*et al*. (1981). Mehrotra *et al.* (1982) reported that slag activated by anhydrite is inferior in strength compared to POP activated slag with an equal amount of OPC activator. It was also reported that the early strength of AAS cement was lower as compared to Portland cement but after two weeks curing it became stronger than Portland cement.

The compressive strength of mortar and concrete mainly depends on the presences of C-S-H gel and ettringite. Ettringite gives the early strength and excess amount of ettringite causes expansion. An increase in lime content results in an increase of C-S-H gel and the compressive strength. However, additions of lime beyond an

optimum value result in the formation of hillebrandite and reduction in compressive strength. These results are in line with the findings of Puertas *et al.* (2000) who carried out factorial experimental designs from which it was concluded that the nature of activator solution is the most statically significant variable in the alkali activation of blast furnace slag.

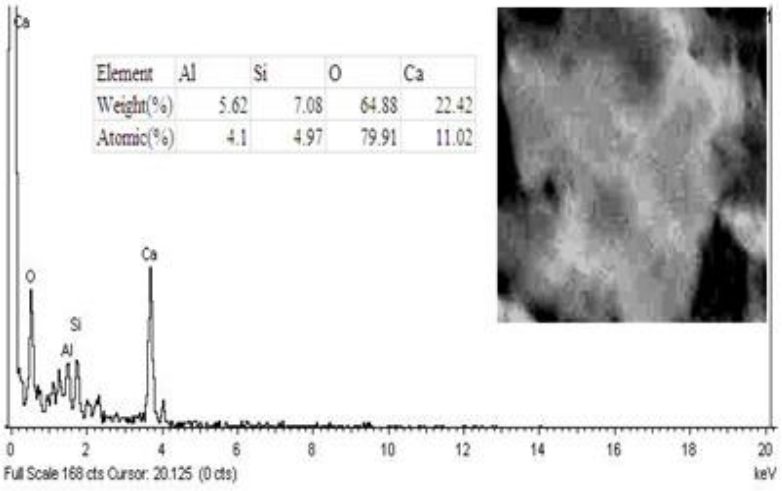

Figure 5.9 EDX analysis of D10 specimen after 90 days curing

The Fourier transmittance infrared (FTIR) spectra of the D10 specimen are given in Figure 5.10 for different curing periods. Analysis of the results showed the bands of O-H at wave numbers 3345-3500 cm^{-1} respectively. The minor band range 441-468 cm^{-1} indicates the presences of small amounts of siliceous silicate material. The stretching vibration band of O-H is banded at wave number of 3345-3500 cm^{-1} due to ettringite phase. The presences of peak at 1465-1492 cm^{-1} is due to the bonding in CO_3^{2-} ions, indicates the presence of some sort of carbonated mineral, possibly due to the absorption of CO_2 from the atmosphere. The bending vibration band of Si-O is observed in wave numbers 1110-1145cm^{-1} due to the formation of calcium-silicate-hydrate. The peaks

found at 1652-1661cm^{-1} indicate the formation of S-O bonds in the mortar specimen. The presences of this bond indicated the formation of secondary gypsum. The S-O and O-H groups are found to be shifted right with the increase in curing period.

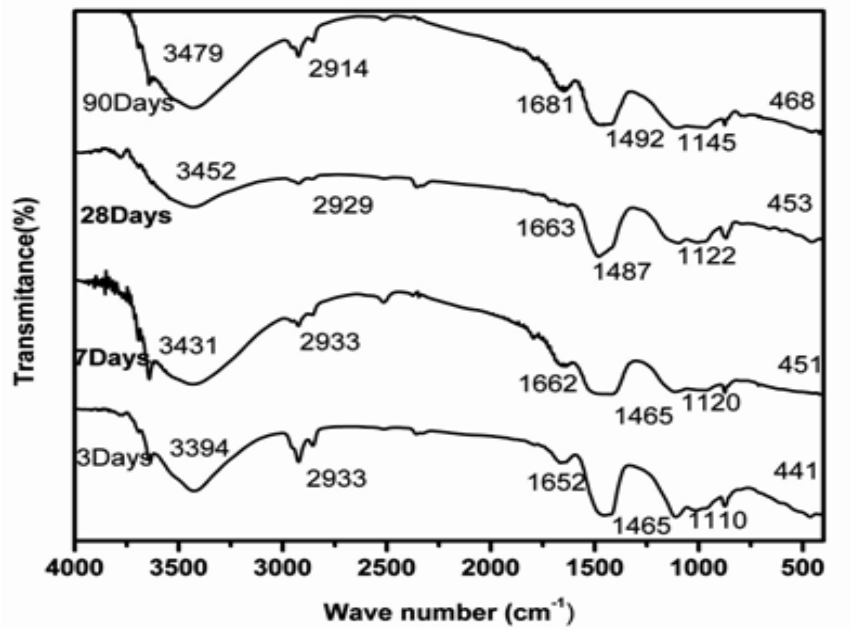

Figure 5.10 FTIR analysis of D10 specimens cured for different days

The hydration mechanism of mortar specimens containing slag-lime-POP mixes was analyzed by thermo gravimetric method and its hydration products are identified. Figure 5.11 shows the TGA curves for D10 samples cured for 3, 7, 28, and 90 days. The total mass loss in these samples, in the temperature range of 0 to 1000 ^{o}C varies between11.4% to 13.5% and the loss of mass is found to increase with the curing period of samples. This indicates that as the curing period increases there is progressive participation of the slag in the hydration reaction and the formation of more amount of C-S-H phase. The hydrated product of C-S-H exhibits permanent endothermic peak in the temperature ranges from 95 ^{o}C to 122 ^{o}C. The endothermic peak corresponding to this temperature range is found to be intensified and the base becomes broader with the curing

period of the samples. This also suggests the formation of more amount of C-S-H phase with the curing period. DSC curves for samples cured at different periods show small exothermic peaks at temperatures of 757 ^{o}C and 883 ^{o}C. This is attributed to the decomposition of calcium carbonate which may be present in the lime or formed during curing and storing of specimens.

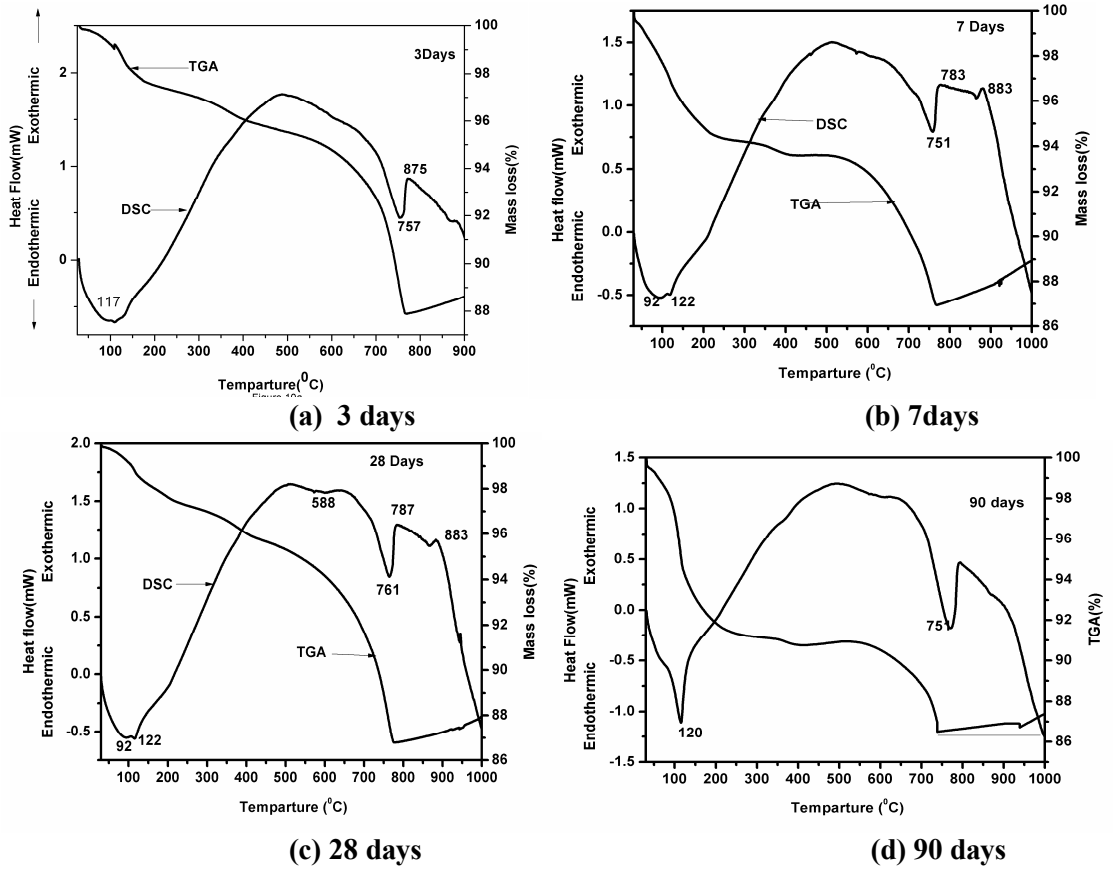

Figure5.11 DSC and TGA of D10 samples cured for different days

The mass loss due to ettringite and C-S-H increased with curing period. A similar result was also obtained by Barbhuiya *et al*. (2009), Ramachandran (2001) and Taylor (1997).

5.3 RESPONSE SURFACE MODEL

Furthermore, optimization of raw materials was done on experimental values of compressive strength of different mixtures with various lime and POP contents cured for

3, 7, 28, 56, and 90 days by response surface plot with the generalized reduced gradient technique. The experimental values of the compressive strength for mixture with various lime and POP contents at above curing periods are compiled and are fitted with the thirdï degree polynomial keeping lime and POP as variable. The regression coefficients of the above said model for each of the representative curing periods are obtained by performing multiple regressions. The fitted response of the third-degree polynomial model shows better agreement with the actual response with lower standard error and higher coefficient of determination (Table 5.1) than other models such as second-degree polynomial, linear etc., due to consideration of interaction terms such as $x_1.x_2$, $x_1^2.x_2$ and $x_1.x_2^2$ which takes into account the high non-linearity which exist between input variables and response of the model along with higher order terms.

Table 5.1 ANOVA test results

Response Model	f_c (3days)	f_c (7days)	f_c (28days)	f_c (56days)	f_c (90days)
Standard error	1.27	1.019	0.874	1.2	1.414
R^2 value	0.881	0.924	0.963	0.951	0.938
F value	21.46	35.56	76.47	56.707	44.19
Significance of F p-value (prob>F)	$7.25x10^{-10}$	$2.22x10^{-12}$	$2.06x10^{-16}$	$8.21x10^{-15}$	$1.68x10^{-13}$
x_1	0.000259	0.002956	$1.52x10^{-6}$	$8x10^{-6}$	0.000216
x_2	$2.15x10^{-7}$	$3.24x10^{-8}$	$1.67x10^{-10}$	$1.24x10^{-9}$	$5.65x10^{-9}$
x_1^2	0.025956	0.025374	$5.2x10^{-5}$	0.00274	0.058552
$x_1.x_2$	0.002981	0.198167	0.07775	0.002856	0.004496
x_2^2	$2.05x10^{-5}$	$2.15x10^{-6}$	$3.98x10^{-8}$	$7.32x10^{-7}$	$1.66x10^{-6}$
x_1^3	0.174076	0.120202	0.001352	0.045246	0.508504

$x_1^2 .x_2$	0.292768	0.916307	0.665232	0.591344	0.42236
$x_1.x_2^2$	0.006977	0.128857	0.114382	0.00399	0.014379
x_2^3	0.000231	$2.8x10^{-5}$	$8.86x10^{-7}$	$2.39x10^{-5}$	$3.26x10^{-5}$

A typical plot showing the dispersion of predicted value with the experimental results for 28 and 90 days cured mortar specimen is shown in Figure 5.12 indicating a very good correlation between observed and predicted values of compressive strength. The statistical model for prediction of compressive strength for different curing periods of 3, 7, 28, 56, and 90 days are given as follows

$$f_c(3\text{ days}) = -2.937 + 1.154x_1 + 10.52x_2 - 0.03109x_1^2 - 0.1279x_1.x_2 - 1.727x_2^2 + 0.0002701x_1^3 + 0.0006127x_1^2.x_2 + 0.007529x_1.x_2^2 + 0.08867x_2^3 \quad (5.1)$$

$$f_c\ (7\text{ days}) = 5.28 + 0.7136x_1 + 9.321x_2 - 0.02488\ x_1^2 - 0.04106x_1.x_2 - 1.605\ x_2^2 + 0.0002474x_1^3 + 0.00004824x_1^2.x_2 + 0.003211x_1.x_2^2 + 0.08389x_2^3 \quad (5.2)$$

$$f_c\ (28\text{ days}) = 6.033 + 1.155x_1 + 10.44x_2 - 0.04349\ x_1^2 - 0.04898x_1.x_2 - 1.742\ x_2^2 + 0.0004741x_1^3 + 0.0001707x_1^2.x_2 + 0.002869x_1.x_2^2 + 0.09084x_2^3 \quad (5.3)$$

$$f_c\ (56\text{ days}) = 4.881 + 1.421x1 + 13x2 - 0.04087\ x12 - 0.1206x1.x2 - 2.021x22 + 0.0003814x13 + 0.000291x12.x2 + 0.007614x1.x22 + 0.09995x23 \quad (5.4)$$

$$f_c\ (90\text{ days}) = 5.968 + 1.296x_1 + 14.18x_2 - 0.02878x_1^2 - 0.1341x_1.x_2 - 2.262x_2^2 + 0.0001432x_1^3 + 0.0005139x_1^2.x_2 + 0.007447x_1.x_2^2 + 0.115x_2^3 \quad (5.5)$$

ANOVA test results show that the selected model for prediction of compressive strength (fc) passed the F test with the values given in Table 5.1 and also significance of

F values, which are the probability that the model will not explain the variations in the response, are very much less than 0.05 which indicates that the selected model is highly significant. The significance of F values (prob>F) of the model less than 0.05 are statistically significant lack of fit at the 95% confidence level (Muthukumar M, Mohan D, 2004). The interaction term $x_{12}.x_2$ is not significant model term for the all fitted models since the p-value is larger than 0.05. The response of the fitted model shows that the term x_{13} is not significant corresponding to curing periods of 3, 7 and 90 days and also the interaction term $x_1.x_2$ is not significant to the response model corresponding to curing period of 7 days.

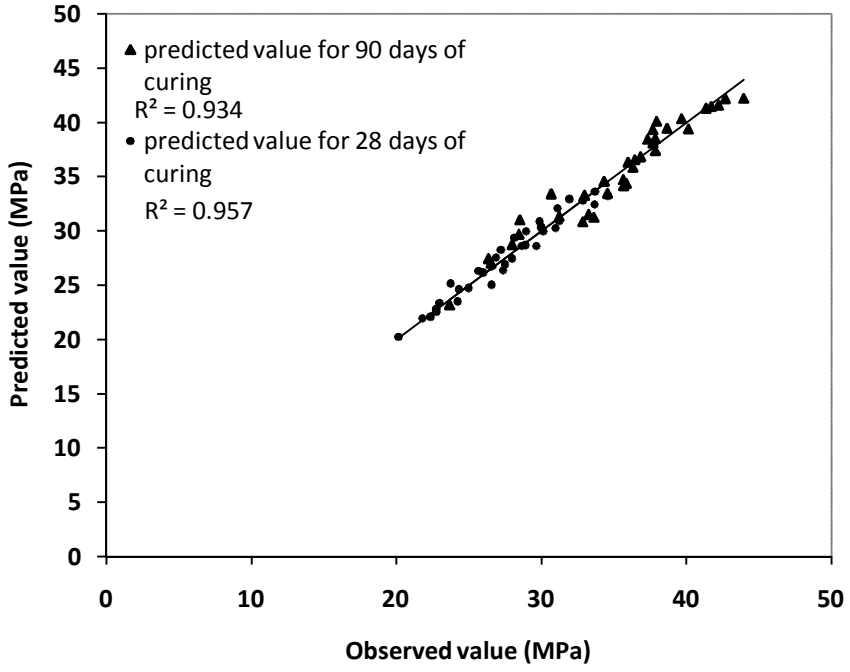

Figure 5.12 Plot between predicted verses observed values of compressive strength

The quadratic term x_1 is not significant term in the response model of 90 days cured sample. F-value of model must be lower than the critical or tabulated F-value if a

particular model is signiýcant. Also F test results proved that the selected models passed the F test with the values given in Table 5.1. The model can be further simplified by neglecting insignificant terms from the corresponding models and analysis can be done by backward stepwise technique.

5.4 OPTIMIZATION

The nonlinear response of the model is optimized using generalized reduced gradient (GRG) algorithm. The above nonlinear method is adopted to obtain the maximum value of the predicted response for each of the fitted models. The predicted response of the fitted model is shown in the form of surface and contour plots for 28 days and 90 days cured mortar specimen (Figures 5.13 and 5.14). It is observed that the response function initially increases with lime content and reached an optimum value, thereafter it shows decreasing trend with further increase in lime content. A similar pattern is also observed with POP content, with the compressive strength remaining almost constant at higher POP contents. The optimum value of the response function is obtained using fitted response surface models by GRG method. The optimum lime and POP content for 90 days cured mortar specimen is found to be 19.12% and 4.26% respectively. However, for other curing periods the optimum values of lime and POP are found to vary from 15.75 to 19.12% and 3.95 to 4.57% respectively. In general, it is observed that with increasing curing period the optimum values of activators are found to be more. This is obvious as the hydration of slag with lime and POP is much slower and a higher dose of activators does not take part in pozzolanic reaction and is left out as free lime and POP. As the curing periods increase, more and more activators are consumed in hydration process, thus increasing the strength.

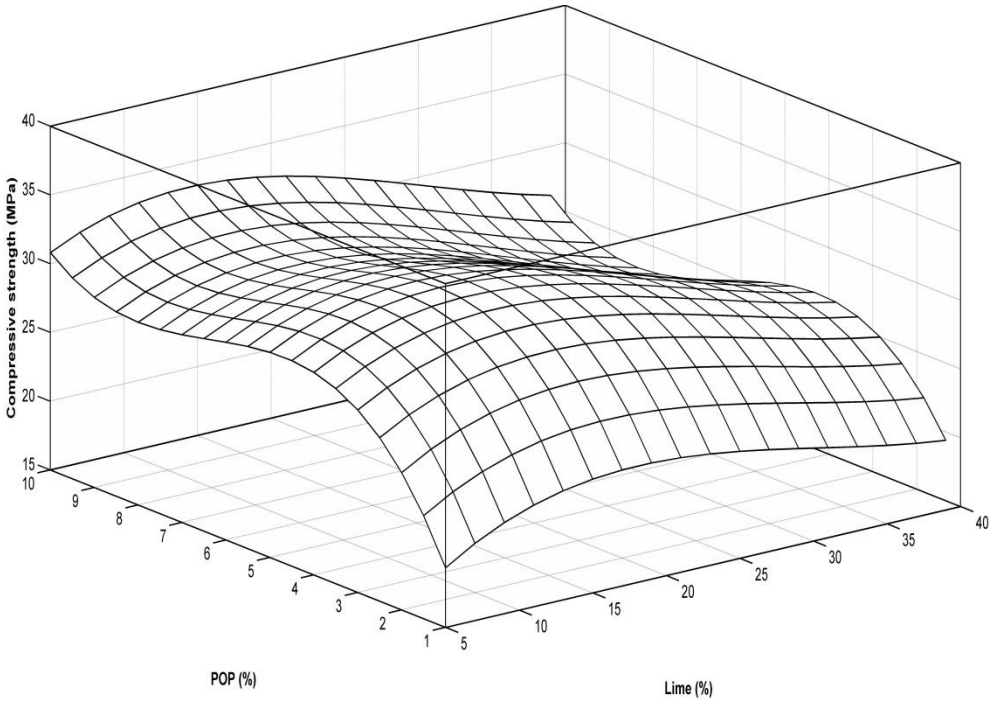

(a) Surface plot

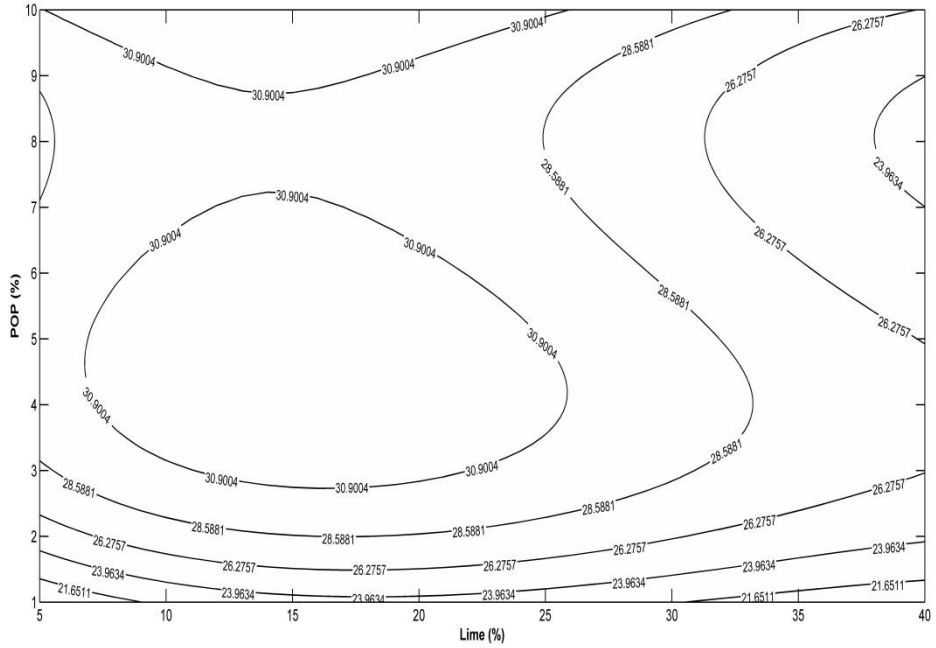

(b) Contour plot

Figure 5.13 Surface and contour plot for predicted compressive strength after 28 days of curing

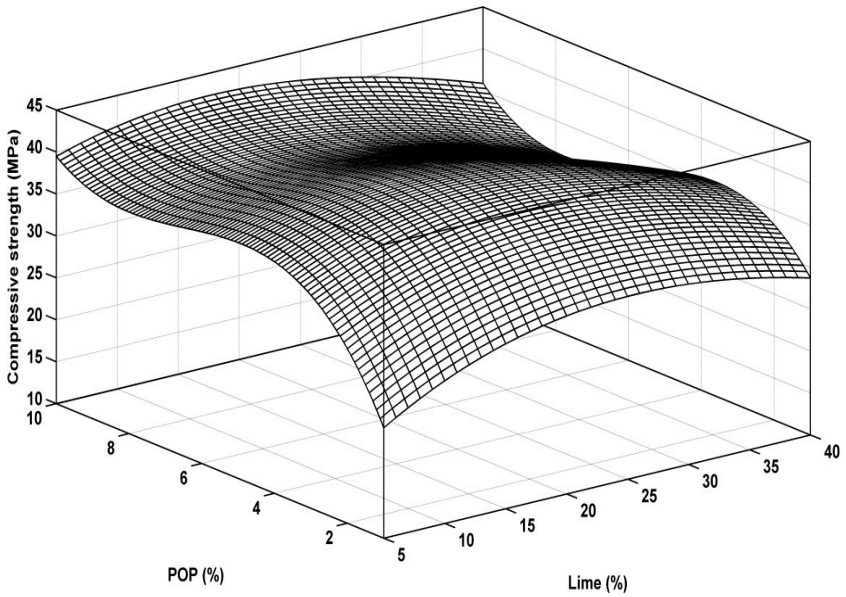

(a) Surface plot

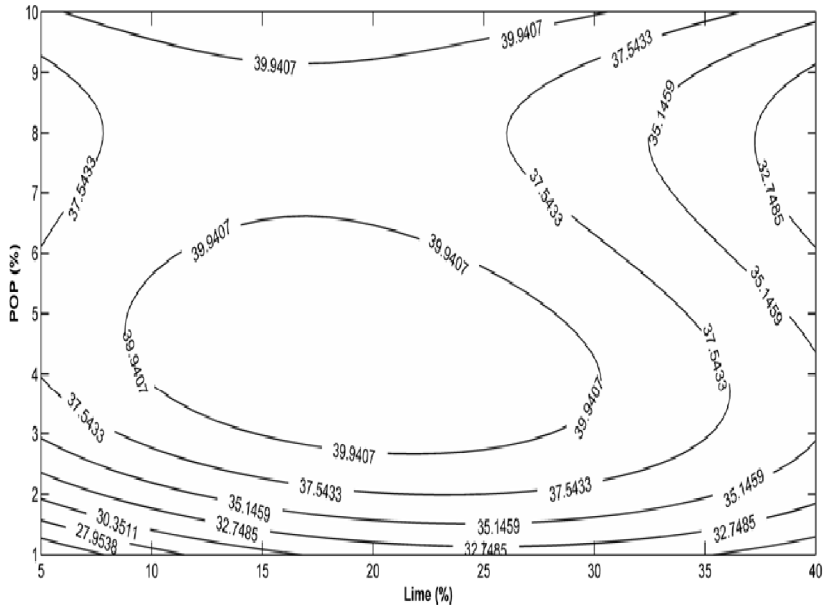

(b) Contour plots

Figure 5.14 Surface and contour plot for predicted compressive strength after 90 days of curing

5.5 POROSITY AND PORE SIZE DISTRIBUTION STUDY

The porosity and pore size distribution of mortar specimens prepared from reference binder and cured for 7, 28, and 90 days are presented in Figure 5.15. From this data it is observed that at 7 days curing, the sample has a porosity of 18.6%, which reduces to 13.2% and 10.7% at 28 and 90 days of curing respectively. The pores present in the sample range from 0.006 to 100 μm with abundance of smaller size voids (diameter < 0.01 μm) whereas the higher diameter pores are lesser in numbers. The porosity declines with increase in the curing period. In 28 days cured specimen, the total porosity is 13.2% with the gel pore (diameter < 0.01 μm) contributing about 1% and the capillary pores (diameter > 0.01 μm) contributing the rest that is 12.2%. In 90 days cured specimen the gel pore contributes about 0.6% and the capillary pores contribute the rest that is 10.1% of the total porosity of 10.7%. The above observations suggest that as the curing period increases the porosity as well as the pore size decreases. This is due to the formation and distribution of more hydration product like AFm, calcium silicate hydrated gel.

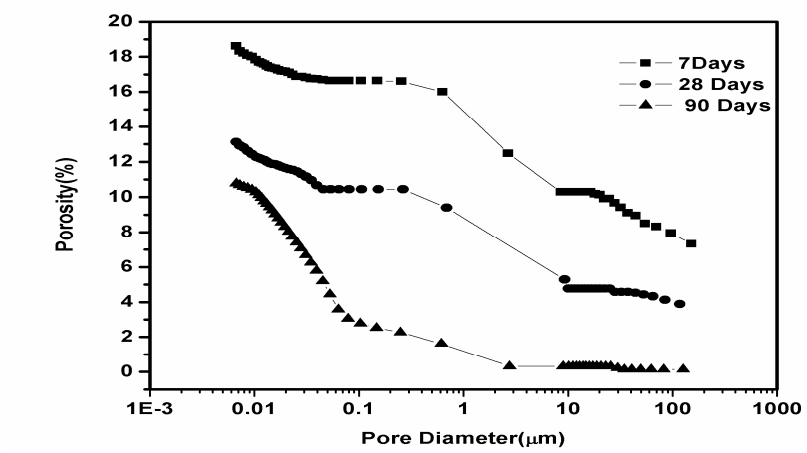

Figure 5.15 Plots between porosity and pore diameter of D5 sample at different curing periods

5.6 SUMMARY

The mechanical properties and optimization of raw material proportions of 36 mixes of slag-lime-POP are studied and presented in this chapter. The mechanical property in terms of compressive strength depends on amount and doses of activator such as POP and lime content. Optimization of raw material proportion has been carried out using response surface models and generalized reduced gradient algorithm and the results of optimized values are well comparable to the experimental values.

CHAPTER VI
RESULTS AND DISCUSSIONS III

6. EFFECTS OF ADMIXTURES

6.1 INTRODUCTION

This chapter presents the test results of experimental studies conducted to evaluate the effects of admixtures on the strength, microstructure, morphology, porosity and drying shrinkage behavior of blast furnace slag activated by lime and POP. The mineral admixtures/additives like silica fume(SF), fly ash(FA), glass powder (GP), ordinary Portland cement (OPC) and chemical admixtures like calcium acetate, calcium formate, calcium nitrate, sodium meta-silicate, sodium hydroxide were used in different proportions with the reference mix (D5). The test programme includes the determination of compressive strength of specimens after different curing periods. Further, the hydration products, microstructure, morphology and chemical bonds of few selected samples were studied and a correlation has been established between these properties with the compressive strength of the respective samples. In addition to this, the pore diameter and pore size distribution in the specimens were measured by mercury intrusion porosimetry test at curing periods of 7, 28 and 90 days for the reference mix and the mix containing different admixtures. The detailed test results are presented in the following sections.

6.2 MINERAL ADMIXTURES

Four different types of mineral admixtures/additives like silica fume, fly ash, glass powder, and OPC are used in this investigation. These are mixed to the reference

binding mixture in different proportions and cubical mortar specimens were prepared out of these new binders. In total 198 numbers of specimens were cast and tested after specified curing periods. Table 3.11 gives the detail proportions of admixtures used, the sample designation along with the compressive strength of specimens after different curing periods. The test results are presented in the following sub-sections.

6.2.1 Compressive strength

The curves in Figure 6.1 show the variation of compressive strength with the curing period for fly ash and OPC added specimens. Figure 6.2 represents the same for silica fume and glass powder added specimens. From these figures it is observed that the compressive strength increases non-linearly with the curing period for all specimens. The compressive strength of reference mix is found to be 33.7 and 42.3 MPa at 28 and 90 days of curing respectively. An addition of fly ash to the reference sample (Figure 6.1) results in an increase in strength up to fly ash content of 30%. Any further addition of fly ash beyond this, results in a fall of strength. The compressive strength of mortar with 30% fly ash is 46.8 MPa and 58.4 MPa at 28 and 90 days of curing respectively. The fly ash used in this test has a specific surface of 334 m^2/kg whereas; the same is 410 m^2/kg for reference binder. Hence, the common concept of fly ash acting as filler to micro voids is ruled out. However, the increased compressive strength of mortar specimen in fly ash added specimen may be attributed to the longer pozzolanic reaction. Bakharev *et al.* (1999) reported a reduction in compressive strength in mortar specimen when the amount of fly ash added to slag activated with 8% liquid sodium silicate is more than 30%.An addition of 5% cement increases this strength to 34.7 and 51.1 MPa and 10% OPC gives a compressive strength of 36.7 and 54.8 MPa respectively. This shows that an addition of

OPC beyond a certain quantity does not improve the strength remarkably. A similar observation was reported by Douglas and Brandstetr (1990) upon addition of OPC in blast furnace slag activated with sodium silicate solution.

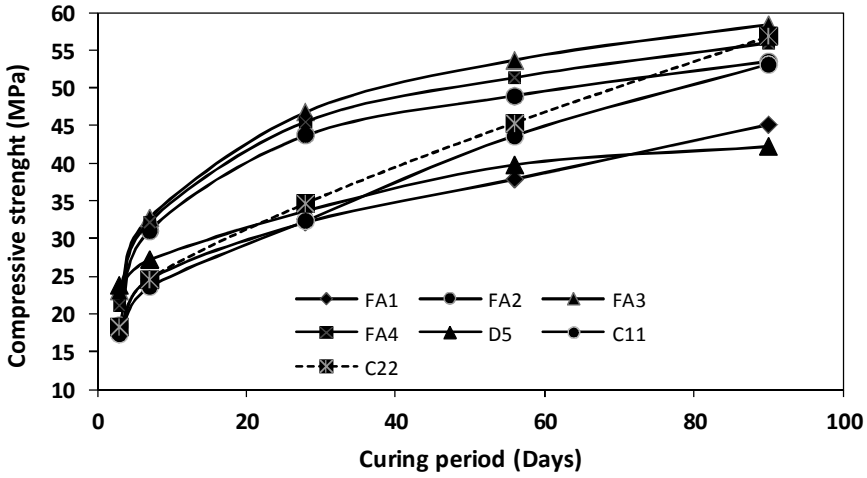

Figure 6.1 Variation in compressive strength with the curing period for fly ash and OPC added specimens

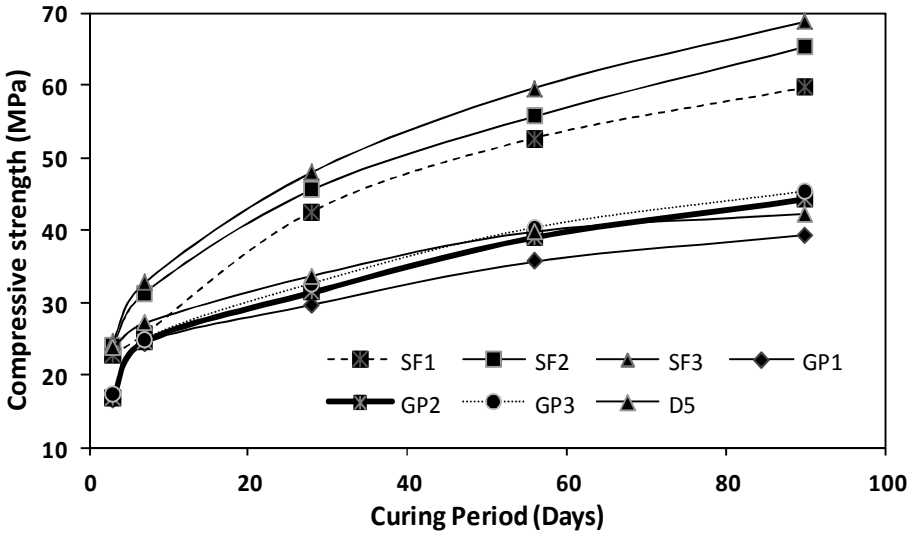

Figure 6.2 Variation in compressive strength with the curing periodfor silica fume and glass powder added specimens

The curves (Figure 6.2) for compressive strength are found to increase both with the curing period and silica fume content. An addition of 5, 10 or 15% silica fume results

in compressive strength of 40.6, 44.6 or 47.0 MPa after 28 days of curing and 59.7, 65.3 or 68.8 MPa after 90 days of curing respectively. This shows a substantial increase in compressive strength upon addition of silica fume. The ultra-fine silica fume with specific surface area of 17256 m^2/kg might act as filler to the pore structure of the mortar. In addition, the increase in strength is attributed to the formation of more quantity of C-S-H gel in the specimen. However, no substantial change in compressive strength is observed when glass powder is added. This may be attributed to the low specific surface area (210 m^2/kg) of the glass powder. A similar result has been reported by Shayan (2004) and Schwarz (2008) that the strength decreases with addition of admixtures with lesser fineness.

6.2.2 Hydration products, microstructure and morphology

The hydration products, morphology and chemical bondformed during the hydration process were studied using XRD, SEM, and FTIR analysis. The XRD pattern of reference sample added with 15% silica fume is shown in Figure 6.3 for different curing periods. A series of compounds such as calcite, quartz, calcium silicate hydrated, and gypsum are found in the hydrated specimens. As the curing period increases, the hydration products or phases are intensified. The crystalline peaks of gypsum, quartz, calcium hydroxide, calcite and amorphous hump of calcium silicate hydrate (C-S-H), appeared at 3 days of curing. Presence of un-reacted lime and gypsum are found in the specimen. As the curing period increases amount of free lime and gypsum diminishes. The peak for quartz almost remains the same for 28, 56, and 90 days cured samples; however, the quartz peak in 3 days cured sample is somewhat smaller with a broad base. In addition to the primary peak of C-S-H, secondary peaks of C-S-H are observed in the

samples cured for longer periods. Specimens cured for longer periods show wide base corresponding to amorphous C-S-H phase.

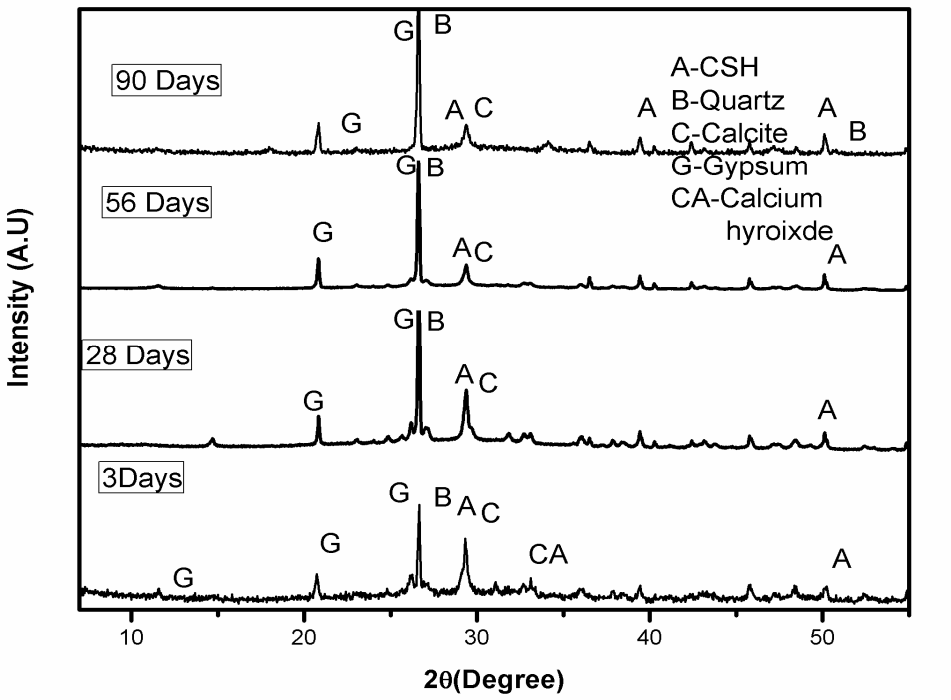

Figure 6.3 XRD patterns of SF3 specimens cured for different periods

The XRD patterns of the specimens, added with different admixtures are shown in Figure 6.4 after a curing period of 90 days. More intensified peaks of C-H-S are found in specimens containing glass powder and OPC. However, the peaks of GP2 and C22 samples at 2ɗ of 29.5^{o} contain C-S-H, wollastonite, additionally hillebrandite is present in GP2 sample whereas other samples at this position mostly give the C-S-H phase. The wide amorphous hump corresponding to C-S-H compounds are found in specimens containing fly ash and silica fume as compared to other specimens. This may be due to the presence of ultra-fine amorphous silica particles in these samples. The formation of more amount of C-S-H resulted in an increase in strength for the specimens containing these admixtures. Qualitative analysis of C-S-H gel (PDF-00-043-1488) in the specimens

was made using X'Pert High Score Plus software which shows that the content of C-S-H gel is more in FA3 specimen followed by C22, SF3 and GP3. It is noted that even though the percentage of C-S-H gel in SF3 sample is slightly lower than other specimens, it registers a high compressive strength. This is mainly due to the low porosity, higher mass density of hydrated sample and homogenous distribution of C-S-H gel in the mass. The diminished intensity of calcium hydroxide peaks with an increased curing time for samples SF3 and FA3 is an indication of participation of calcium hydroxide in hydration process and formation of more amount of C-S-H gel.

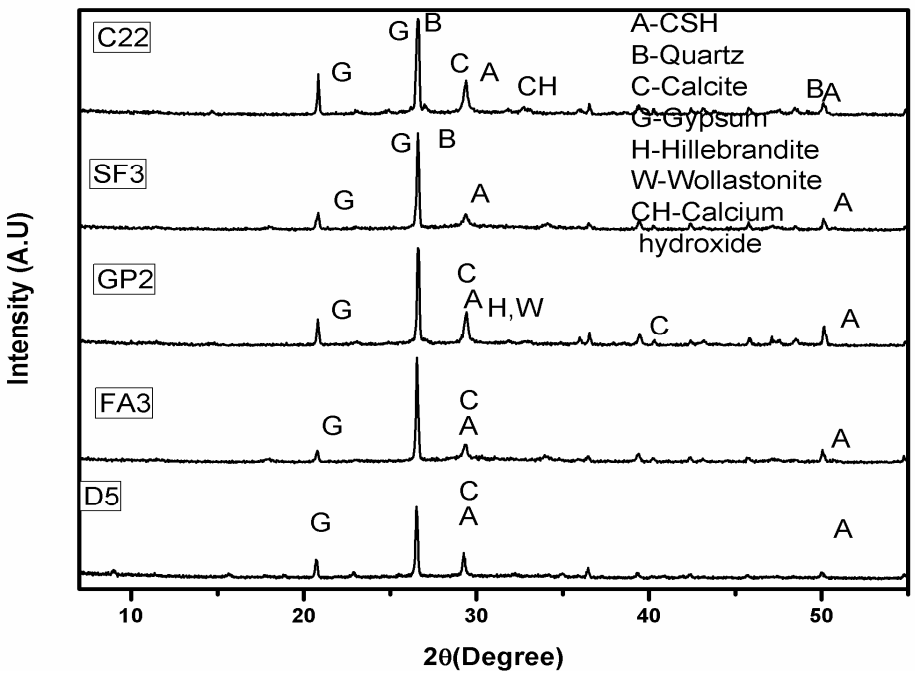

Figure 6.4 XRD patterns ofmortar specimens cured for 90 days

The microstructure and hydration products of specimens cured for different periods are studied using SEM analyzer. Figure 6.5 shows the microstructure of SF3 specimens cured for different periods. Abundance of needle-like structures are found in the specimens cured for 3 days. Usually needle like crystals appeared during the early period of hydration. As curing proceeds the needle shaped crystals are seen wrapped with

gel like substances of calcium silicate hydrate. A further increase in the curing period resulted in an increase of crystal concentration and more C-S-H gel appeared. This results in an increase in strength and hardness of specimens. At early curing periods, in some areas, more solid hydrated products appeared while other smaller areas are found porous with inhomogeneous distribution of hydration products and voids. However, at later days of curing; common fibrous type of irregular grains forming a reticular network of calcium-silicate-hydrated gel is found. The 90 days cured sample is fully filled with a fibrous network of calcium-silicate-hydrate. The presence of this hydration product results in enhancing the strength of mortar sample. The SEM analysis shows compounds that are identified earlier from XRD analysis.

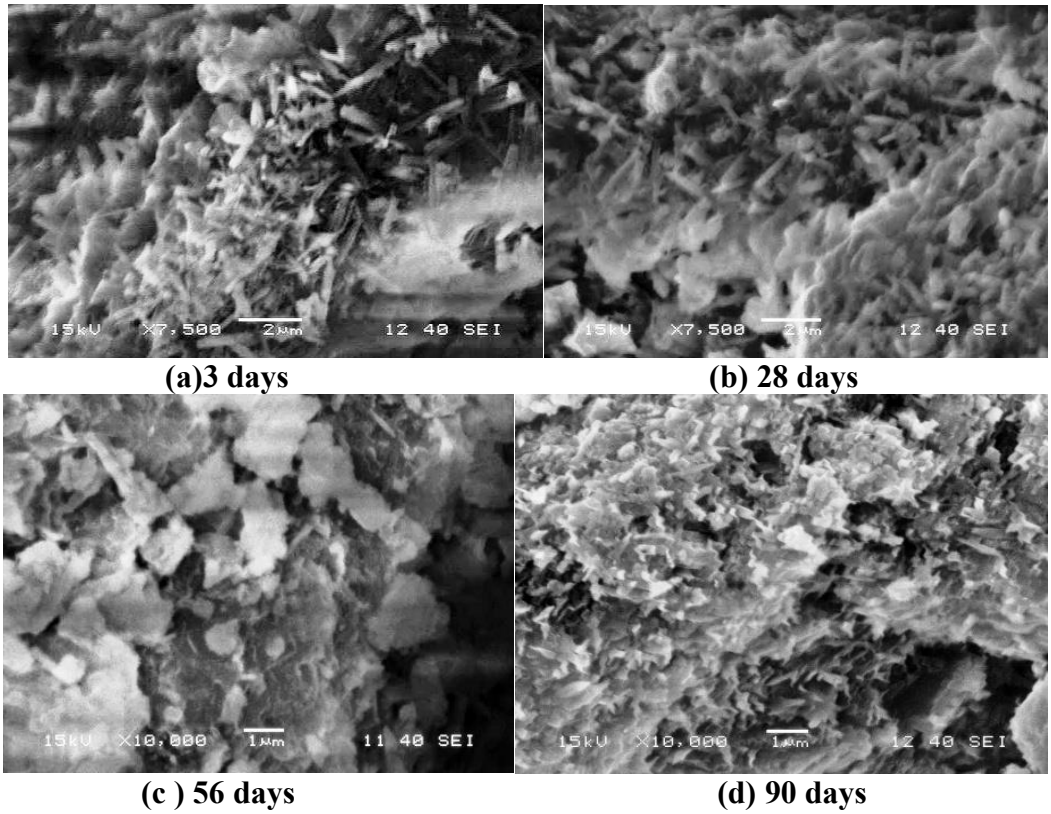

(a)3 days **(b) 28 days**

(c) 56 days **(d) 90 days**

Figure 6.5 Microstructure of silica fume added specimen for different curing periods

The SEM images of reference sample and the specimens added with fly ash, silica fume, glass powder, and OPC at 90 days curing period are shown in Figures 6.6 and 6.7. The microstructure images show that the silica fume containing specimen is more homogenous, uniform and dense as compared to other samples. The C-S-H gel is found to be evenly distributed over the mass and the voids diameters as well as numbers are much smaller. On the other hand, the fly ash added sample shows an abundance of calcium alumino-silicate hydrates and aggregation of C-S-H. This mostly imparts strength to the sample. In glass powder added sample, needle shaped mono-sulphate aluminate (AFm phase) and C-S-H gel are found. However, the structure is not dense as compared to silica fume sample. Further, it is seen that the structure is neither homogeneously distributed nor are the products themselves homogeneous.

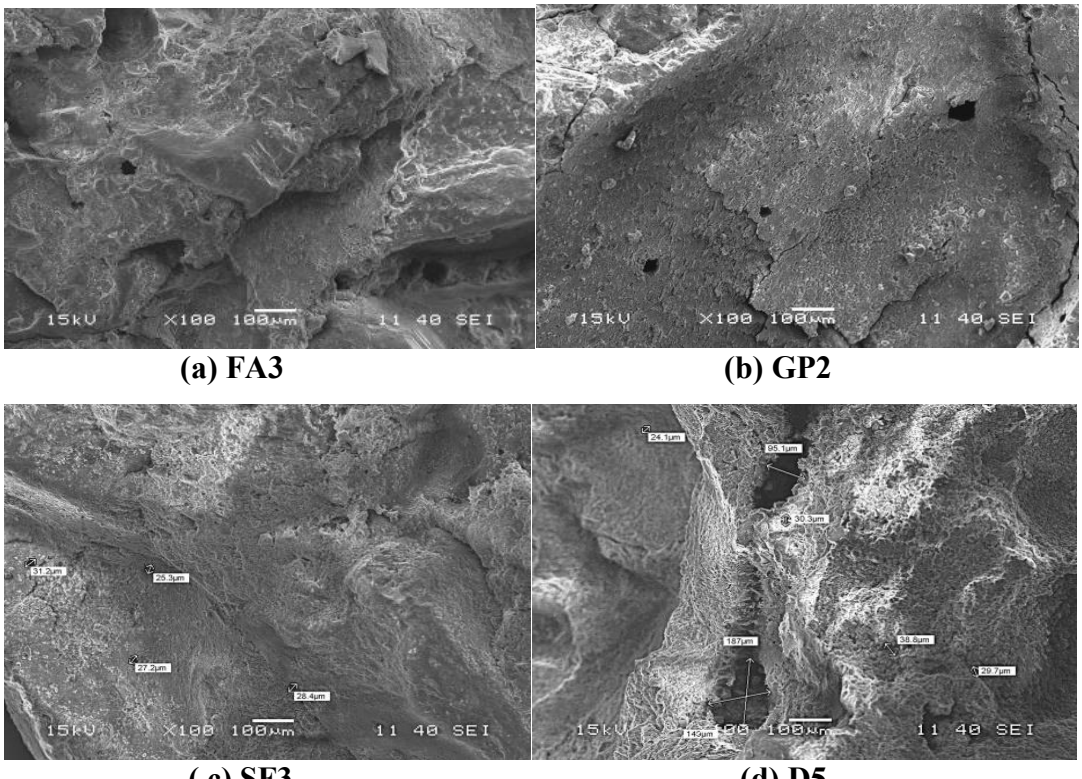

(a) FA3 **(b) GP2**

(c) SF3 **(d) D5**

Figure 6.6 Surface morphology for specimens after 90 days curing

For instance, in some areas more solid hydrated products appear while other areas are highly porous. The OPC added sample shows fibrous C-S-H gel and plate shaped calcium hydroxide phases. The SEM image of reference sample shows uneven distribution of hydration products, some unreacted slag powder, and smaller quantities of calcium silicate hydrate. The ultimate structure of hydrated cement at the micrometer scale is that of C-S-H, which is considered to be responsible for the strength of samples, and the structure of C-S-H plays an important role in revealing the mortar strength and other physical properties.

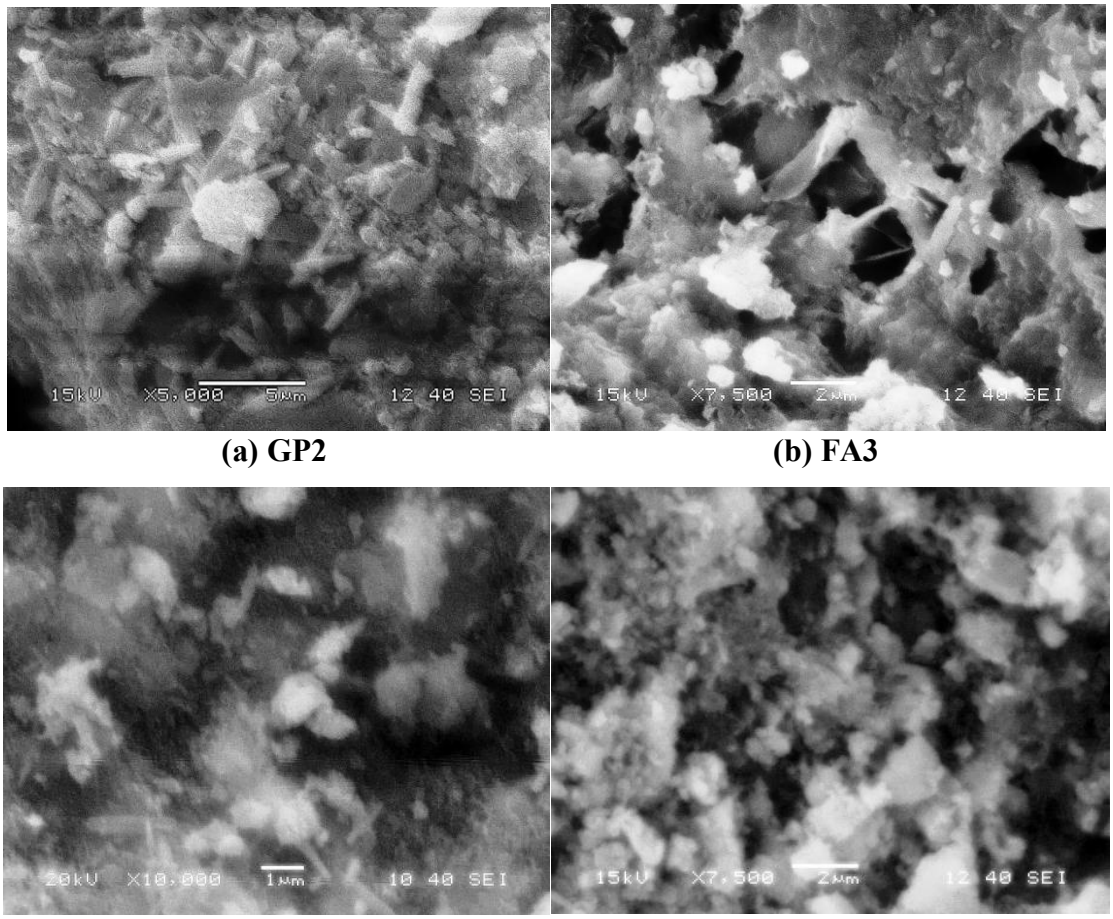

(a) GP2 **(b) FA3**

(c) D5 **(d) C22**

Figure 6.7 Microstructures of mortar specimens cured for 90 days

The FTIR spectra of SF3 specimen cured for different periods are shown in Figure 6.8. The spectrum shows bands at 990-960 cm^{-1} corresponding to the stretching vibration of Si-O-Si and at 458-464 cm^{-1} associated with bending vibration. The bending vibration band characteristic for O-H is banded at wave number 882 cm^{-1}. The stretching vibration band of O-H is banded at wave number of 3375-3448 cm^{-1} due to the presence of calcium hydroxide phase. The presence of peak at 1456-1498 cm^{-1} is due to the bonding in CO_3^{2-} ions, indicates the presence of some sort of carbonated mineral, possibly due to the absorption of CO_2 from the atmosphere. The Si-O bond is found to shift towards higher frequency with increase in curing period. The stretching band of time indicating the progress of the hydration process and the formation of more calcium silicate hydrated gel during the reaction. Especially, at 90 days curing the spectra of C-O bond shows weaker double peaks at wave length 2500 cm^{-1}.

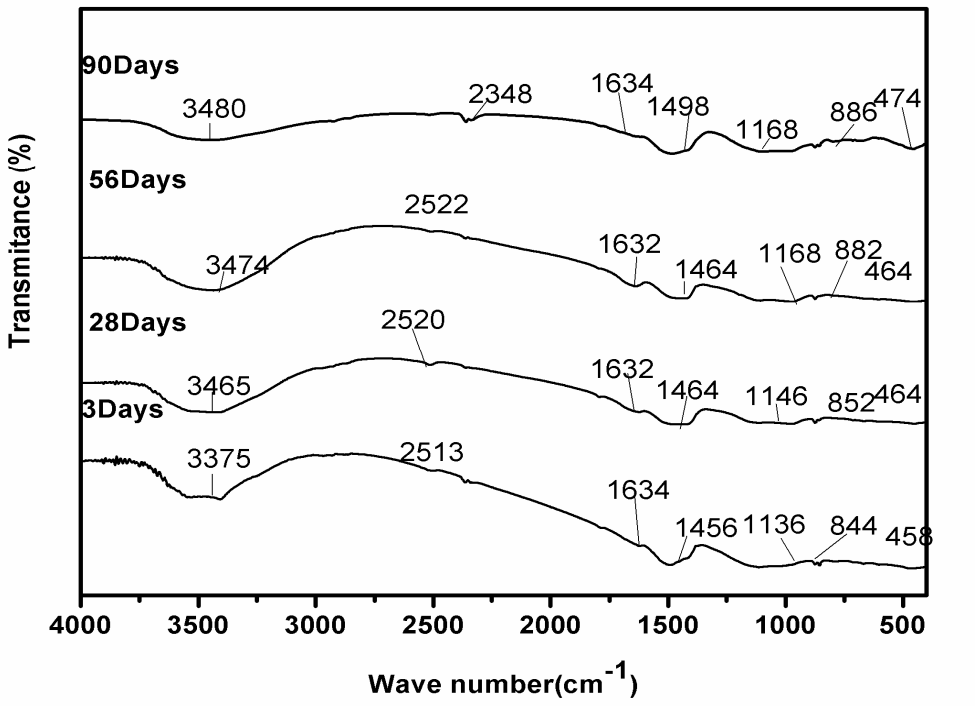

Figure 6.8 FTIR spectra for SF3 specimen after different curing periods

The FTIR spectra of the 90 days cured samples of the reference binder and the reference binder added with admixtures are given in Figure 6.9. The FA3 of sample has band at 3433, 1626, 1517, 1144, 1004, 797, 663, and 457 cm^{-1}. The band appeared at 3433 and 1144 cm^{-1} is associated with O-H bond and indicates the formation of mono-sulphate aluminate (AFm) phase and the broadband at 1626 -1517 $cm^{-1}$is also the characteristics for AFm phase. The band at 474 cm^{-1} is associated with O-Si-O or O-Al-O bond bending vibration. Silica fume contained sample (SF3) has shown the band at 3464, 1616, 958, 872, and 446 cm^{-1}. The band at 3461 and 1616 cm^{-1} are associated with O-H and S-O bond respectively, but the consumption of sulphate is found to be less, as compared to FA3 specimen. This indicates the formation of C-S-H gel is more than the AFm phase in SF3 as compared to FA3 and vice versa. A similar observation has also been reported by Sakulich (2010), Ramachandran (2001) and Taylor (1997). The low frequency band of

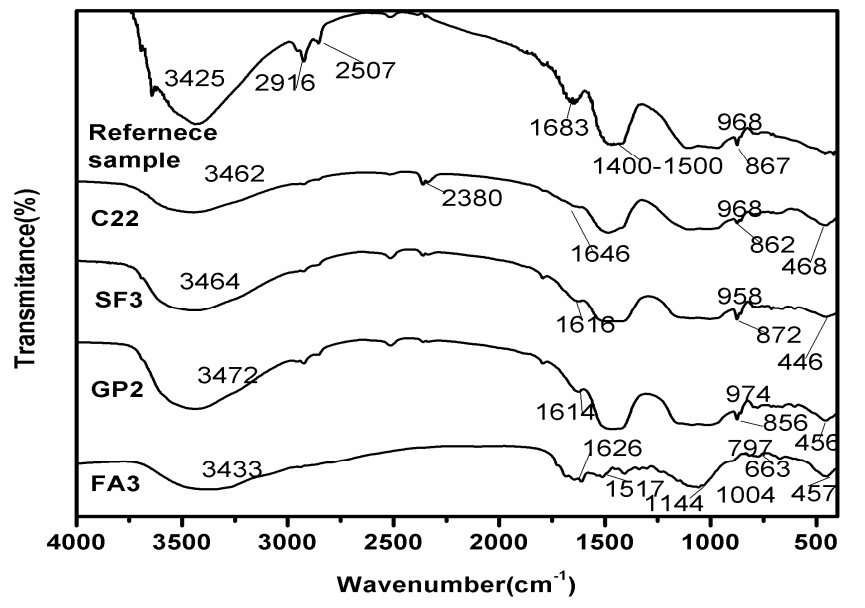

Figure 6.9 FTIR spectra for specimens containing different admixtures after 90 days of curing

446 cm-1 is the characteristics of v4-SiO4 and it indicates the formation of O-Si-O bond. As compared to other specimens, the v4-SiO4 bond of SF3 specimen is found to shift more towards lower frequency. This indicates that larger quantity of silica taking part in the reaction.

The hydration mechanisms for the binder containing different admixtures were analyzed by thermo-gravimetric analysis and the hydration products formed are shown in Figure 6.10. Differential scanning calorimeter (DSC) curve exhibits an endothermic peak at 92 ^{o}C to 206 ^{o}C for all samples. The results of thermo-gravimetric analysis (TGA) show the mass loss of 3.75, 2.69, 3.7, 2.1 and 3.67% for SF3, OPC, FA3, GP2 and D5 specimens in the above temperature range. There is also a mass loss peak related to the decomposition of uncombined calcium hydroxide between temperature range of 400 ^{o}C to 551 ^{o}C in reference sample and OPC added samples, and the occurrence of a mass loss peak due to the decomposition of un-reacted calcium carbonate at temperatures range 560 ^{o}C to 794 ^{o}C. The mass losses in the temperatures range from 560 ^{o}C to 794 ^{o}C are 6.4, 4.58, 6.1, 9.61 and 7.01% for GP2, SF3, FA3, OPC and D5 specimens respectively. The SF3 sample mixture presents an expressive loss of mass between 92 ^{o}C and 220 ^{o}C related to the decomposition of gypsum, calcium silicate hydrate. The total mass loss in SF3 samples are 3.5% and3.75% for curing periods 28 and 90 days respectively. The mass loss is found to increase with the curing period of samples which attributes the formation of C-S-H and causes gain in strength after longer curing of samples.

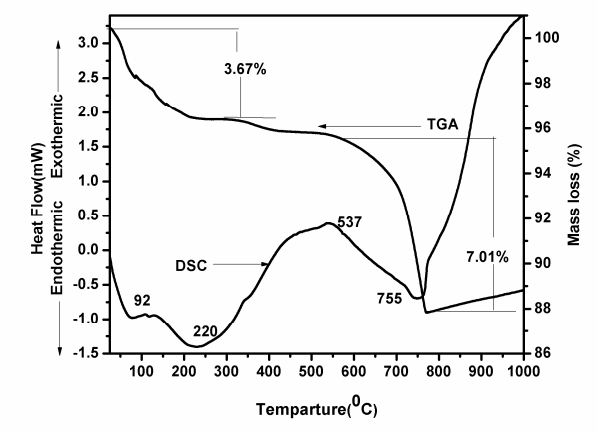

(a) D5 after 90 days curing

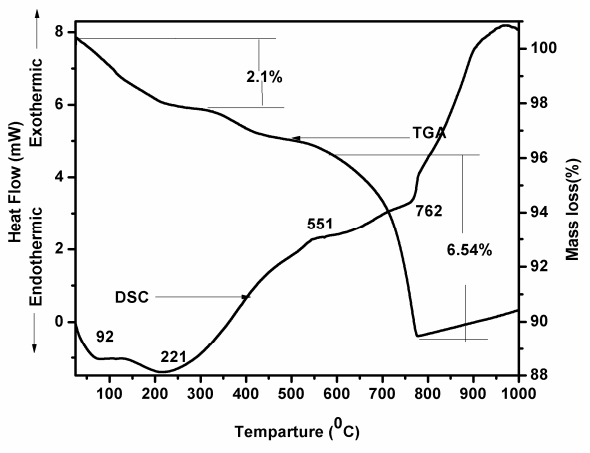

(b) GP2 after 90 days curing

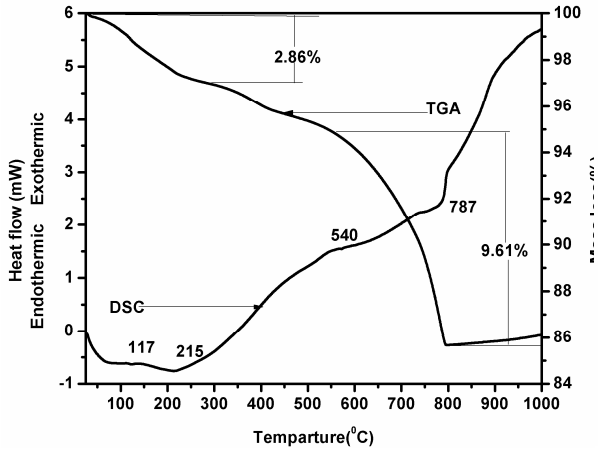

(c) C22 after 90 days curing

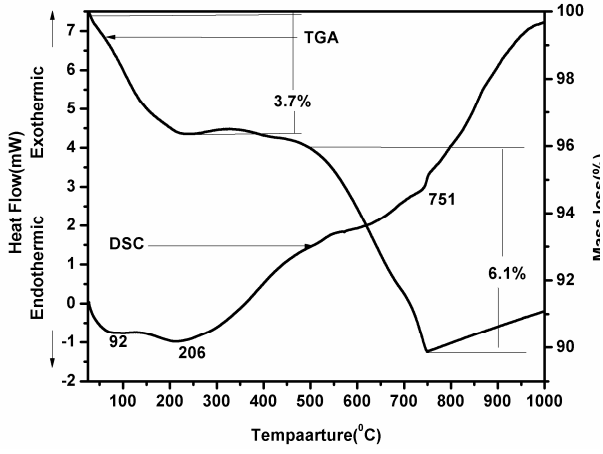

(d) FA3 after 90 days curing

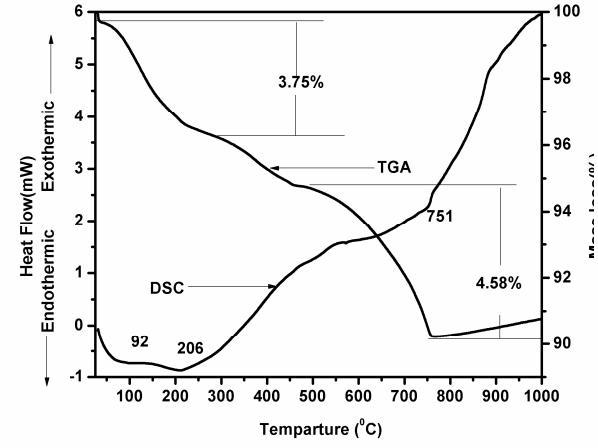

(e) SF3 after 90 days curing

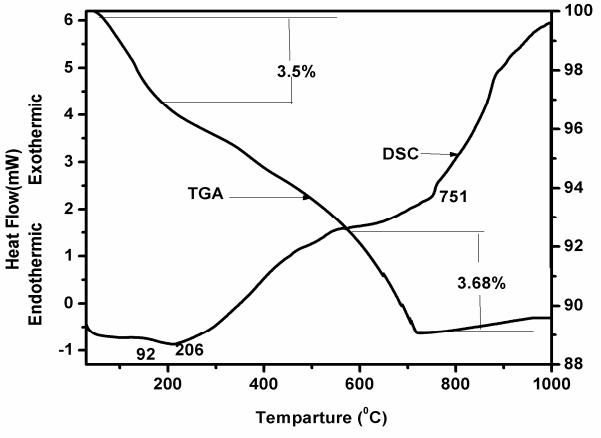

(f) SF3 after 28 days curing

Figure 6.10 DSC and TGA curves for specimens containing different mineral admixtures

6.2.3 Porosity and pore size distribution

The relationship between porosity and pore diameter of SF3 sample is presented in Figure 6.11. The porosity and pore size is found to reduce with an increase in curing period. The pores are distributed in sizes varying from 0.006 to 100 μm. The porosity of 7 days cured sample is 14.8%. However, the smaller size pores (diameter <0.01 μm) contribute only 3.2% to total porosity. The other significant difference between the reference sample and SF3 sample is the distribution of pore size at a given curing period. The reference sample shows the presence of large number of pores of higher diameter than the SF3 sample. The porosity of SF3 changed from 10.06 to 7.5% with an increase in the curing period from 28 to 90 days. Silica fume added samples exhibit a significant lower measured porosity than that of the reference sample for both gel pore and capillary pore.

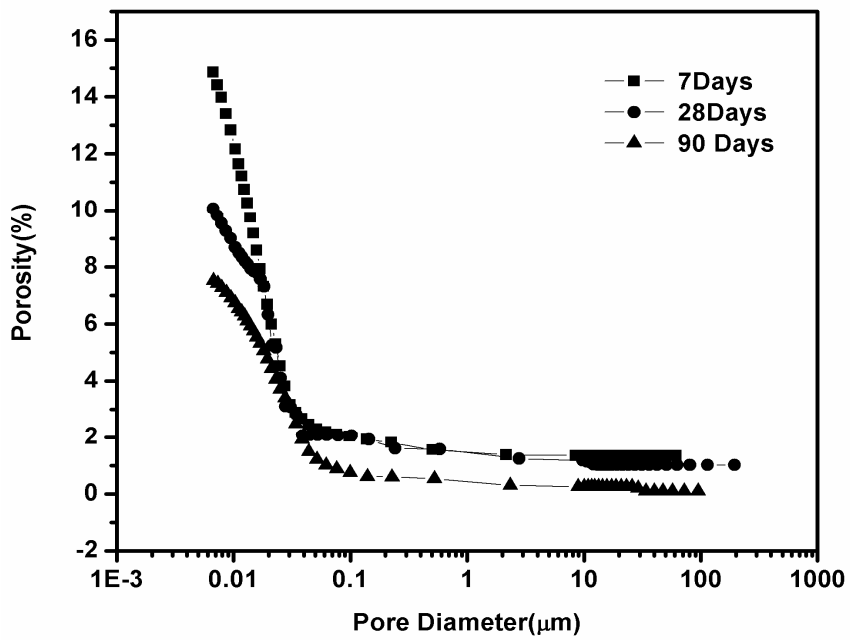

Figure 6.11 Porosity and pore size distribution in SF3 sample after different curing periods

The porosity and pore size distribution of reference sample and reference sample with different admixtures after 90 days curing period are presented in Figure 6.12. It is found that the pores are distributed in sizes varying from 0.006 to 100μm. However; the pores in SF3 specimen are more uniformly distributed over the measured pore size range from 0.1 to 100 μm.The porosity and pore size distribution for samples containing fly ash are almost identical with the reference sample, both showing the same porosity and identical distribution of pore size in the sample. SF3 mortar has lowest porosity among all five mortar samples for a given curing age. SF3 specimens also showed uniformly distributed pores over the measured pore size range. This shows that silica fume acts as a filler material in the reference sample and helps in homogenizing the specimen. The higher mechanical strength of SF3 specimen may be attributed to the above factor.

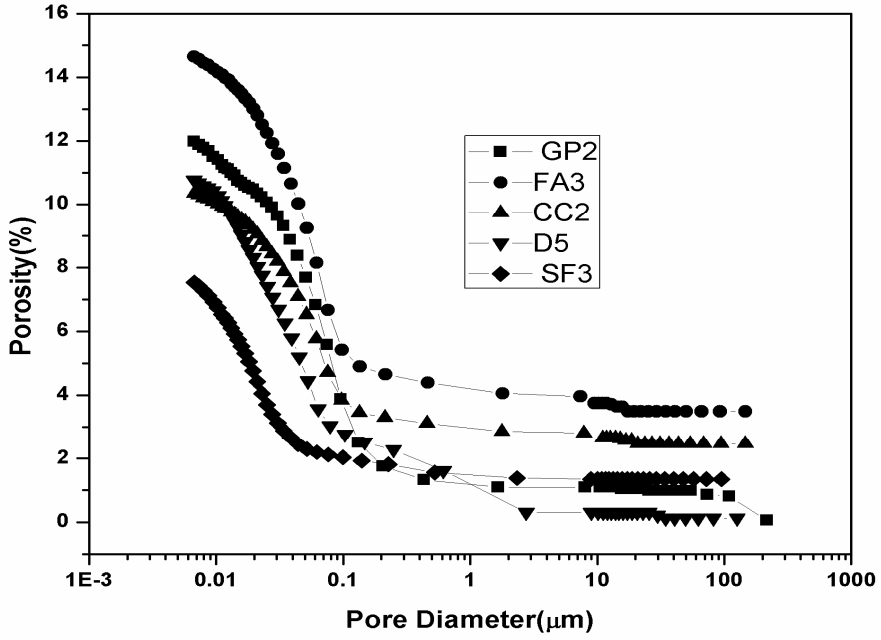

Figure 6.12 Porosity and pore size distribution in mortar specimens containing different admixtures after 90 days of curing

6.2.4 Drying shrinkage behaviour

The drying shrinkage behaviors of D5 specimen and D5 specimen with mineral admixtures like fly ash and silica fume were determined after curing periods of 3, 7 and 28 days. These are presented in Figure 6.13. It is seen that an addition of mineral admixtures reduces the drying shrinkage value. The minimum value is found for specimens added with silica fume and the highest value is for the reference mortar. The drying shrinkage values of all the specimens are found to increase with the curing period.

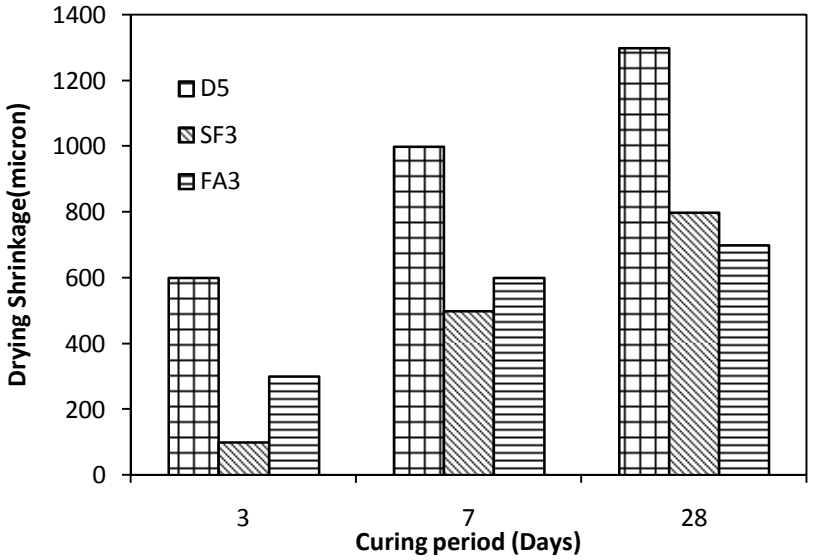

Figure 6.13 Drying shrinkage of specimen with mineral admixture for different curing period

6.3 CHEMICAL ADMIXTURES

Five different types of chemical admixtures such as calcium formate, calcium acetate, sodium-meta-silicate, calcium nitrate, and sodium hydroxide are used in this investigation. These are mixed to the reference binding mixture in different proportions and mortar the specimens were prepared. A total 780 numbers of mortar specimens were cast and strength of mortar cubes was determined after 3, 7, 28, 56 and 90 days of curing

period. Table 3.12 gives the detail proportions of chemical admixtures used, the sample designation along with the compressive strength of mortar specimens after different curing periods. The test results are presented in the following sub-sections.

6.3.1 Compressive strength

The relationship between compressive strength and curing period of specimens with different chemical admixtures are presented in Figures 6.14 to 6. 18. The result indicates that the addition of calcium based chemical admixtures give lower strength at early period and at later period results higher strength. But sodium based admixtures give equal or same strength as reference sample in both early and later curing period. The addition of calcium acetate and sodium-meta-silicate is able to increase the final strength at lesser percentages that is 2 and 0.5% respectively. The samples with 0.5% sodium-meta-silicate and 2% calcium acetate give the maximum strength which are 44 and 58 MPa respectively at 90 days. The results show that the addition 1% of calcium nitrate and gave 48 MPa at 90 days and an excess addition of admixtures decreases the strength.

The effect of sodium meta-silicate on the strength of lime activated slag cement was studied by varying its contents as 0.5, 1, 2 and 4 %. The result is presented in Figure 6.14. From this figure, it is observed that the compressive strength is increased by the addition of sodium meta-silicate and 0.5% sodium meta-silicate gives the highest strength at 90 days. From the results it observed that there are no changes in strength by addition of sodium meta-silicate beyond 0.5%. A higher dose of chemical reduces the strength. The reduction of strength might be due to presence of sodium calcium sulphate.

The effect of calcium acetate on the strength of lime activated slag cement was studied by varying its contents as 0.5, 1, 2 and 4 %. The variation of compressive strength with curing period for different proportions of admixture is presented in Figure 6.15. From this figure, it observed that the compressive strength is increased with addition of calcium acetate up to 2% and after that the strength falls. A further increase in the content of calcium acetate results in a reduction of strength. The higher strength might be due to high calcium ion concentration in the pore solution which increases the pH and accelerates the reaction of the mix. The high calcium concentration is directly responsible for activation of the slag.

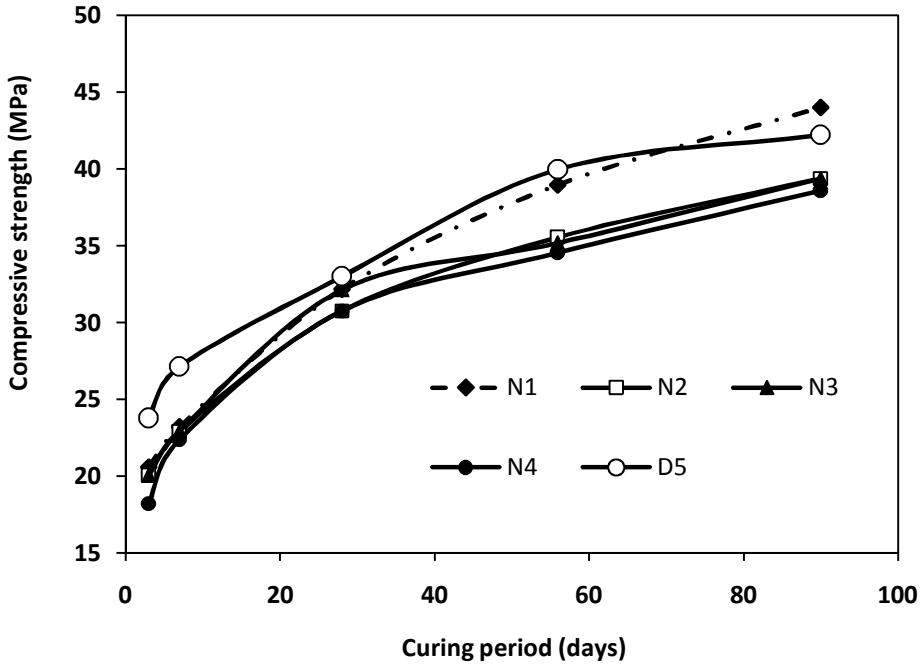

Figure 6.14 Variation in compressive strength with the curing period for sodium meta-silicate added samples

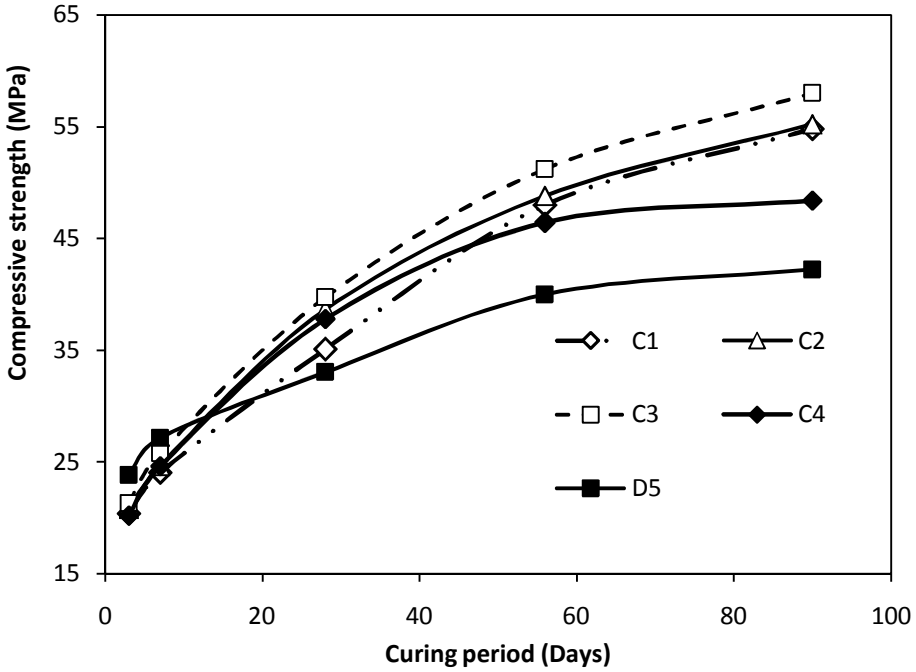

Figure 6.15 Variation in compressive strength with the curing period for calcium acetate added samples

The variation of compressive strength with the curing period for calcium formate added samples is presented in Figure 6.16. Similarly, in this case also the strength is improved with addition of calcium formate up to 2% after that the strength decreases in the same way as observed for calcium acetate. From Figures 6.15 and 6.16, it is observed that the compressive strength is increased by the addition of calcium acetate and calcium formate up to 2%. The chemical admixture, calcium acetate seems to be more reactive than the calcium formate. At 2% chemical content calcium acetate specimen gave 13.7% higher strength than calcium formate for 90 days curing period. The maximum strength of mortar specimens is 51.12 MPa for optimum dose of calcium formate.

The variation of compressive strength with the curing period is presented in Figure 6.17 for specimen containing calcium nitrate. The calcium nitrate was varied as

0.5, 1, 2, and 4 % to the reference binder mix. From this figure, it is observed that the strength of specimens is declined with increase of amount in calcium nitrate. However, an increase in curing period results in an increase in the compressive strength. One percent calcium nitrate in the reference binder gave the strength of 49.6 MPa for 90 days cured mortar specimens, which is the highest strength among all these proportions. A reduction in the compressive strength of mortar specimens is observed for specimens added with different amounts of calcium nitrate at early days of curing.

The effect of sodium hydroxide on compressive strength of lime activated slag cement was studied. The variation in compressive strength for reference specimen and specimen added with 0.5, 1, 2, and 4 % sodium hydroxide content with different curing period is presented in Figure 6.18. From this figure, it observed that the compressive strength increases with the addition of sodium hydroxide and 1% sodium hydroxide gives the highest strength after 90 days curing that is 48.8 MPa.

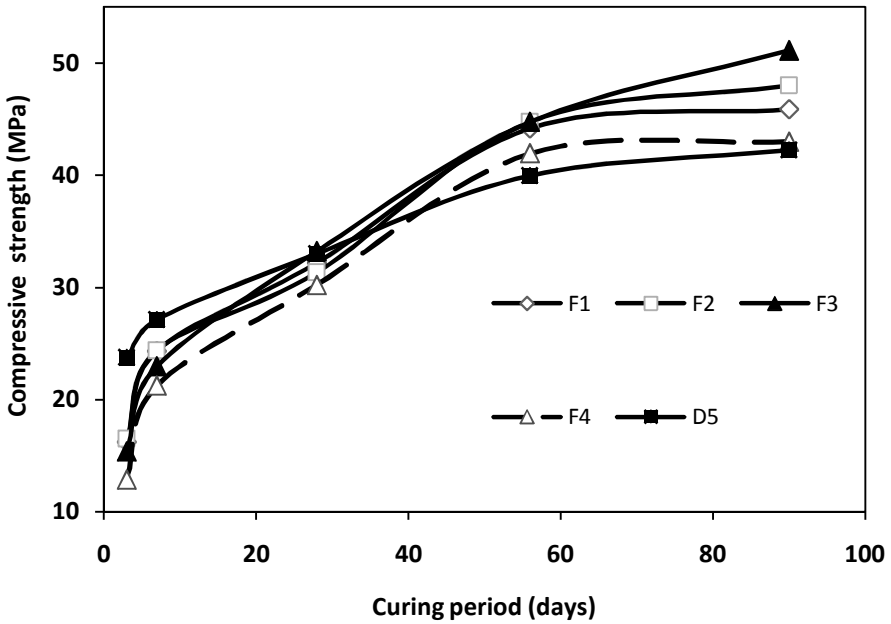

Figure 6.16 Variation of compressive strength with the curing period for calcium formate added samples

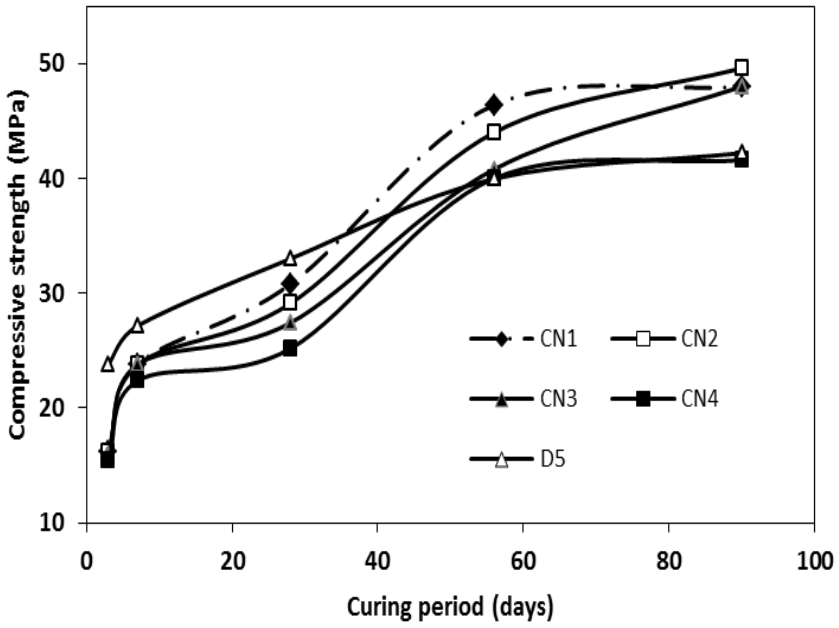

Figure 6.17 Variation in compressive strength with the curing periodfor calcium nitrate added samples

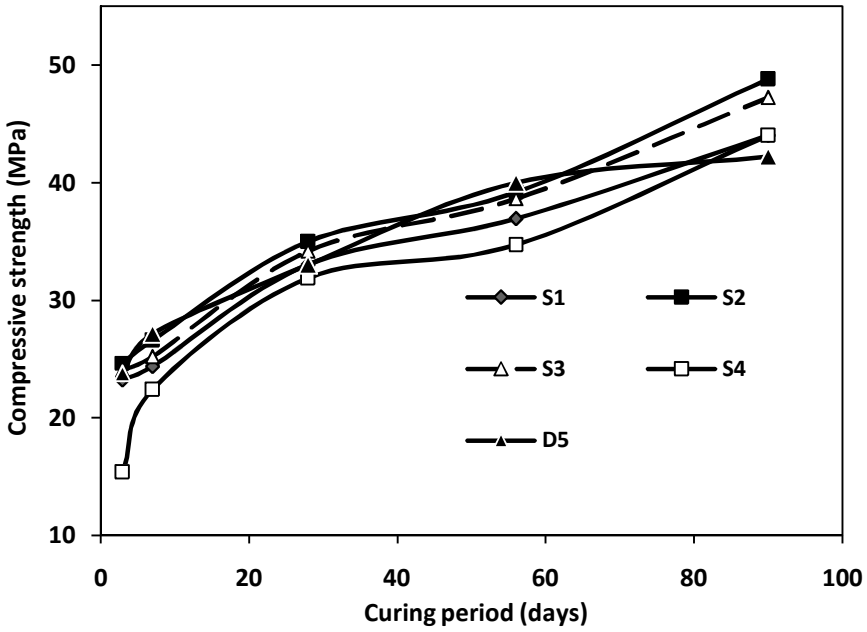

Figure 6.18 Variation in compressive strength with the curing periodfor sodium hydroxide added samples

6.3.2 Hydration products and microstructure

The hydration products, morphology and chemical bond during the hydration period were studied by using XRD, SEM and FTIR analysis. The XRD pattern of different sample added with chemical admixture is shown in Figure 6.19. A series of crystalline and amorphous compounds such as qartz, aragonite, sodium-calcium-sulphate, calcium sulphate hydrate gismondine, gypsum and calcium silicate hydrated are found in the hydrated specimens. In calcium acetate and calcium formate specimen, the chemical compounds such as aragonite, gismondine, calcium silicate hydrate, and gypsum are found. In the sample added with sodium meta-silicate, sodium-calcium-sulphate, and calcium sulphate hydrate including phases like CSH and gypsum are obtained. Similarly, specimens containing sodium hydroxide showed same chemical compounds as that observed with sodium meta-silicate specimens. The strength may be equal or lesser than the reference specimen due to formation of sodium-calcium-sulphate in sodium based salt specimen.

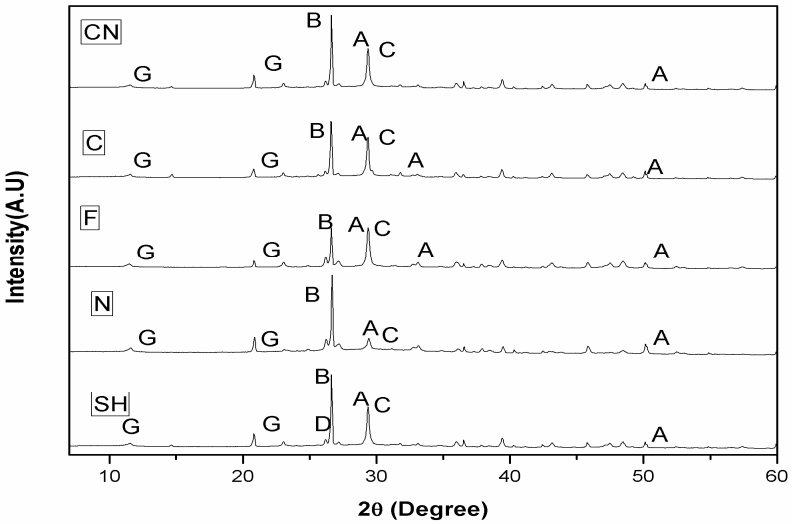

Nomencleture: A-CSH, Sodium calcium sulphate, C-Aragonite, B-Quartz, D-Gismondine G-Gypsum

Figure 6.19 XRD patterns for chemical admixture added specimen after 90 days curing

The microstructure and hydration products of specimens containing different chemical admixtures and cured for 90 days are studied using SEM analyzer. Figure 6.20 shows the abundance of needle and gel like structures in all specimens.

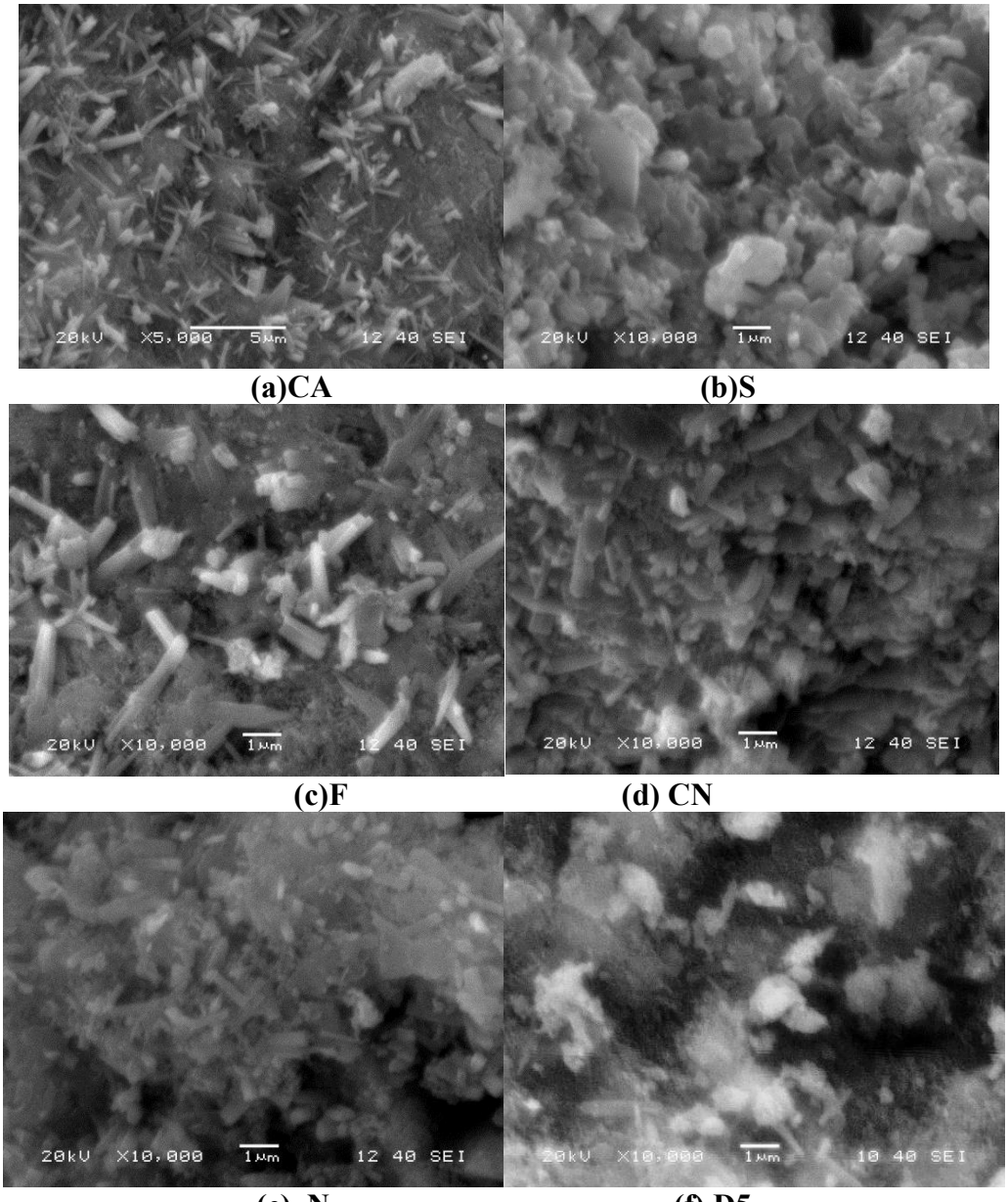

(a)CA **(b)S**

(c)F **(d) CN**

(e) N **(f) D5**

Figure 6.20 SEM images for chemical admixture added specimen after 90 days curing

The needle shaped crystals are seen wrapped with gel like substances of calcium silicate hydrate. In specimen containing calcium acetate and calcium formate, the microstructure is filled with needle shaped and gel like substances. These substances might be Aft phase and calcium silicate hydrate respectively. The presence of these hydration products enhances the strength of sample. However, in sodium based specimen like sodium meta-silicate and sodium hydroxide, lesser quantity of needle shaped Aft phase and common fibrous type of irregular grains forming a reticular network of calcium-silicate-hydrated gel are found. The reference sample shows uneven distribution of hydration products, some unreacted slag powder, and lesser quantities of calcium silicate hydrate. This results in lower compressive strength in mortar specimens containing sodium based chemicals as compared to calcium based specimens.

The FTIR spectra of mortar specimens containing different chemical admixtures and cured for 90 days are given in Figure 6.21.

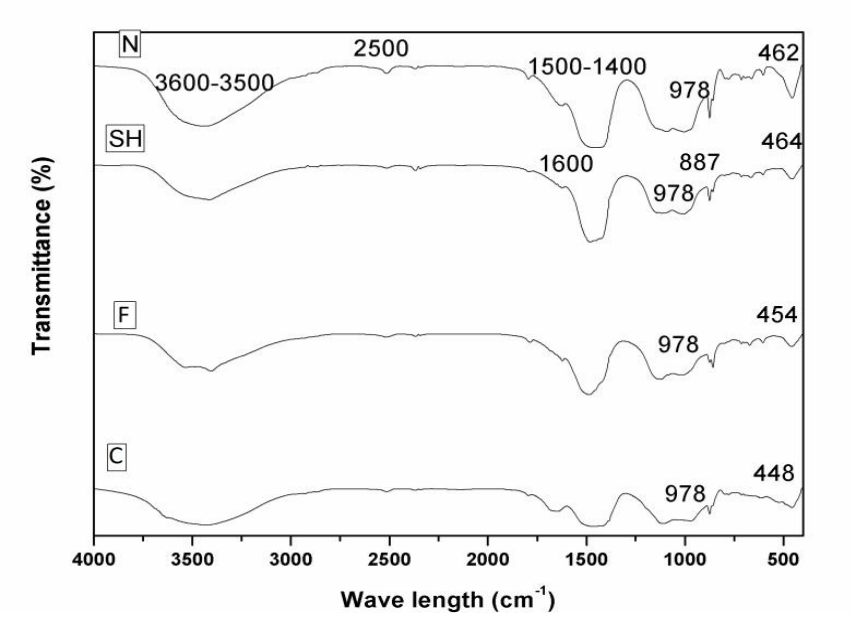

Figure 6.21 FTIR spectra for chemical admixture added specimen after 90 days curing

The specimen containing calcium acetate has band at 3433, 1626, 1517, 1144, 1004, 797, 663, and 457 cm^{-1}. The band appeared at 3433 and 1144 cm^{-1} is associated with O-H bond and indicates the formation of mono-sulphate aluminate (AFm) phase and the broad band at 1626-1517 cm^{-1}represents the AFm phase. Calcium formate contained sample has shown the band at 3464, 1616, 978, 872, and 448 cm^{-1}. The frequency band of 464-448 cm^{-1} is the characteristics of $v4SiO_4$ and it indicates the formation of O-Si-O bond. As compared to other specimens, the $v4\text{-}SiO_4$ bond in specimens containing calcium formate is found to be shifted more towards lower frequency. This indicates that large quantity of silica took part in the reaction and formation of C-S-H, which imparts the strength. A similar observation has also been reported by Sakulich (2010), Ramachandran (2001) and Taylor (1997).

The hydration mechanism for reference specimen and specimen with chemical admixture were analyzed by thermo-gravimetric method by measuring the amount of hydrates and different chemical compounds formed. The TGA and DSC curves for specimen added with calcium acetate, calcium formate, sodium meta-silicate and reference samples after 90 days of curing period are shown in Figure 6.22. DSC curve exhibits an endothermic peak in the temperature range of 92^{o}C to 206^{o}C for all samples. The mass loss peak between 92^{o}C and 206^{o}C is the characteristics of the presence of CSH and gypsum. There is also a mass loss peak related to the decomposition of uncombined calcium hydroxide between 400^{o}C to 551^{o}C in all specimens. Specimens with calcium acetate show more mass losses in the temperature range between 400^{o}C to 551^{o}C. This may be due to the presence of higher amount of calcium hydroxide in the specimen. The

occurrence of a mass loss peak in the temperatures range of 560 ^{o}C to 794 ^{o}C is the characteristics of the decomposition of calcium carbonate. This is found in specimens containing all chemicals.

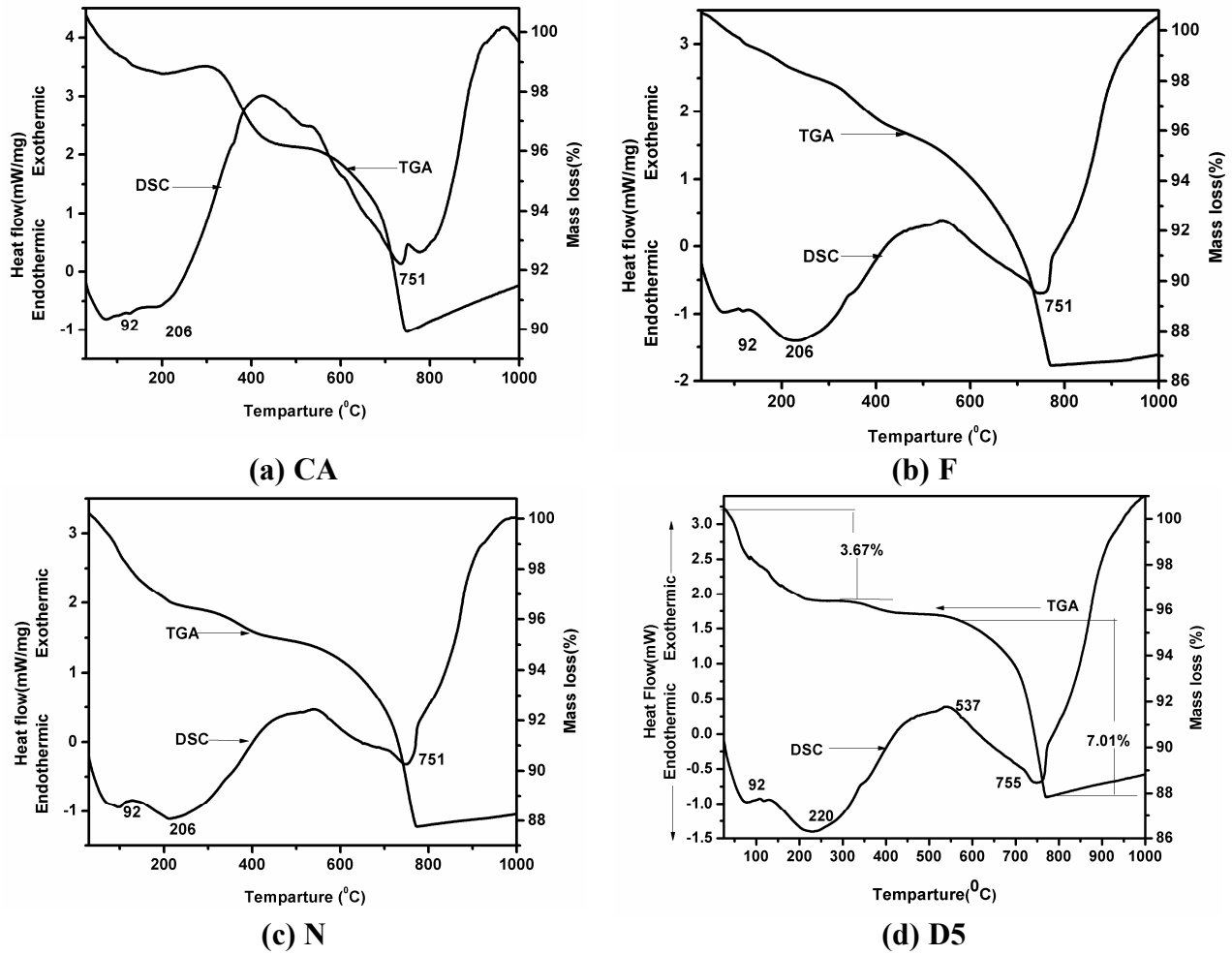

Figure 6.22 DSC and TGA for chemical admixture added specimen after 90 days curing

6.4 SUMMARY

The effects of mineral admixtures such as silica fume, fly ash, glass power and additive OPC on the strength, hydration products and porosity of lime activated slag has been investigated and presented in this chapter. Out of the several admixtures used in this

experimental investigation, silica fume was found to be a better admixture as it yields higher strength and lower porosity. The effect of chemical admixture on strength and hydration products of lime activated slag cement was also presented in this chapter. The calcium based chemicals are found to yield higher compressive strength than sodium based chemicals both at early age and later stage.

CHAPTER VII
RESULTS AND DISCUSSIONS IV

7. EFFECTS OF CURING CONDITIONS

7.1 INTRODUCTION

The effects of curing conditions on strength, hydration products, microstructure, and morphology of lime activated slag specimen cured under different conditions have been evaluated and presented in this chapter. The mortar specimens were cured under different curing temperatures in water tanks such as 27, 45, 60 and 75 ^{o}C for curing periods of 3, 7, 14, 30, 56, and 90 days. The binding mix containing 20% lime and POP contents of 1, 1.5, 2, 2.5, 5, and 10 % was used to prepare the mortar specimens. The test results are presented in terms effects of curing temperature, curing period, POP content on strength, hydration products, microstructure and morphology. The compressive strength obtained in this experimental program was compared with the results of Benghazi *et al*. (2009). Further, the effects of curing temperature and POP content on compressive strength are analyzed. Response surface plot and generalized reduced gradient technique is used to optimize the curing temperature for a given curing period and POP content. In addition to this, the mortar specimens were also cured in autoclave. These specimens were prepared with D5 binding mix (mix containing 20% lime and 5% POP) and D5 mix added with silica fume or fly ash in different proportions and were cured in autoclave at a temperature of 210 ^{o}C and pressure of 2 MPa for 1, 2, 3, and 4 hours. The test results are presented in terms effects of admixtures, curing period on strength, hydration products, microstructure, and morphology.

7.2 COMPRESSIVE STRENGTH

7.2.1 Effects of curing period

The typical relationship between compressive strength and curing period for D10 and D1.5 sample cured under different curing temperatures are presented in Figures.7.1 and 7.2 respectively. The result shows that the compressive strength of slag-lime-POP mix increases non-linearly with curing period. Initially, the rate of strength gain is high up to 28 days curing, followed by a mild increase in strength. It is observed that the strength continues to increase up to 90 days for all the specimens. However, specimens cured at low temperatures show an upward trend even after 90 days of curing while the strength of specimens cured at higher temperatures either stabilized or show an insignificant increase in strength. This leads to a cross over effect of strengths. Specimens cured at higher temperature shows a high early strength gain. However, as the curing period increases the strength gain in the specimens cured at comparatively lower temperature is more than that of the specimens cured at higher temperatures. High temperature favors rapid pozzolanic reaction at early stages of curing. However, the distribution of hydration products is not uniform leading to a formation of non-homogenous and porous structure. This phenomenon results in lower ultimate strength for specimens cured at higher temperatures and this leads to the crossover effects. The 28 and 90 days strength of mortar specimens cured at 60 ^{o}C temperature are higher than specimens cured either at 27, 45, 75 or 90 ^{o}C. The compressive strength of mortar specimens containing D10 binder and cured in water at 60 ^{o}C temperature are 45.2 MPa and 47.7 MPa after 28 days and 90 days curing whereas D1.5 sample attains strength of 34.87 MPa and 36.58 MPa respectively under similar curing conditions.

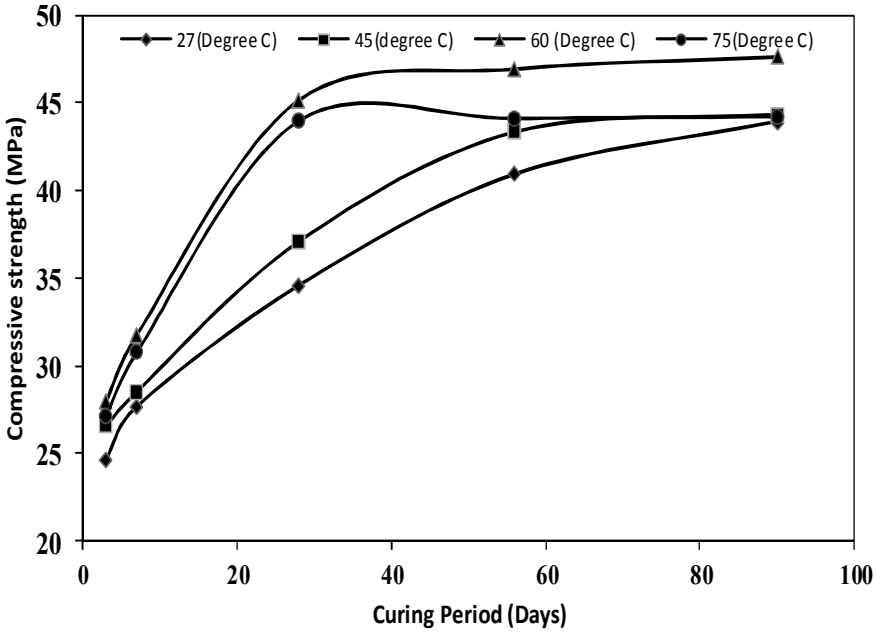

Figure 7.1 Variation of compressive strength with curing period for D10 sample

The results of compressive strength tests indicate that the strength is a function of raw material proportions, curing period and the curing temperature. Verbeck and Helmuth (1986) and Esclante Garcia (2001) reported the crossover effect in mortar specimens cured at different temperatures. The degree of hydration of the cement phases has been reported to be higher at increased temperatures in the early stages, but later, the situation is reverse. A higher curing temperature increases the rate of hydration at early ages. However, it does not allow reaction products to become uniformly distributed within the pores of hardening paste. Carino (1991) and Carino and Tank (1992) on the other hand reported that the crossover effect does not occur in hot cured high strength concrete.

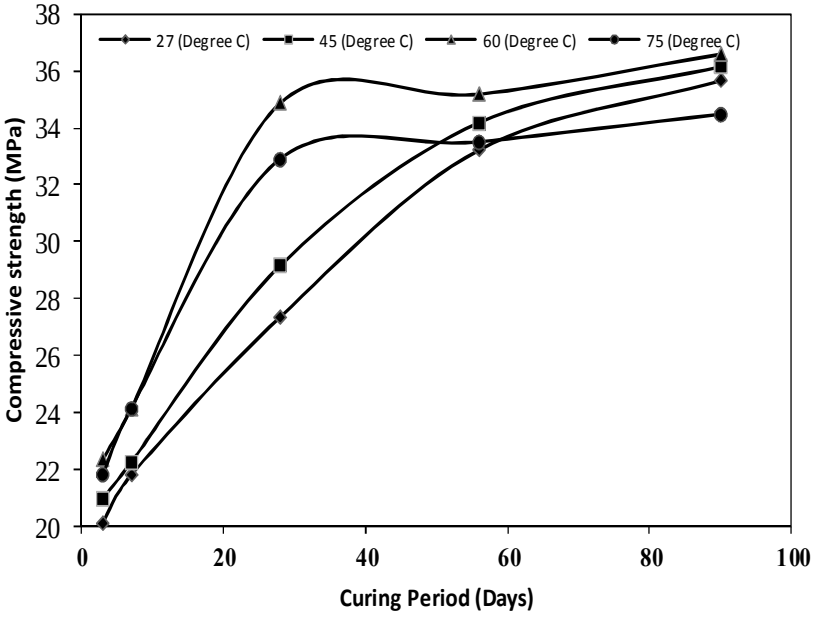

Figure 7.2 Variation of compressive strength with curing period for D1.5 sample

7.2.2 Effects of plaster of Paris content

For the mix containing 20% lime, the effect of plaster of Paris on strength for different curing period has been determined. The variation of compressive strength with plaster of Paris content under curing temperatures of 75 ^{o}C and 27 ^{o}C are presented in Figures 7.3 and 7.4 respectively. The result shows that the compressive strength of mix increases with plaster of Paris content. The increase in strength with POP content is more distinct in the early ages of curing. At later curing periods, especially after 28 days and for higher curing temperature that is at 75 ^{o}C no substantial gain in strength is recorded with an increase of POP content. An insignificant change in strength of 2.19% is observed when the POP content is increased from 5% to 10% for 90 days cured specimens at curing temperature of 75 ^{o}C.

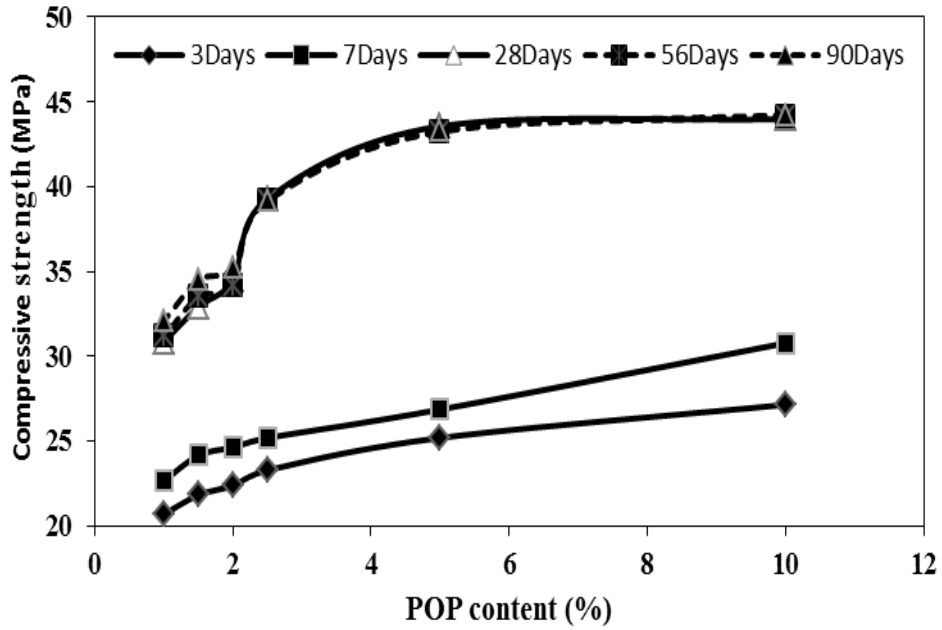

Figure 7.3 Variation of compressive strength with POP content at curing temperature of 75 ^{o}C

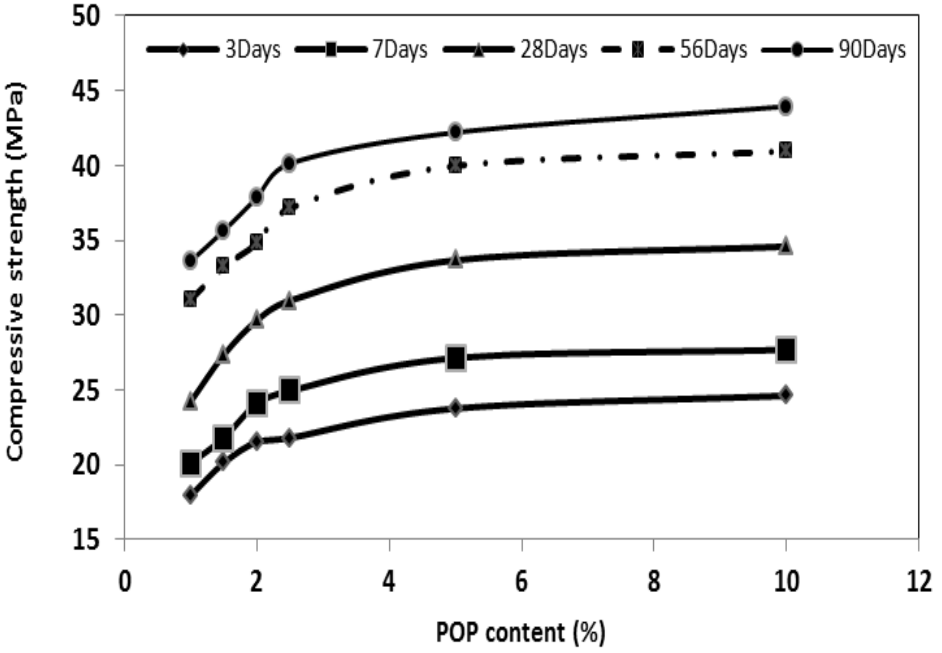

Figure 7.4 Variation of compressive strength with POP content at curing temperature of 27 ^{o}C

However, specimens cured at 27 ^{o}C shows a marginal improvement in the compressive strength with POP content. The test results show that the compressive strength of mix increases both with curing period and plaster of Paris content. The compressive strength of mortars containing 10% plaster of Paris is about 3 to 4% higher than samples containing 5% plaster of Paris both at the early and later curing periods. At a given POP content, an increase in curing temperature results in a substantial increase in strength. The increase in strength with curing period is more prominent at low POP contents. The results indicate that for the raw materials used in the present testing program, the optimum amount of plaster of Paris is about 5%.

7.2.3 Effects of curing temperature

The relationship between compressive strength and curing temperature for D10 sample is presented in the Figure 7.5. The result shows that the compressive strength of the mix cured for a specified period increases with the curing temperature up to 60 ^{o}C. Thereafter, the strength decreases with further increase in the curing temperature. At low curing temperatures of 27 ^{o}C and 45 ^{o}C, the compressive strength is found to increase with the curing period. However, sample cured at 60 ^{o}C and 75 ^{o}C shows an improvement in strength up to 28 days beyond which no significant increase in strength is noticed. The strength is found to stabilize with curing period. The results further indicate that for all curing periods and comparable testing conditions, the samples cured at 60 ^{o}C give the highest strength as compared to other curing temperatures.

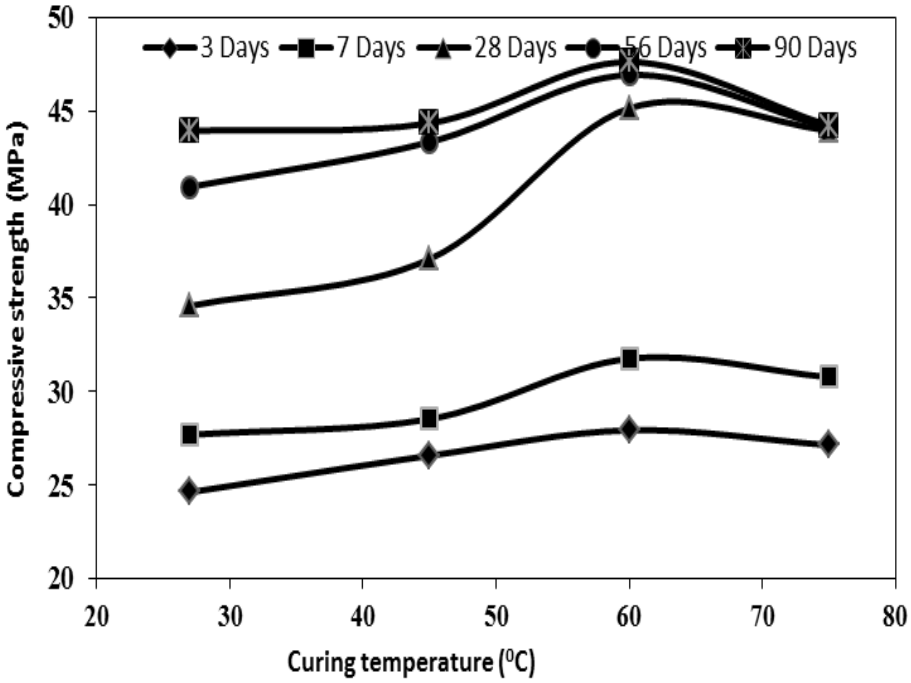

Figure 7.5 Relationship between compressive strength and curing temperature for D10 sample

7.3 HYDRATION PRODUCTS AND MORPHOLOGY

The effect of temperature on strength of some selected samples due to formation of hydration products, morphologyand chemical bonds during the hydration process has been studied using XRD, SEM, and FTIR analysis. The XRD pattern of D5 sample at 90 days curing period and different curing temperatures is shown in Figure 7.6. The chemical compounds such as calcite, quartz, calcium silicate hydrated, gypsum, wairakite, and wollastonite are found in the hydrated specimens. The peaks of calcium silicate hydrate, quartz, gypsum, wairakite, and calcite appeared in the specimen cured under 75 ^{o}C and the peaks are more intensified.

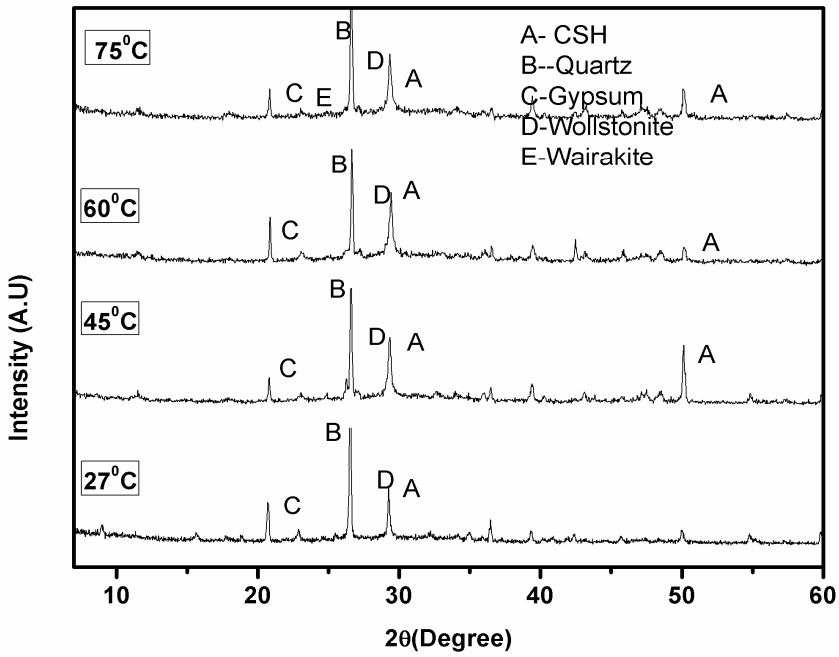

Figure 7.6 XRD patterns of D5 sample after 90 days curing

However, specimen cured at 60 ^{o}C shows the compounds like calcium silicate hydrate, quartz, and gypsum whereas quartz, calcite, C-S-H, and wollastonite appeared in the specimen cured at 45 ^{o}C temperature. The compounds like calcium silicate hydrate, quartz, and gypsum appear for the sample cured under 27 ^{o}C temperature. It is observed that the amount and type of chemical compounds formed during hydration is a function of curing temperature. In general, higher curing temperature favours higher amount of hydration products.

The hydration product wairakite is formed in a porous area of hydrated mortar when the sample is cured at 75 ^{o}C. On the other hand, specimen cured at 60 ^{o}C shows compounds like calcium silicate hydrate and gypsum and these compounds are responsible in imparting higher compressive strength to the specimen. The compressive strength of mortar cured at 75 ^{o}C is slightly lower than that of the specimen cured at 60

^{o}C. This is mainly due to the porous structure and non-homogenous distribution of hydration products in the specimen.

The XRD patterns of D5 sample cured at 27 ^{o}C and 75 ^{o}C for 7 days and 90 days curing are shown in Figure 7.7. These figures show that the hydration peaks for specimen cured at 75 ^{o}C are more intensified than the specimen cured at 27 ^{o}C. This is more prominent at 7 days cured specimen than 90 days cured specimen. This shows that higher curing period favours formation of more hydrated products at early ages of curing. However, with increase in curing period this difference gradually vanishes and at 90 days curing the intensity of hydration peaks are almost same for both curing temperatures.

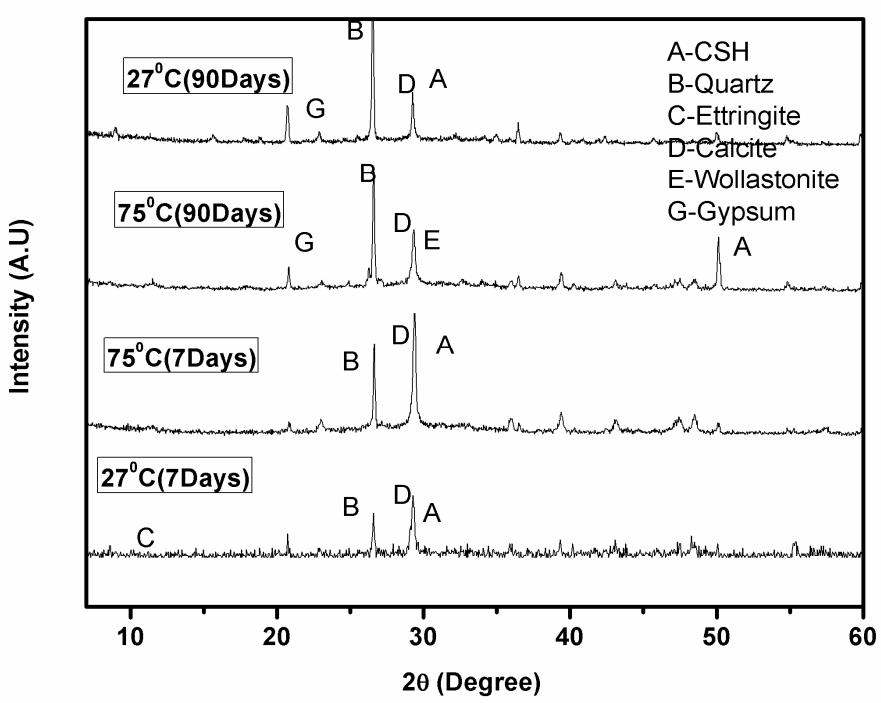

Figure 7.7 XRD patterns of D5 sample cured for 7 days and 90 days

The microstructure and hydration products of specimens cured for different periods and different curing temperature are studied using SEM analyzer. Figure 7.8 shows the

microstructure of D5 specimens cured in water at temperatures of 27, 45, 60, and 75 ^{o}C after a curing period of 7days.Abundance of needle-like structure is found in specimens cured for 7 days at curing temperatures of 27 ^{o}C and 45 ^{o}C whereas the samples cured at higher temperature that is at 60 ^{o}C and 75 ^{o}C show the presence of both needles like structures of ettringite as well as C-S-H gel.

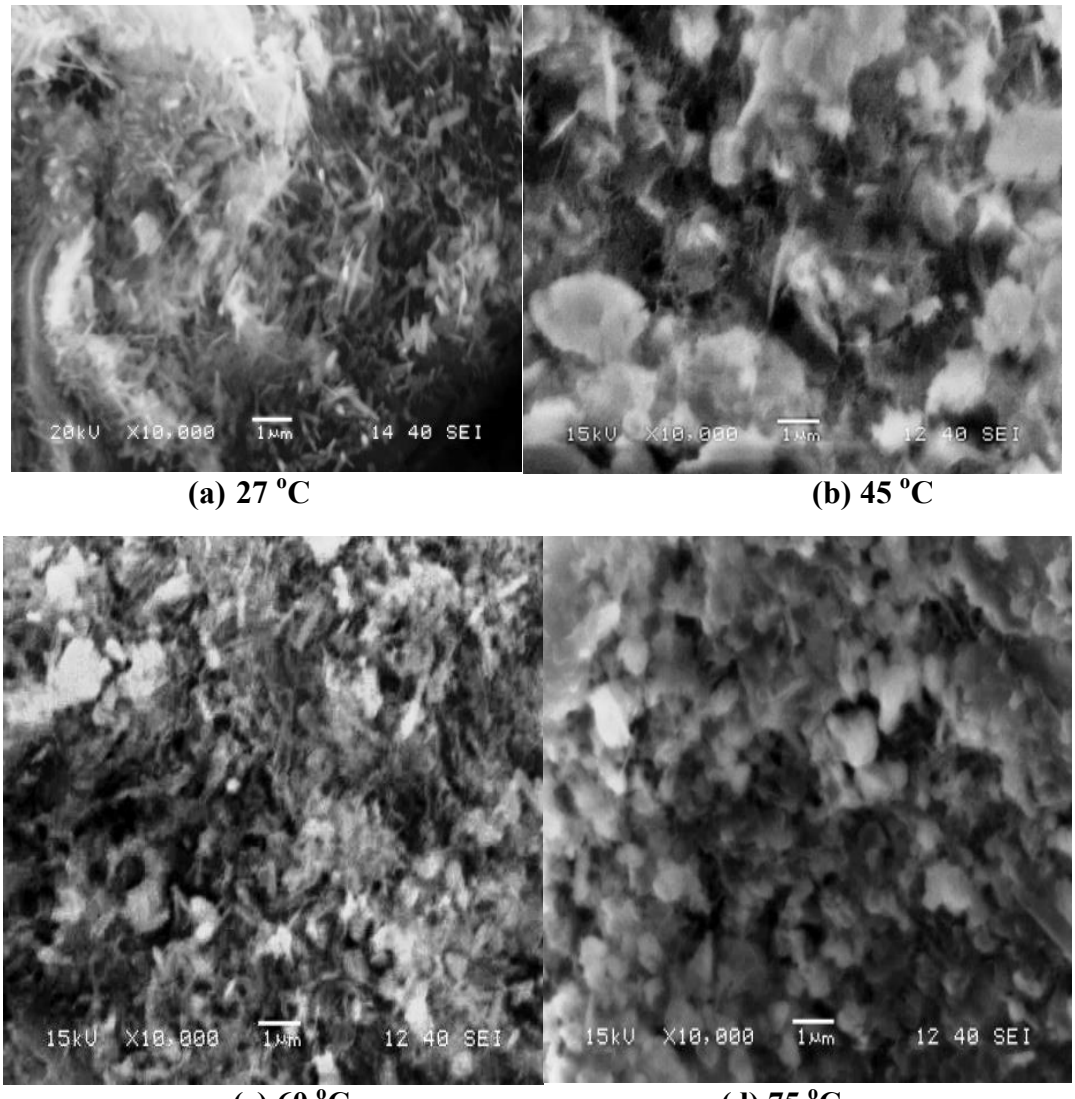

(a) 27 ^{o}C **(b) 45 ^{o}C**

(c) 60 ^{o}C **(d) 75 ^{o}C**

Figure 7.8 Microstructure of D5 specimens on 7 days curing under different temperatures

The microstructure of D5 specimen cured for 90 days in water at temperatures of 27, 45, 60 and 75 ^{o}C is shown in Figure 7.9. The structure seems to be more compact compared to samples cured for 7 days and most of the pore spaces are filled with these compounds. However, absence of the hydration products is noticed in few spaces in the specimens cured at low temperatures. As curing period increases, the low temperature cured specimens gradually add the hydration products and these are more uniform and homogeneously distributed over the mass as compared to samples cured at 75 ^{o}C. This leads to a gradual and steady increase in strength for specimens cured at low temperatures.

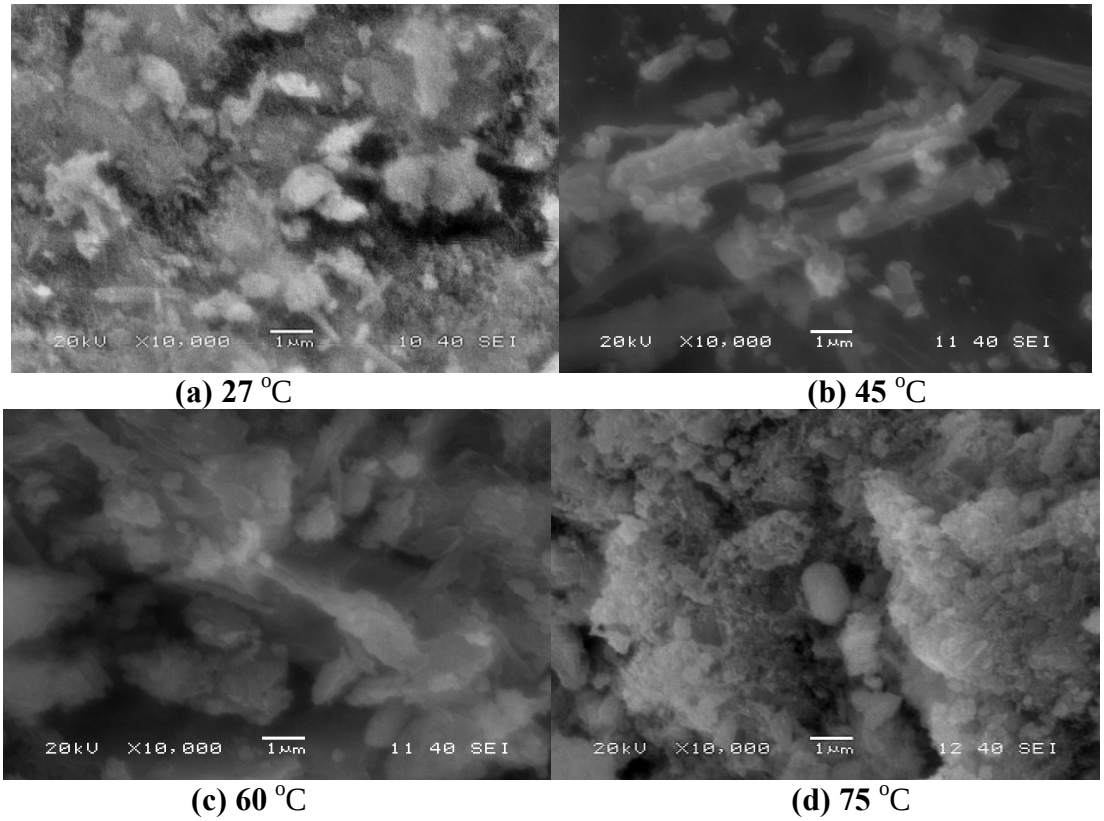

(a) 27 ^{o}C **(b) 45 ^{o}C**

(c) 60 ^{o}C **(d) 75 ^{o}C**

Figure 7.9 Microstructure of D5 specimens cured for 90 days under different temperatures

However, with the increase in curing period a non-homogeneous distribution of hydration products are observed especially samples cured at 75 ^{o}C temperature (Figure 7.9). Further, it is observed that with increase in curing period the needle like compounds of ettringite are gradually converted to mono-sulphate aluminates (AFm phase). In addition to this, with the increasing curing period more fibrous network of C-S-H gel are formed. These compounds add to the compressive strength of specimens. The SEM analysis shows compounds that are identified earlier from XRD analysis.

The FTIR spectra of D5 mortar samples cured for 90 days with different curing temperature are given in Figure 7.10. The band appeared at 3428-3471 cm^{-1} is associated with O-H bond and indicates the formation of mono-sulphate aluminate (AFm) phase and the band at 1652-1670 cm^{-1} is the characteristics for AFm phase [Ramachandran(2001), Taylor(1997)]. The band at 457-480 cm^{-1} is associated with O-Si-O or O-Al-O bond bending vibration. A similar observation has also been reported by Sakulich (2010). The low frequency band of 457-480 cm^{-1} is the characteristics of v4-SiO_4 and it indicates the formation of O-Si-O bond. The v4-SiO_4 bond is found to shift more towards lower frequency as the curing temperature is raised from 27 ^{o}C to 75 ^{o}C. This specifies that large quantity of silica took part in the reaction resulting in the formation of higher amount of C-S-H gel. The presence of peak at 1427-1448 cm^{-1} is due to the bonding in CO_3^{2-} ions. This indicates the presence of carbonated minerals in the waste lime used in this testing program and possibly due to the absorption of CO_2 from atmosphere in subsequent periods of curing and testing.

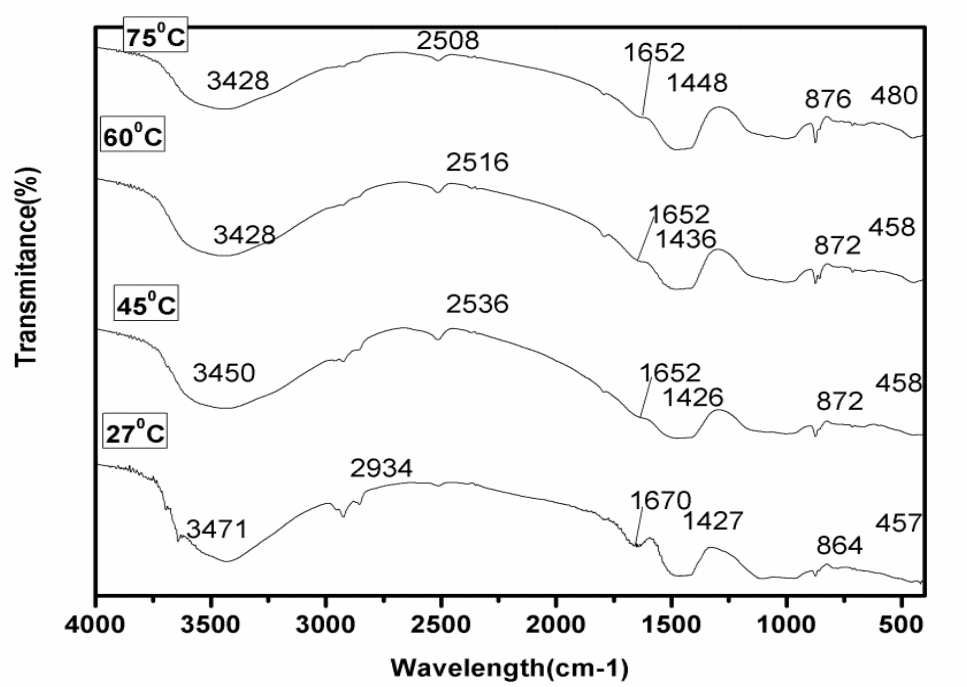

Figure 7.10 FTIR spectrums for D5 sample after 90 days curing under different temperature

7.4 RESPONSE SURFACE MODEL

The experimental values of the compressive strength of mortar specimens containing different amount of POP and cured under different temperatures and periods such as 3, 7, 28, 56 and 90 days are compiled. The predictive models for compressive strength of specimens having constant lime content of 20% are developed using second degree polynomial in which POP and curing temperature are taken as explanatory variables for different curing ages of 3, 7, 28, 56 and 90 days. The regression coefficients of the above said model for each of the representative curing periods are obtained by performing multiple linear regressions.

Response surface models for the prediction of compressive strength of mixture having constant lime content of 20% have been presented through equations (7.1 to 7.5).

The predictive capability of developed models in terms of R^2 value shows that the fitted response surface model can perform well with very low standard square error (SSE) in the range of 12.46 to 72.11 and root mean square error (RMSE) in the range of 0.832 to 2.002. Predictive models for compressive strength taking POP and temperature as inputs are as follows,

$$f_c\,(\text{day } 3) = 14.4 + 1.366P + 0.1753T - 0.06974P^2 + 0.000912PT - 0.001367T^2 \quad (R^2=0.9015) \tag{7.1}$$

$$f_c\,(\text{day } 7) = 15.45 + 2.139P + 0.1755T - 0.1367P^2 + 0.003434PT - 0.001455T^2 \quad (R^2=0.8867) \tag{7.2}$$

$$f_c\,(\text{day } 28) = 12.98 + 3.661P + 0.3822T - 0.2744P^2 + 0.01016PT - 0.002367T^2 \quad (R^2=0.8988) \tag{7.3}$$

$$f_c(\text{day } 56) = 23.04 + 3.544P + 0.2413T - 0.2501P^2 + 0.009195PT - 0.002316T^2 \quad (R^2=0.9377) \tag{7.4}$$

$$f_c\,(\text{day } 90) = 26.91 + 3.681P + 0.193T - 0.2574P^2 + 0.007169PT - 0.002238T^2 \quad (R^2=0.9479) \tag{7.5}$$

Figure 7.11 shows the actual verses the predicted values of compressive strength and it is observed that the entire model developed here can predict the output response i.e. compressive strength with high correlation coefficient. Among the various model developed, the model for prediction of compressive strength for curing ages 3, 56 and 90 shows high correlation coefficient of 0.9015, 0.9377 and 0.9479 respectively.

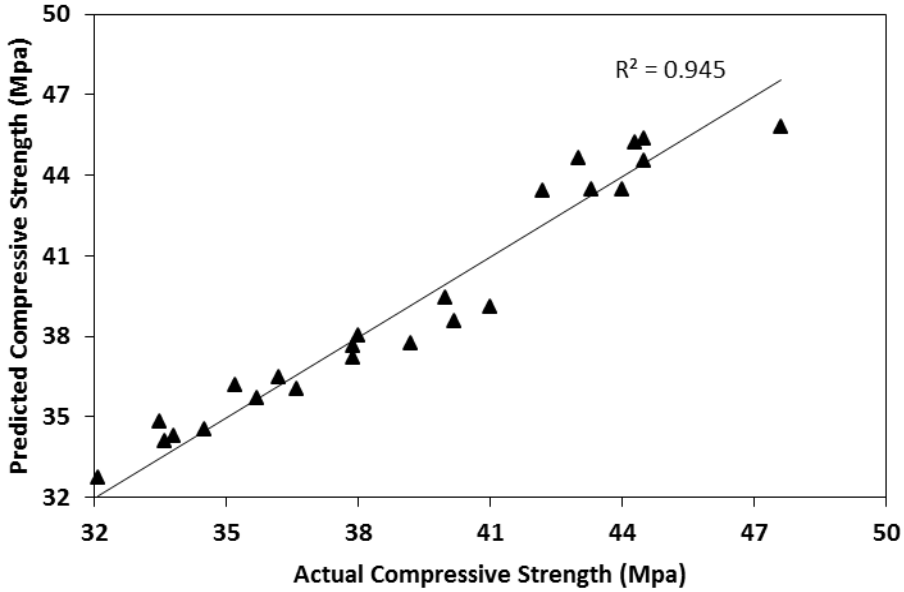

Figure 7.11 Actual versus predicted values of compressive strength

7.5 OPTIMIZATION

The nonlinear response of the model is optimized using generalized reduced gradient (GRG) algorithm. The above nonlinear method is adopted to obtain the maximum value of the predicted response for each of the fitted models. The predicted response of the fitted model is shown in the form of surface and contour plots for 90 days cured mortar specimen (Figure 7.12). It is observed that the response function initially increases with increase in POP content up to the optimum value and thereafter, it shows decreasing trend with further increase in POP content. A similar pattern is also observed for curing temperature with the compressive strength. The optimum value of the response function is obtained using fitted response surface models by GRG method. The optimum values of POP content and curing temperature for 90 days cured mortar specimen are found to be 7.927% and 55.82^{o}C respectively. However, for other curing periods the optimum values of POP content and curing temperature are found to vary from 8.059 to 10% and 67.45 to 75 ^{o}C respectively. In general, it is observed that the optimum values of

activator such as POP are found to decrease with increase in curing period. This is obvious as the hydration of slag with lime and POP is much slower and a higher dose of activators does not take part in pozzolanic reaction and is left out as free lime and POP. As the curing period increases, more and more activators are consumed in hydration process, thus increasing the strength.

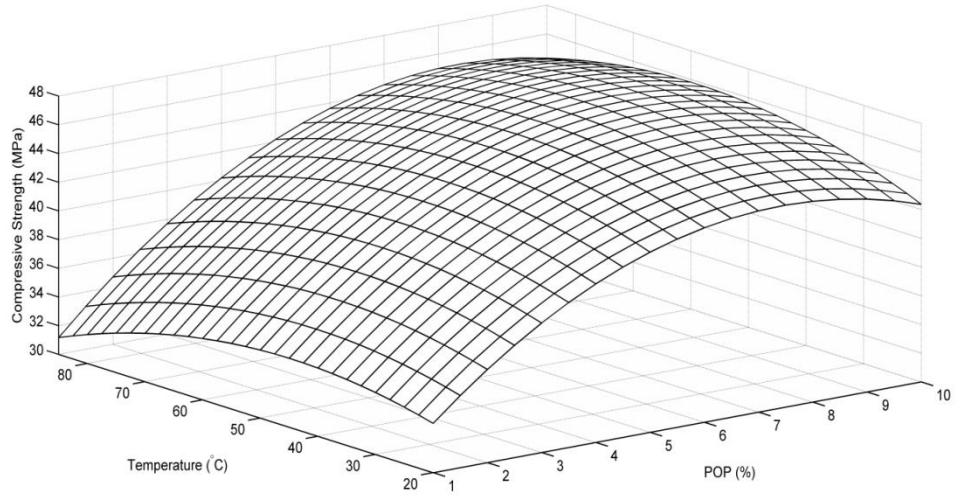

(a) Response Surface model

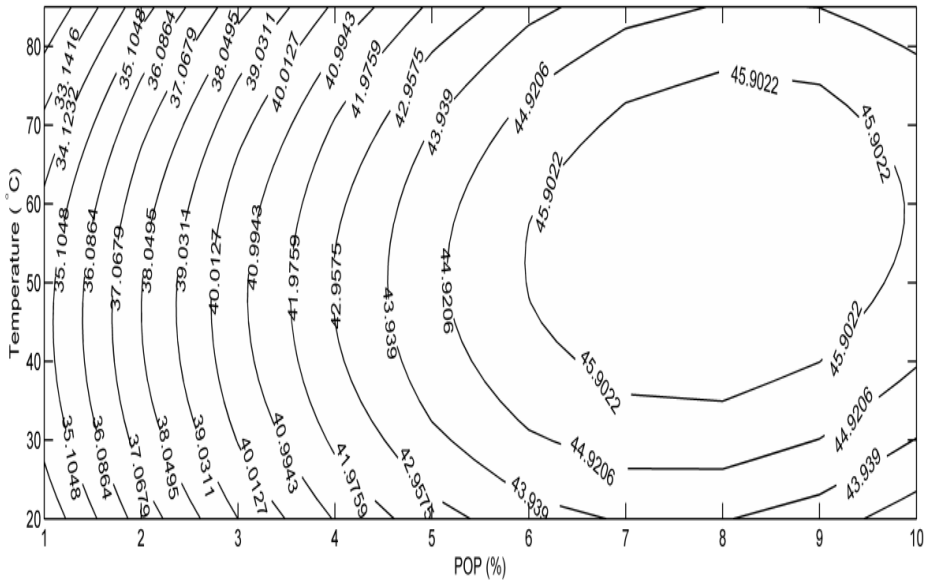

(b) Contour plot

Figure 7.12 Response surface model and contour plot showing variation of compressive strength with curing temperature and POP content

7.6 AUTOCLAVE CURING

Few mortar specimens prepared with D5 binding mix and D5 mix added with silica fume or fly ash in different proportions were cured in autoclave at a temperature of 210 ^{o}C and pressure of 2MPa for 1, 2, 3, and 4 hours. The proportion of silica fume and fly ash in the reference mix was varied as 5, 10, 15% and 10, 20, 30%. These specimens are designated as SF1, SF2, SF3 and FA1, FA2, FA3 respectively. The test results are presented in terms effects of admixtures, curing period on strength, hydration products, microstructure and morphology of lime activated slag cement.

7.6.1 Compressive strength

The compressive strength of autoclave cured mortar specimens and specimens cured in water tanks at 27 ^{o}C were determined after specified curing periods and are given in Table 3.14.The compressive strength values obtained were plotted with autoclaving time and is presented in Fiure.7.13. The compressive strength of mortar specimens was improved due to the addition of either fly ash or silica fume to the reference sample. These curves show that the compressive strength increases rapidly with autoclaving time only up to about 2 hours, beyond that only a marginal gain in strength is observed. For comparable test conditions silica fume added specimens show higher compressive strength followed by sample added with fly ash and the reference sample. The compressive strength of the mixture containing 15% of silica fume attained a value of 56 MPa at 4 hour of autoclaving. The enhancement in compressive strength is 33.33% as compared to that obtained for mortar specimens prepared out of the reference binder at a comparable curing time. The reference sample added with 30% fly ash showed 16.9% higher strength than that obtained for the reference sample at the same autoclaving time.

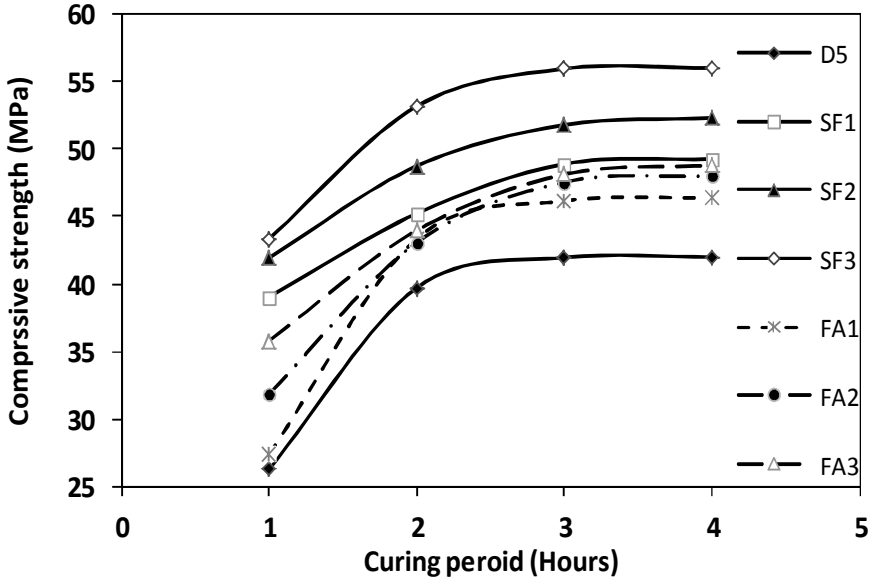

Figure 7.13 Variation of compressive strength with autoclaving time

The compressive strength of mortar specimens obtained from autoclave curing is compared with that of the normal water curing at 27 ^{o}C. The autoclave curing timings of 1, 2, 3, and 4 hour are represented as AC01, AC02, AC03, and AC04 respectively whereas the normal water curing periods of 7, 28, and 90 days are represented as WC07, WC28, and WC90 respectively. Figure 7.14 shows the compressive strength of reference sample and samples added with different proportions of admixtures for similar curing conditions whereas Figure 7.15 gives the compressive strength of specimens with similar compositions cured under different conditions. For similar curing conditions SF3 samples gave the highest compressive strength compared to all other specimens. The samples cured in an autoclave for 2h give almost equal strength to 28days water cured specimens. The 7 days water cured specimens gave strength which is even lower than the 1h autoclave cured specimens. This indicates that high temperature and pressure curing favor quick formation of hydration products and much faster gain of strength. However,

the strength of 4 hour autoclave cured SF3 specimens is slightly lower than the strength of specimens cured in water for 90 days. Similar observations are made for specimens containing different proportions of admixtures.

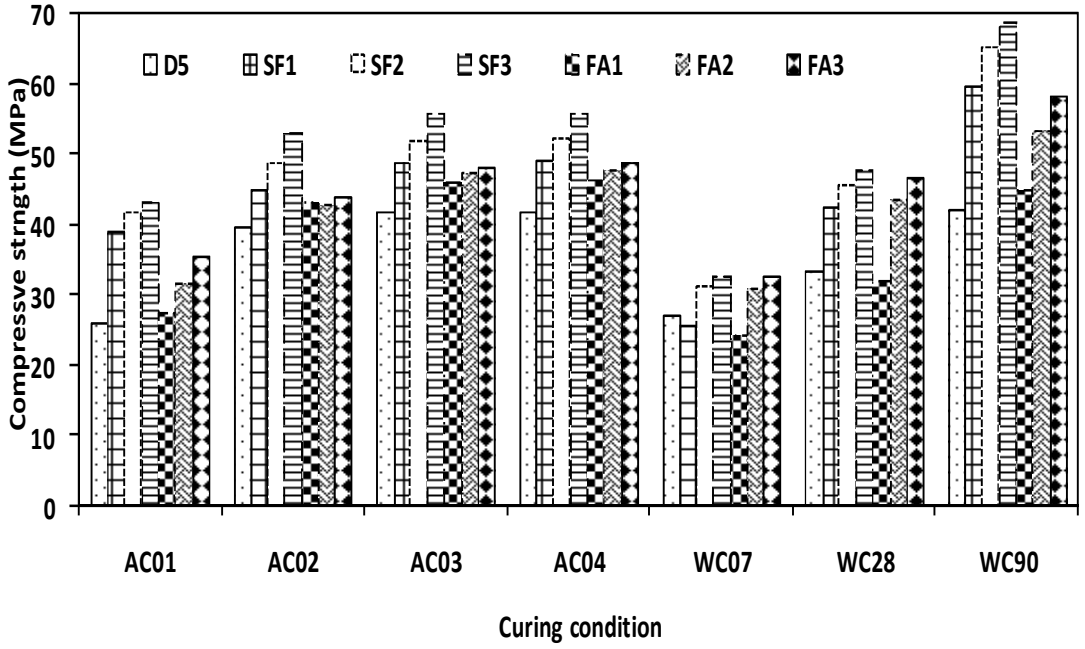

Figure 7.14 Compressive strength of mortar specimen cured under different conditions

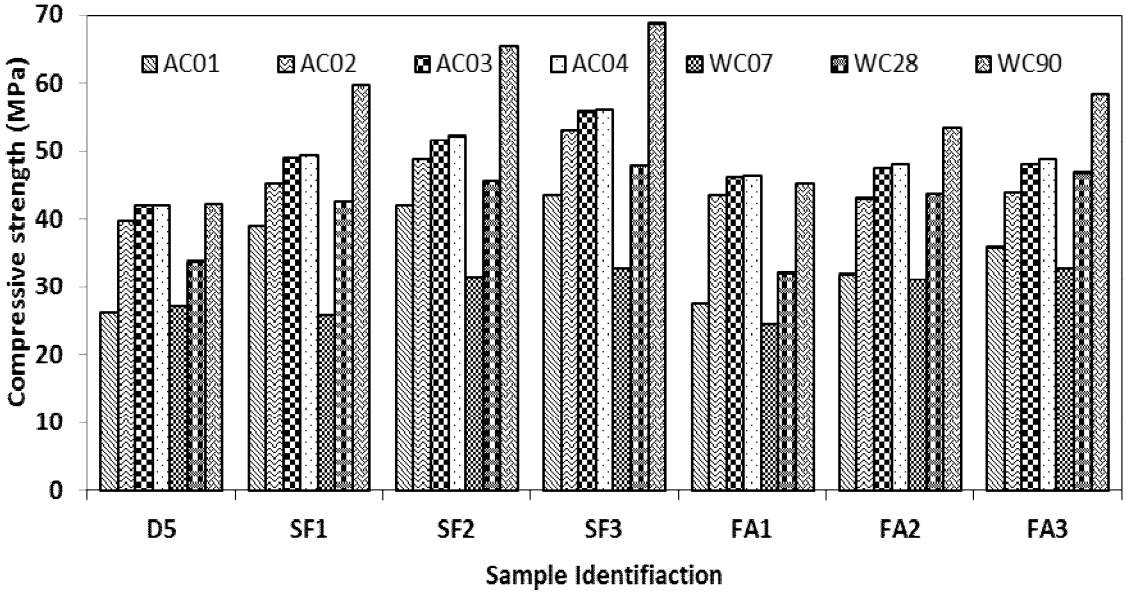

Figure 7.15 Compressive strength of identical mortar specimen cured under different condition

Furthermore, no appreciable gain in strength is observed with increase in the curing period in autoclave cured specimens beyond 2 hours whereas samples cured in water at standard temperature show a continuous increase in strength up to 90 days of curing, though the rate of gain of strength in early curing period is more than the later curing periods. The figures indicate that the ultimate strength of specimen cured in an autoclave with additives or without additives is slightly lower as compared to normal water cured specimen.

7.6.2 Hydration products and morphology

The formation of hydration products and microstructure during the hydration process was studied using XRD and SEM analysis. The XRD patterns of the D5, FA3 and SF3 mortar specimens cured for 90 days in water at 27 ^{o}C are shown in Figure 7.16. The chemical compounds such as C-S-H, calcite, quartz, gypsum are found in specimen cured in water. Calcium silicate hydrate compounds are found with wide amorphous humps in SF3 and FA3 specimens as compared to D5 specimens. This may be due to the presence of ultra-fine amorphous silica particles in these samples. The formation of more calcium silicate hydrated resulted in an increase of the strength of mortar specimens containing these admixtures. It is noted that the percentage of C-S-H gel in SF3 sample is slightly lower than FA3 specimens but higher than D5 specimens. However, it registers the highest compressive strength. The additional strength of SF3 specimens over FA3 specimens may be mainly due to the low porosity, higher mass density of hydrated sample and homogenous distribution of C-S-H gel in the mass. The XRD pattern of D5, SF3 and FA3 sample after 4 hour of curing in the autoclave is shown in Figure 7.17. The chemical compounds such as calcite, quartz, calcium silicate hydrated, gismondine (PDF-

00-020-0452), tobermorite (PDF-00-045-1480), and xonolite (PDF-00-029-0379) are obtained. The chemical compounds such as gismondine, tobermorite, and xonotlite are not found in samples cured at standard temperature of 27 ^{o}C. The C-S-H phase in specimens cured in autoclave is found in the form of Ŭ-dicalcium silicate hydrate (Ŭ-C_2S) and tobermorite. The Ŭ-dicalcium silicate hydrate (Ŭ-C2S or $Ca_2(HSiO_4)OH$) normally causes an increase in porosity and reduction in strength. However, with the presence of silica, Ŭ-C_2S gets converted to tobermorite ($C_5S_6H_5$) on continued heating, thus imparting higher strength to the specimens. [Bezerra*et al.* (2012)]. The XRD pattern of SF3 specimen also shows higher amount of tobermorite as compared to specimens containing fly ash and reference sample. The higher compressive strength of SF3 mortar specimens over FA3 and D5 specimens are mainly due to the higher tobermorite content coupled with low porosity, higher mass density, and homogenous distribution of C-S-H gel in SF3 mortar specimens. This shows that silica fume acts as filler in the micro-voids of the specimens and also participates in the pozzolanic reaction.

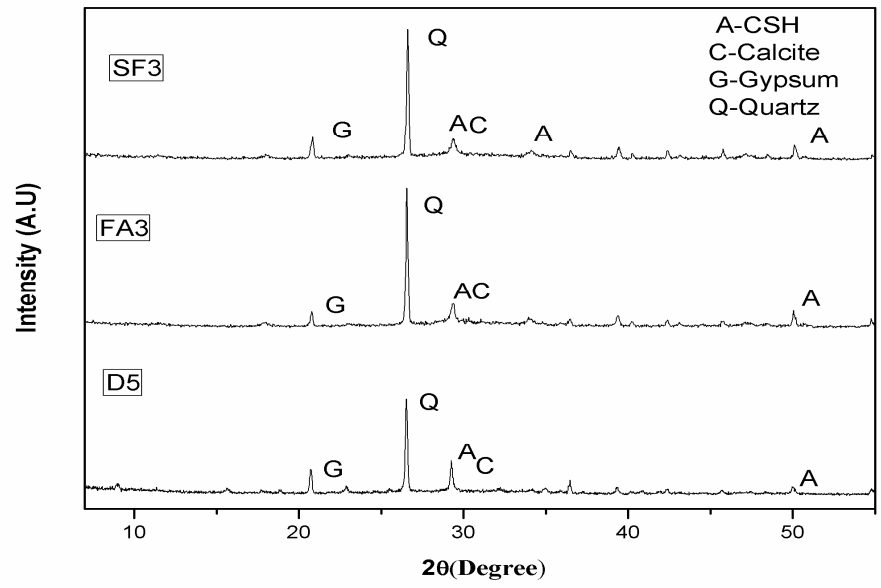

Figure 7.16 XRD patterns of specimens cured in water for 90 days

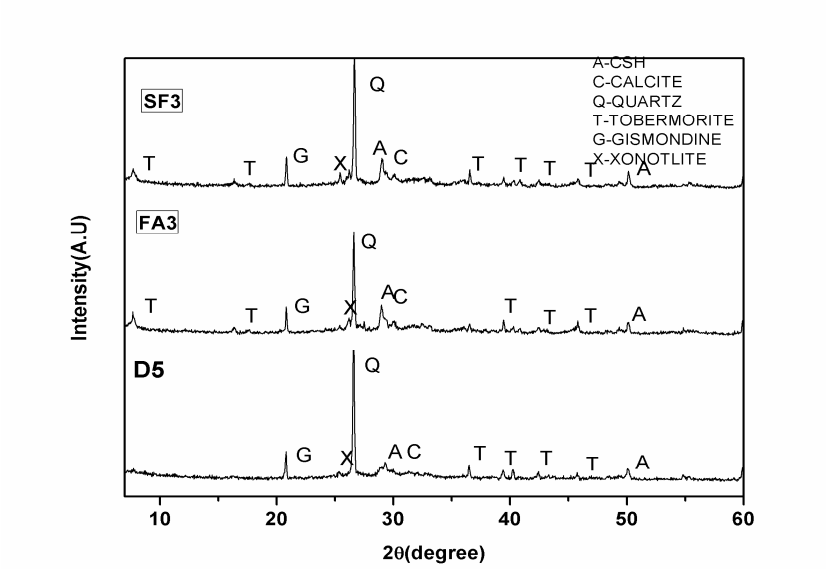

Figure 7.17 XRD patterns of specimens cured in autoclave for 4 hours

The microstructure of the hydration products of D5, FA3 and SF3 specimens cured under different conditions is given in Figure 7.18. Abundance of reticulated plate-shaped structure of tobermorite and C-S-H is found in SF3 and FA3 specimens. A combination of needle and plate shaped structure is found in reference sample. The needle and plate shaped structures are due to formation of tobermorite which normally appear in specimens that are cured at elevated temperature. The occurrence of tobermorite is also confirmed from XRD analysis. The microstructure of the hydration products of D5, FA3 and SF3 specimens cured under different conditions is given in Figure 7.18. The SEM images of D5, FA3 and SF3 specimens cured for 4 hour in autoclave are shown in Figures 7.18 (a) to 7.18 (c) respectively. Abundance of reticulated plate-shaped structure of tobermorite and C-S-H is found in SF3 and FA3 specimens. A combination of needle and plate shaped structures are found in reference sample. The needle and plate shaped structures are due to formation of xonotlite and tobermorite which normally appear in specimens that are cured at elevated temperature. The presence of

tobermorite in specimens cured in autoclave is also established from XRD analysis. Similarly SEM images of D5, FA3 and SF3 specimens cured for 90 days in water at 27 ^{o}C are shown in Figure 7.18 (d) to (f) respectively. The needle and plate shaped structures of xonotlite and tobermorite are absent in these samples. However, the hydration product C-S-H is found in abundance in these specimens. Figures 7.19 (a) to (c) show the surface morphology of D5, FA3 and SF3 specimens cured in autoclave whereas Figures 7.19(d) to (f) show the surface morphology of D5, FA3 and SF3 specimens cured in water at 27 ^{o}C. The microstructure images show that the silica fume and fly ash containing specimen are denser as compared to the reference samples both for specimens cured in water or in autoclave. The C-S-H gel is found to be homogenous, uniform and evenly distributed over the mass and the voids diameters as well as numbers are much smaller especially in water cured samples as compared to specimens cured in autoclave. Specimens containing fly ash show an abundance of calcium alumino-silicate hydrates and aggregation of C-S-H as compared to specimens containing silica fume at comparable test conditions. This shows that silica fume also acts as a filler material and helps in homogenizing the specimen in addition to contributing to pozzolanic reaction. The higher mechanical strength of SF3 specimen is attributed to the above factor. Further, a homogenous distribution of hydration products in specimens cured in water for 90 days makes these specimens stronger than the specimens cured for 4 hour in autoclave, although the amount of hydration products in autoclaved specimens seemed to be more than the normal water cured specimens.

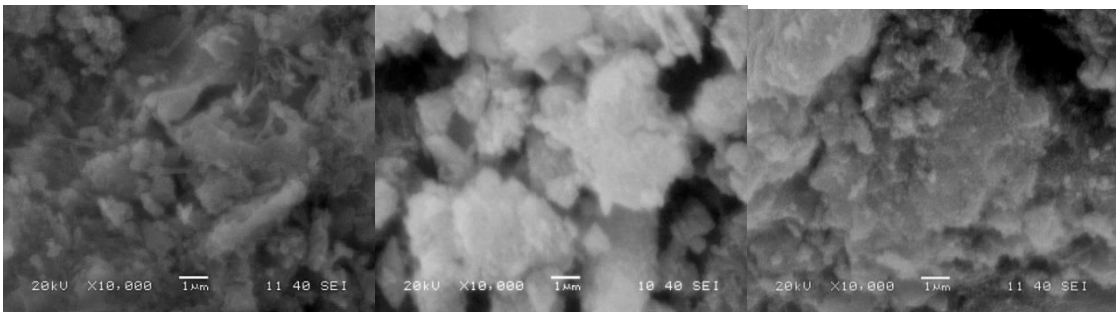

(a) D5-AC04 (b) FA3-AC04 (c) SF3-AC04

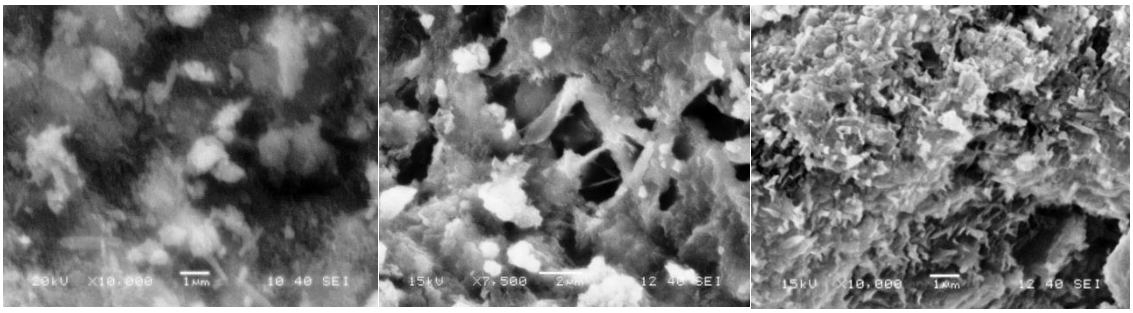

(d) D5-WC90 (e) FA3-WC90 (f) SF3-WC90

Figure 7.18 Microstructure of specimens cured in autoclave and water

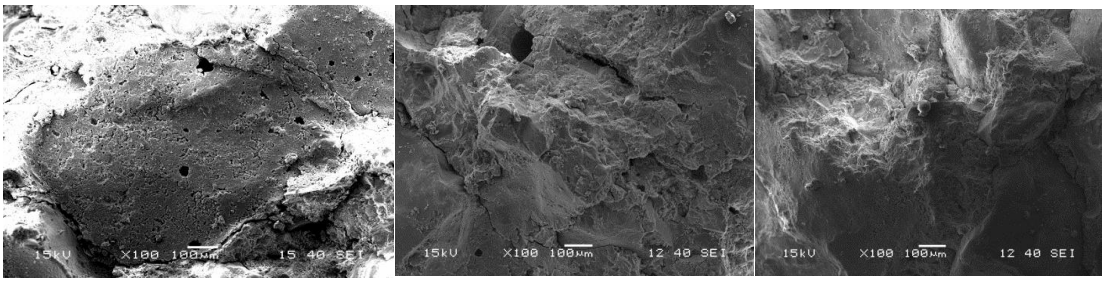

(a) D5-AC04 (b) FA3-AC04 (c) SF3-AC04

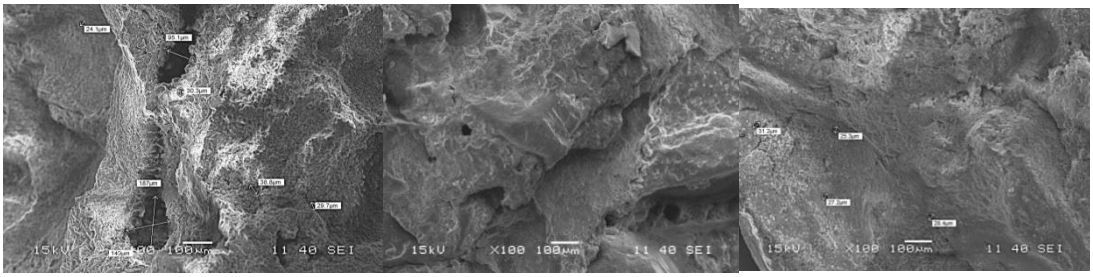

(d) D5-WC90 (e) FA3-WC90 (f) SF3-WC90

Figure 7.19 Morphology of specimens cured in autoclave and water

The microstructure images show that the silica fume and fly ash containing specimen are more homogenous, uniform and dense as compared to the reference

samples. The C-S-H gel is found to be evenly distributed over the mass and the voids diameters as well as numbers are much smaller especially in water cured samples as compared to autoclaved specimens. On the other hand, the fly ash added sample shows an abundance of calcium alumino-silicate hydrates and aggregation of C-S-H. This shows that silica fume mainly acts as a filler material and helps in homogenizing the specimen. The higher mechanical strength of SF3 specimen is attributed to the above factor. Further, a homogenous distribution of hydration products in 90 days water cured specimens makes these specimens more stronger than the specimens cured for 4 hour in autoclave, although the amount of hydration products in autoclaved specimens seemed to be more than the specimens cured in normal water at a given raw material composition.

The hydration mechanism of slag-lime mortar was analyzed by thermo-gravimetric method and its hydration products are identified. Figure 7.20 shows the TGA and DSC curves of D5 and SF3 specimens cured in autoclave for 4 hour and in water for 90 days. In autoclave cured sample the total mass loss varies from 14.3 to 16%. The total mass loss in these samples for water cured specimens is 9.9% to 14.3% in the temperature range of 0 ^{o}C to 1000 ^{o}C. The higher mass-loss in autoclaved samples compared to normal water cured samples indicates that higher amount of hydration products is formed in autoclaving curing. This is also evident from the XRD patterns of these samples. However, the compressive strength of water cured specimens after 90 days of curing are somewhat higher than the corresponding 4 hour of autoclaving specimens. This can be explained from the morphology of these samples. The 90 days water cured samples show a more homogeneous distribution of hydration products than the corresponding autoclave

cured specimens. DSC curve exhibits an endothermic peak at 92 ^{o}C to 20 ^{o}C for samples cured in water.

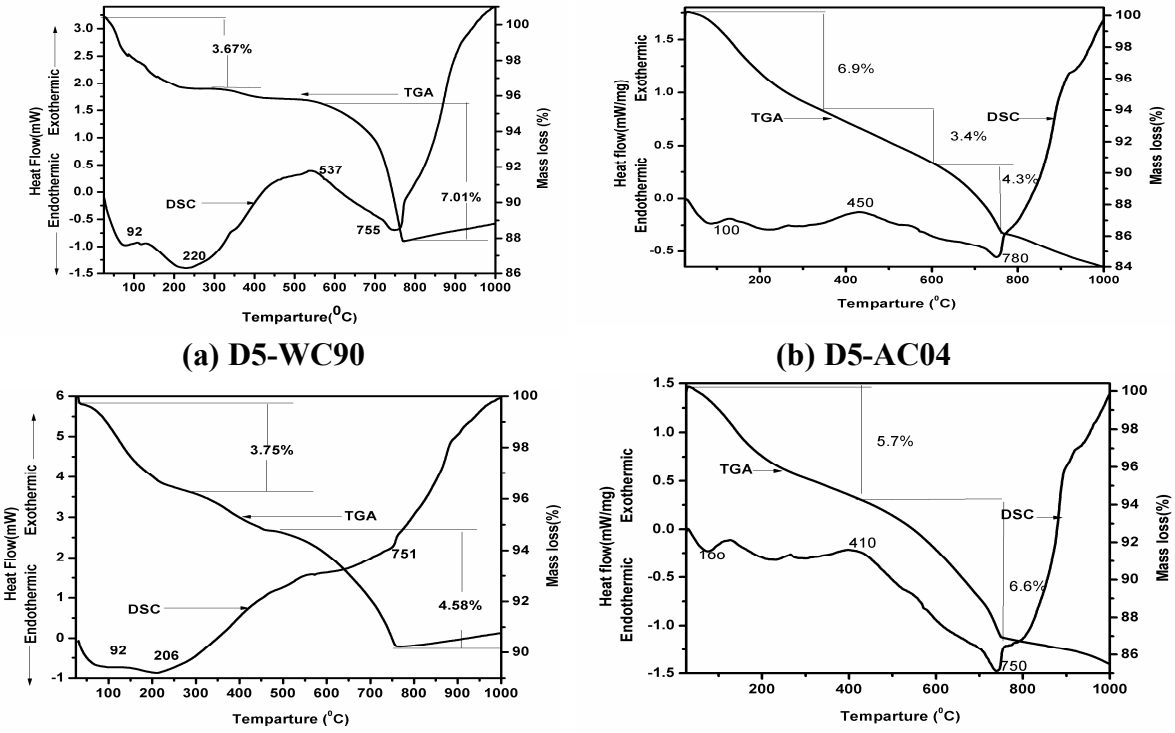

(a) D5-WC90 **(b) D5-AC04**

(c) SF3-WC90 **(d) SF3-AC04**

Figure 7.20 TGA and DSC of specimens cured in autoclave and water

A mass loss of 3.75 and 3.67% is observed in this temperature range for SF3 and D5 specimens respectively. The mass loss peak between 92^{o}C and 206^{o}C is characteristics of presence of gypsum and C-S-H. A mass loss peak in temperature range from 560 ^{o}C to 794 ^{o}C is seen. This is due to the decomposition of calcium carbonate. The mass loss in the temperature ranges of 560^{o}C to 794°C is 4.58 and 7.01% for SF3 and D5 specimens. The TGA curve of autoclave cured SF3 specimen showed two stages of thermal decomposition; the first stage began at the onset temperature near 25°C and ended around

410 °C and the second took place from 410 °C to 780 °C. The first stage might be caused by dehydration of calcium silicate hydrate, tobermorite and xonotlite with mass loss of 5.7%. The second stage representing a large mass loss of 6.44 % mostly involved the decomposition of calcium carbonate.

7.7 SUMMARY

The effects of curing conditions like water curing with high temperature and autoclave curing on strength, hydration products, microstructure, and morphology of lime activated slag cement have been evaluated and presented in this chapter. In general, the high temperature curing imparts higher strength at early ages; however, a specimen cured at low temperature registers a higher compressive strength than specimens cured at higher temperatures.

CHAPTER VIII
SUMMARY AND CONCLUSIONS

8. SUMMARY AND CONCLUSIONS

8.1 SUMMARY

The objective of the present research is to prepare and characterize a sustainable binding material using industrial by-product as an alternate to Portland cement. To achieve the above objective, an extensive review on studies related to the physical, chemical and mechanical properties along with microstructure and morphology of slag activated by various activators have been made. Based on this, the scope of the present study is defined and the same has been summarized in chapter 2. Indian standard codes of practice are followed to conduct various tests and chapter 3 presents the details of materials used, the testing procedure adopted and the variables studied. The experimental test results pertaining to the physical properties and chemical analysis of hydration products in slag-lime-POP mixes are presented in chapter 4, while chapter 5 presents the mechanical strength of mortar specimens prepared out of this binding mixture along with a technique for optimization of raw material proportions. Chapter 6 deals with the effects of different mineral and chemical admixtures on strength and hydration products. Chapter 7 delineates the effects of curing temperature including curing in autoclave conditions on strength and hydration products. In the present chapter the conclusions drawn from the test results are summarized.

8.2 CONCLUSIONS

The physical properties of 42 slag-lime-plaster of Paris mixes along with the study on hydration products and microstructure corresponding to their respective initial and final setting times has been made based on which the following conclusions are drawn:

1. The normal consistency value of slag-lime-plaster of Paris mixes increases with increase in either lime or plaster of Paris content. The consistency for these mixes varies over a wide range from 28.89 to 37.4% whereas this value is about 30% for ordinary Portland cement (OPC).
2. The initial and final setting time of the mixes decrease with increase in either lime and/or plaster of Paris content. An addition of borax retards the setting time and a borax content of 0.4% by mass in the binding mixture gives the setting time that is normally prescribed for OPC.
3. The soundness of this binder varies between 1 mm to 3 mm, which is lower than that of the value prescribed for OPC by Bureau of Indian Standards.
4. X-ray diffraction analysis shows a series of crystalline compounds such as calcium-sulphate-hydrate, portlandite, calcium-silicate-hydrate and calcite which influence the hardening process.
5. SEM analysis for the early stages of setting reveals the presence of calcium-aluminate-silicate-hydrate (C-A-S-H) gels in the mixes instead of calcium-silicate-hydrate (C-S-H) gel which is normally found in hydration products of OPC. However, after 24 hours of setting both C-S-H and C-A-S-H phases are found.

6. FTIR analysis shows a shift of S-O and O-H bands with wave number, indicating that the hydration process continues with setting time and confirms the formation of calcium-sulphate-hydrate gel during the reaction.

Based on the compressive strength of 36 slag-lime-POP mixes optimization has been done and an optimum mix of raw materials (reference mix) has been obtained. Various properties such as compressive strength, microstructure, porosity and drying shrinkage have been investigated for mortar specimens prepared from the reference mix and the following conclusions are arrived at:

1. The compressive strength of the slag-lime-POP mixes depends on proportions of slag, lime and POP. An optimum dose of lime exists and no further significant increase in strength is achieved beyond this dose. A higher dosage of lime reduces the strength. The compressive strength increases non-linearly with POP content. No appreciable increase in strength is observed beyond 5% POP content. Also, the strength of the mixes increases with curing period.
2. Response surface models are introduced for respective curing periods with high coefficient of determination and the chosen model was proved to be statistically significant based on ANOVA tests. Optimization of the fitted model has been carried out using a generalized reduced gradient (GRG) algorithm and the results of optimized values are well comparable to the experimental values.
3. The optimum composition of raw materials is found to vary marginally with the curing period. The optimum proportion of lime and POP for 90 days cured specimens is found to be 19.12% and 4.26% respectively.

4. Microstructure and hydration product studies show the presence of compounds like ettringite and C-S-H gel, which mainly enhance the strength. An addition of lime beyond an optimum value results in the formation of hillebrandite and reduction in compressive strength.
5. The total porosity and the size of pores decrease with an increase in curing period. Particularly, a substantial reduction in capillary pores is observed with an increased curing period.

Several mineral and chemical admixtures have been added to the reference mix and various properties like compressive strength, microstructure, porosity and drying shrinkage were studied. The conclusions drawn from the experimental results are:

1. The strength of mortar specimens mainly depends on the curing period, type, amount, and the fineness of the mineral admixtures. For the present test variables, silica fume added samples gave the highest compressive strength than other mixes at comparable test conditions.
2. The porosity and pore size distribution in mix are found to be a function of the type of admixture, its quantity and the curing period. Silica fume added mix is less porous and shows uniform distribution of pores over the measured pore size range. This may be due to the presence of micro fine particles, which function as filler material and also participate in pozzolanic reaction.
3. X-ray diffraction analysis shows a series of compounds such as calcium silicate hydrated, gypsum, quartz, and calcite. A wider amorphous hump corresponding to the C-S-H compound is observed in specimens containing fly ash and silica fume

compared to reference specimen and specimens containing OPC and glass powder. SEM analysis also confirms the existence of these components in the hydrated specimens as a calcium silicate hydrated gel. The FTIR spectrum shows a shift of Si-O, O-H, and Al-O bonds with wave number indicating that the hydration process continues with curing time and confirms the formation of calcium silicate hydrated gel during the reaction.

4. From DSC and TGA curve the absence of calcium hydroxide peak is observed except OPC sample. A correlation is established between the developed strength with the type of mineral admixture through analysis of hydration products and the microstructure. For the present test variables silica fume is found to be a better admixture compared to fly ash, glass powder, and OPC.
5. It is seen that an addition of mineral admixtures reduces the drying shrinkage value. However, the drying shrinkage values of all the specimens are found to increase with the curing period.
6. In brief, the findings of the investigation show that the strength of lime activated slag cement improves by addition of calcium based admixtures like calcium acetate, calcium formate and calcium nitrate up to 2% to the reference binder (D5) and after that it decreases. However, an addition of sodium based admixtures results no appreciable change in strength over the reference sample.
7. The SEM image of specimens containing calcium based chemicals such as calcium acetate and calcium formate shows abundance of needle shaped Aft phase of calcium aluminate tri-sulphate and gel like substance of calcium silicate hydrate. The presence of these hydration product results in enhancing the strength of mortar specimens

containing calcium acetate and calcium formate. However, in sodium based specimen these phases are found in lesser quantity.

8. The v4-SiO_4 bond is found to shift more towards lower frequency for the specimen containing calcium formate indicating that large quantity of silica took part in the reaction and formation of CSH gel, which imparts higher strength to the specimen compared to the specimens containing other chemicals.

The effects of curing temperature and curing under autoclave conditions on the compressive strength of mortar specimens and hydration products are investigated. Based on experimental results following conclusions are drawn:

1. The curing temperature is found to influence both the early and late age strengths of lime activated slag cement. Higher curing temperature favors an early strength gain but the strength at a later age is found to be lower than the samples cured at moderate temperatures. Samples cured at low temperature show a rising trend of strength even after 90 days of curing whereas the strengths of high temperature cured specimens get stabilize much earlier. A crossover effect of strength is noticed between low and high temperature cured specimens.
2. For the present test variables and conditions, the highest 90 days compressive strength was found to be 47.63MPa for D10 specimen cured at temperature of 60 ^{o}C. The microstructure of specimen cured at 60 ^{o}C is found to be more homogenous and dense with the hydration products distributed more evenly compared to other specimens.
3. D5 binding mix added with silica fume shows higher compressive strength than the reference sample (D5) or the reference sample added with fly ash under same curing

condition. The highest compressive strength is found to be 68.8 MPa for a mortar specimen containing D5 binder with 15% silica fume and cured for 90 days in water at 27 ^{o}C. The samples cured in an autoclave for 2 hours give almost equal strength to specimens cured in water at normal temperature for 28 days. No appreciable gain in strength is observed in mortar specimens cured in autoclave beyond 2 hours whereas samples cured in water at normal temperature show a continuous increase in strength up to 90days.

4. The specimens cured in water for 90 days show a low porosity, higher mass density and more homogeneous distribution of hydration products than the 4 hours autoclaved specimens. This contributes to higher strength of the samples.
5. X-ray diffraction analysis shows a series of hydration compounds such as calcium silicate hydrated, gismondine, xonotlite, and tobermorite in samples cured in autoclave whereas absence of gismondine, xonotlite and tobermorite is observed in samples cured in water at normal temperature of 27 ^{o}C. Furthermore, tobermorite structures having different morphology such as foiled and semi-transparent are observed in the spherical pores in autoclaved samples. A high temperature and pressure curing favors quick formation of hydration products and it results much faster gain of strength.
6. The gradual shifting of v4-SiO_4 bond towards lower frequency with increase in temperature indicates the formation of more amounts of C-S-H with increased curing period. The optimum dose of raw materials is found to vary marginally based on curing temperature and curing period of specimens.

7. Based on the findings of the experimental investigation, it perceives that activation of slag using lime and plaster of Paris is a viable process.

The objective of the present investigation is to understand the properties of slag activated by lime and plaster of Paris through an extensive experimental program. Therefore, the test results obtained from present investigation builds a high level confidence that alkaline activated slag can be used as an alternate cementing material which has similar physical, chemical and mechanical properties to that of the OPC.

8.3 BROAD RECOMMENDATIONS

A cementing material of 43 grade can be prepared by activating slag with 20% lime and 5% POP. Cementing material with higher grade such as 53 grade can be manufactured by activating slag with suitable mineral admixtures like silica fume. The rate of gain in strength in lime activated slag cement is comparatively lower than that of OPC, PPC, or PSC and hence, higher curing period is recommended for this type of binding material.

8.4 SCOPE FOR FUTURE RESEARCH WORK

The present thesis pertains to the study on the physical, chemical, and mechanical properties of lime activated slag cement. Due to time constraint all other aspects related to other properties like durability of lime activated slag could not be studied. The future research work should address the following:

1. The present work can be extended to study the durability of concrete made out of this cementing material.
2. The drying shrinkage and autogenous shrinkage of this binding material can be studied in detail.
3. The performance of concrete made out of this cementing material under chemical environment may be studied.

REFERENCES

[1] Aitcin P.C. (1958), ñDurable concrete: Current practice and future trendsò, *Proceedings of V. Mohan Malhotra Symposium*,American concrete institute ACI J., 54, 1063-1081.

[2] Aldea C.M., Young F., Wang K., Shah S.P. (2000), ñEffects of curing conditions on properties of concrete using slag replacementò, *Cement and Concrete Research*,30, 465ï 472.

[3] Bakharev T., Sanjayan J.G., Cheng Y. B. (1999), ñAlkaline activation of Australian slag cementsò, *Cement and Concrete Research*, 29(1), 113ï 120.

[4] Bakharev T., Sanjayan J.G., Cheng Y.B. (1999), ñEffect of elevated temperature curing on the properties of alkali-activated slag concreteò, *Cement and Concrete Research*,29(10), 1619ï 1625.

[5] Bakharev T., Sajayan J.G., Cheng Y.B. (2001), ñResistance of alkali-activated slag concrete to alkali-aggregate reactionò, *Cement and Concrete Research*, 31(2), 331-334.

[6] Barbhuiya S.A., Gbagbo J.K., Russell M.I., Basheer P.A.M. (2009), ñProperties of fly ash concrete modified with hydrated lime and silica fumeò, *Construction and Building Materials*, 23(10), 3323-3329.

[7] Bezerra1 U.T., Martinelli A.E., Melo D.M.A., Melo M.A.F., Oliveira V.G. (2011), ñThe strength retrogression of special class Portland oilwellcementò, *Ceramica*, 57, 150-154.

[8] Benghazi, Z., Zeghichi, L., Hamdane, A. (2009), ñStudy of Alkali activated pozzolana/ Slag cementò, *1st International conference on Sustainable Built Environment Infrastructures in Developing Countries, ENSET Oran (Algeri*a), 335-342.

[9] Bellmann F., Strak J. (2009), ñActivation of blast furnace slag by a new methodò, *Cement and Concrete Research*, 38(8) 644-650.

[10] Ben Haha M., Saout G.L., Winnefeld F., Lothenbach B. (2011), ñInfluence of activator type on hydration kinetics, hydrate assemblage and microstructural development of alkali activated blast-furnace slagsò, *Cement and Concrete Research,* 41(3), 301-310.

[11] Bijen, J., Niel, E. (1981), ñSuper sulphated cement from blast furnace slag and chemical gypsum available in the Netherland and neighboring countriesò, *Cement and Concrete Research*, 11(3), 307-322.

[12] Box G.E.P., Draper N.R.(1987),ñEmpirical Model Building and Response Surfacesò, *New York: John Wiley & Sons, Inc;1987*

[13] Brough A.R., Katz A., Bakharev T., Sun G., Kirkpatrick R., Struble L.(1996), ñMicrostrutural aspects of zeolite formation in alkali activated cements containing high levels of fly ashò, *Materials Research Society Proceeding*, 370 , 199ï 208.

[14] Brough, A. R., Holloway, M., Sykes, J., Atkinson, A. (2000), ñSodium silicate based alkali-activator slag mortars: Part II The retarding effect of additions of sodium chloride or malic acidò, *Cement and Concrete Research*, 30 (9), 1375ï 1379.

[15] Brough A.R., Atkinson A. (2002), ñSodium silicate-based alkali-activated slag mortars. Part I. Strength, hydration and microstructureò, *Cement and Concrete Research,* 32 , 865ï 879

[16] Carino N.J. (1991), ñThe Maturity method, Handbook on Nondestructive Testing of concreteò, *V.M. Malhotra and N.J Carino eds.*,101-146,CRC press Boca Raton, FL, Nawy.

[17] Carino N.J., Tank, R.C.(1992), ñMaturity functions for concrete made with various cements and admixturesò, *American concrete institute Material Journal*, 89(2), 188-196.

[18] Chandra, S. (1996). ñWaste materials used in concrete manufacturing.ò *Westwood*, *New Jersey*, *U.S.A.*, 235-282.

[19] Chang, J. J. (2003) ñA study on the setting characteristics of sodium silicate-activated slag pastesò, *Cement and Concrete Research*, 33, 1005ï 1011.

[20] Cheng Q.C., Sarkar S.L.(1994),ñA study of rheological and mechanical properties of mixed alkali activated slag pastesò, *Advanced Cement Based Materials*, 1(4):178-81.

[21] Collins F., Sanjayan J.G. (2000),ñEffect of pore size distribution on drying shrinkage of alkali-activated slag concreteò, *Cement and Concrete Research*, 30, 1401-1406.

[22] Davidovits, J. (1991), ñGeopolymers: Inorganic polymeric new materialsò, Journal of Thermal of Thermal Analysis, 37, 1633-1656.

[23] Davidovits, J. (1994), ñProperties of Geopolymer Cementsò, *Paper presented at the First International Conference on Alkaline Cements and Concrete*s, Kiev State Technical University, Kiev, Ukraine.

[24] Dongxua L., Xuequan W., Jinlina S., Yujiang W. (2000), ñThe influence of compound admixtures on the properties of high-content slag cementò, *Cement and Concrete Research* , 30,45ï 50

[25] Douglas E., Brandstetr J. (1990),ñA preliminary study on the alkali activation of ground granulated blast furnace slagò,*Cement and Concrete Research* ,20(5):746-756.

[26] Douglas E., Bilodeau A., Brandstetr J., Malhotra V.M. (1991),ñAlkali activated ground granulated blast furnace slag concrete: Preliminary investigationò, *Cement and Concrete Research*, 21(1):101-108.

[27] Dutta, D. K., Borthakur, P. C. (1990), ñActivation of low lime high alumina granulated blast furnace slag by anhydriteò, *Cement and Concrete Research*, 20(5), 711-722.

[28] Escalante-Garcia J.I., Sharp J.H. (2001),ñThe microstructure and mechanical properties of blended cements hydrated at various temperaturesò, *Cement and Concrete Research,* 31(5), 695-702.

[29] Escalante-Garcia J.I., Palacios-Villanueva V.M., Gorokhovsky A.V., Mendoza-Suarez G., Fuentes A.F. (2002),ñCharacteristics of a NaOH-activated blast furnace slag blended with a fine particle silica wasteò, *Journal of American Ceramic*, 85(7), 1788ï 1792.

[30] Escalante-Garcia J.I., Gorokhovsky A.V., Mendonza G., Fuentes A.F. (2003), Effect of geothermal waste on strength and microstructure of alkali-activated slag cement mortarsò,*Cement and Concrete Research,* 33, 1567ï 1574.

[31] Ezzian K., Bougara A., Kadri A., Khelafi H., Kadri E. (2007),ñCompressive strength of mortar containing natural pozzolan under various curing temperatureò, *Cement and Concrete Composite*, 29(8), 587ï 593.

[32] Feret, R., (1939), RevuedesMateriaux de construction et desò, *Travaux Publics,* 355-361.

[33] Fernandez-JimenezA., Puertas F. (1997), ñAlkali-activated slag cements: kinetic studiesò, *Cement and Concrete Research*, 27(3), 359ï 368.

[34] Fernandez Jimenez A., A. Palomo A.(2003), ñCharacterisation of fly ashes. Potential reactivity as alkaline cementsò, *Fuel* 82, 2259ï 2265.

[35] Fernando Pacheco-Torgala, Joao Castro-Gomesb, SaidJalalic, (2008), ñAlkali-activated binders: A review: Part 1. Historical background, terminology, reaction mechanisms, and hydration productsò, *Construction and Building Materials*, 22(7), 1305ï 1314.

[36] Gifford P.M., Gillot J.E. (1996), ñAlkali-silica reactions (ASR) and alkali-carbonate reaction (ACR) in activated blast furnace slag cement (ABFSC) concreteò, *Cement and Concrete Research*, 26, 21ï 26.

[37] Glukhovsky V.D., Krivenko P.V., Rostovskaya G.S., Timkovich V.J., Pankratov V.L.(1983), United States Patent No 4410365, 18 Oct 1983.

[38] Glukhovsky V. D., Zaitsev Y., Pakhomow V. (1983), ñSlag-alkaline cements and concrete structures, properties, technological and economic aspects of the useò, *SilicInd*, 10, 197-200.

[39] Gruskovnjak A., Lothenbach B., Winnefeld F., Figi R., Ko S.C., Adler M., Mader U. (2008),ñHydration mechanisms of super sulphated slag cementò, *Cement and Concrete Research*, 38(7), 983-992.

[40] Gong, C., Yang, N.(2000), ñEffect of phosphate on the hydration of alkali activated red-mud slag cementious materialsò, *Cement and Concrete Res*earch, 30 (7), 1013-1010.

[41] Hong S.Y., Glasser F.P. (1999), ñAlkali binding in cement pastes. Part I. The Cï Sï H phaseò, *Cement and Concrete Research*, 29, 1893ï 1903

[42] Hong S.Y., Glasser F.P. (2002) ñAlkali absorption by Cï Sï H and Cï Sï Aï H gels. Part II.ò *Cement and Concrete Research*, 32, 1101ï 1111.

[43] Hong S.Y., Glasser F.P. (2004), ñPhase relations in the CaOï SiO_2ï H_2O system to 200 ^oC at saturated steam pressureò, *Cement and Concrete Research*, 34, 1529 ï 1534.

[44] IS: 4031 ï 1988 (PT 4). Method of physical test for hydraulic cement: Part 4 Determination of standard consistency of cement paste, *Bureau of Indian Standards*, New Delhi, 1988.

[45] IS: 4031 ï 1988 (PT 5). Method of physical test for hydraulic cement: Part 5 Determination of initial and final setting time, *Bureau of Indian Standards*, New Delhi, 1988.

[46] IS: 4031 ï 1988 (PT 3). Method of physical test for hydraulic cement: Part 3 Determination of soundness, *Bureau of Indian Standards*, New Delhi, 1988.

[47] IS:650-1991.Standard sand for testing cement specification. Bureau of Indian Standards, New Delhi,1991.

[48] IS: 4031 ï 1988 (PT-6). Method of physical test for hydraulic cement: Part 7 Determination of compressive strength of Ordinary Portland Cement. Bureau of Indian Standards, New Delhi,1988.

[49] IS: 4031 ï 1988 (PT-7). Method of physical test for hydraulic cement: Part 7 Determination ofcompressive strength of masonry cement. Bureau of Indian Standards, New Delhi,1988.

[50] Jolibois, P., Nicol, A. (1952), Revue des Materiaux de Construction et desò, *Travaux Publics*; 437:33.

[51] Jiang W. (1997), ñAlkali Activated Cementitious Materials*:* Mechnism, Microstructure and Propertiesò, Ph.D. Thesis, The Pennsylvania StateUniversity, Pennsylvania.

[52] John V.M., Cincotto M.A., Sjostrom C., Agopyan V., Oliveira C.T.A. (2005),ñDurability of slag mortar reinforced with coconut fibreò, *Cement and Concrete Composite,* 27, 565ï 574.

[53] Kim, J.C., Hong, S. Y. (2001), ñLiquid concentration changes during slag cement hydration by alkali activationò, *Cement and Concrete Research*, 31 (2), 283ï 285.

[54] Kim J.K., Han H.S., Song, Y.C. (2002),ñEffect of temperature and aging on the mechanical properties of concrete. Part I. Experimental resultsò, *Cement and Concrete Research,* 32(7), 087ï 1094.

[55] Krivenko, P. D. (1994), ñAlkaline cementsò, Paper presented at the first international conference on alkaline cements and concrete.ò Kiev, Ukraine. 1994), 11-14 October.

[56] KunhanandanNambiar E.K., Ramamurthy K.(2006),ñModels relating mixture composition to the density and strength of foam concrete using response surface methodologyò,*Cement and Concrete Composites*, 28(9),752ï 60

[57] Lasdon L.S., Fox R.L., Ratner M.W. (1973),ñNonlinear Optimization Using the Generalized Reduced Gradient Methodò, *Technical Report,* Case Western Reserve University.

[58] Maghsoud A., Amir A.N., Komeil G. (2008), ñResponse surface methodology and genetic algorithm in optimization of cement clinkering processò, *Journal of Applied Sciences*, 15(8), 2732ï 38.

[59] Malolepszy J., Nocun-Wczelik W. (1988), ñMicrocalorimetric studies of slag alkaline bindersò, *Journal of Thermal Analysis,* 33, 431ï 434.

[60] Macphee D.E. (1989),ñSolubility and aging of calcium silicate hydrates in alkaline solutions at 25 °Cò, *Journal of the American Ceramic Society*, 72, 646ï 654.

[61] Mehrotra V.P., Sai A.S.R., Kapur P.C. (1982), ñPlaster of Paris activated supersulfated slag cementò, *Cement and Concrete Research,* 12 (4), 463-73.

[62] MeloNeto A.A., Cincotto M.A., Repette W.(2010), ñMechanical properties, drying and autogenous shrinkage of blast furnace slag activated with hydrated lime and gypsumò, *Cement and Concrete Composite*, 32(4), 312-318.

[63] Myers R.H., Montgomery D.C. (2002), ñResponse Surface Methodology: process and product optimization using designed experimentò, *A Wiley-Interscience Publication*;2002

[64] Muthukumar M., Mohan D. (2004), ñStudies on polymer concretes based on optimized aggregate mix proportion.ò *European Polymer Journal* 40(9), 2167ï 2177.

[65] Murmu M., Singh S.P. (2012). ñSome studies on physical and mechanical properties of cold process cement.ò*International Conference on Advancements in Engineering and Technology*, ICAEM-2012, Hyderabad.

[66] Naceri, A., Bouglada, M. S., Grosseau, P. (2009), ñMineral Activator and Physical Characteristics of Slag Cement at Anhydrous and Hydrated Statesò, *World Academy of Science, Engineering and Technology*,32, 137-139.

[67] Naceri A., Bouglada M. S., Belouar, A. (2011), ñActivation of Slag Cement by Hydrated Limeò, *Applied Mechanics and Material*, (71-78), 706-711.

[68] Neville A.M. (1995), *Properties of concrete, Longman*: New York; 1995.

[69] Palacios M., Puertas F. (2007),ñEffect of shrinkage-reducing admixtures on the properties of alkali-activated slag mortars and pastesò, *Cement and Concrete Research*, 37, 691ï 702.

[70] Phillips J.C., Cahn D.C. (1973),ñRe-use glass aggregate in Portland cementò, *Proc. 3rd Mineral Waste Utilisation Symposium*, 385-390.

[71] Puertas F.(1995),ñCementos de escoriasactivadas. Situacio an actualy per spectivas de futureò, *Material Construction,* 45(239), 53-64.

[72] Puertas F., Martinez-Ramirez S., Alonso S., Vazquez T. (2000),ñAlkali activated fly ash/slag cements:Strength behavior and hydration productsò, *Cement and Concrete Research*, 30 (10), 1625-1632.

[73] Puertas F., Fernandez-Jimenez A. (2003),ñMineralogical and microstructure characterization of alkali-activated fly ash/slag pastesò, *Cement and Concrete Composites*, 25(3), 287ï 293.

[74] Puertas F., Fernandez-Jimenez A., Blanco-Varela M.T. (2004), ñPore solution in alkali-activated slag cement pastes. Relation to the composition and structure of calcium silicate hydrateò, *Cement and Concrete Research*, 34, 195ï 206.

[75] Puertas F., Palacios M., Manzano H., Dolado J. S., Rico A., Rodríguez J. (2011), ñA model for the C-A-S-H gel formed in alkali-activated slag cementsò, *Journal of the European Ceramic Society*, 31(12), 2043ï 2056.

[76] Purdon A.O. (1940), ñThe action of alkalis on blast furnace slagò, *Journal of the Society of Chemical Industry*, 59,191ï 202.

[77] Ramachandran V.S. (2001). *Handbook of analytical techniques in concrete sciences and technology.* New York: LLC Norwich; 2001.

[78] Rashada A.M., Zeedan S.R., Hassan A.H. (2012), ñA preliminary study of autoclaved alkali-activated slag blended with quartz powderò, *Construction and Building Materials*, 33, 70ï 77.

[79] Raymond A. C., Kenneth C. H.(1999),ñMercury porosimetry of hardened cement pastesò, *Cement and Concrete Research,* 29,933ï 943.

[80] Rousekova I., Bajza A., ZivicaV. (1997),ñSilica fume-basic blast furnace slag systems activated by an alkali silica fume activatorò, *Cement and Concrete Research,* 27(12):1825ï 1828.

[81] Sakulich A.R. (2010),ñCharacterization of Environmentally friendly Alkali activated slag cements and Ancient Building materialsò, PhD Thesis, Materials Sciences Engineering, Drexel University.

[82] Samtur H.R. (1974),ñGlass Recycling and Reuseò, University of Wisconsin, Madison Institute for Environmental Studies, Report No. 17.

[83] Savastaro J.H., Warden P.G., Coutts R.S.P. (2001), ñGround iron blast furnace slag as a matrix for cellulose ï cement materialsò, *Cement and Concrete Composite*, 23, 389-397.

[84] Schwarz N., Neithalath N. (2008),ñInfluence of a fine glass powder on cement hydration: Comparison to fly ash and modeling the degree of hydrationò, *Cement and Concrete Research,* 38 (4), 429ï 436.

[85] Serdar A. (2013), ñA ternary optimisation of mineral additives of alkali activated cement mortarsò, *Construction and Building Materials*, 43,131ï 138.

[86] Shao Y., Lefort T., Moras S., Rodriguez S. (2000), ñStudies on concrete containing ground wasteglassò, *Cement and Concrete Research* 30 (1), 91ï 100.

[87] Sharath S., Sandesh V., Yaragal S.C., Babu Narayan K.S., Suryanarayan K. (2012), ñMicrostructure Analysis of Concrete Subjected to Elevated Temperatures using Mercury Intrusion Porosimetryò, *International Journal of Earth Sciences and Engineering,* 5(4), 1063-1067.

[88] Shayan A., Xu A.(2004), ñValue-added utilisation of waste glass in concreteò, *Cement and Concrete Research,* 34 (1), 81 ï 89.

[89] Shi C., Li Y. (1989), ñInvestigation on some factors affecting the characteristics of alkali-phosphorus slagò, *Cement and Concrete Res*earch, 19(4), 527ï 533.

[90] Shi C., Tang X., Li Y. (1991), ñThermal activation of phosphorus slagò *IL Cemento*, 88 (4), 219-225.

[91] Shi C., Wu X., Tang M. (1991), ñHydration of alkali-slag cements at 150 °Cò,*Cement and Concrete Research*, 21, 91ï 100.

[92] Shi C., Day R.L.(1993),ñChemical activation of blended cement made with lime and natural pozzolanaò, *Cement and Concrete Res*earch, 23(6),1389-96.

[93] Shi C., Day R.L. (1999), ñEarly strength development and hydration of alkali-activated blast furnace slag/fly ash blendsò, *Advance in Cement Research,* 11(4),189-196.

[94] Shi C., Hu S. (2003),ñCementitious properties of ladle slag fines under autoclave curing conditionsò, *Cement and Concrete Research,* 33, 1851ï 1856.

[95] Shi C.,Wu Y., Riefler C., Wang H. (2005),ñCharacteristics and pozzolanic reactivity of glass powdersò, *Cement and Concrete Research,* 35(5), 987ï 993.

[96] Shi C., Roy D., Krivenko, P. (2006), Alkali-activated cements and concrete. London: Taylor & Francis, (2006).

[97] Singh M., Garg M.(1995), ñActivation of Gypsum Anhydrite Slag Mixturesò, *Cement and Concrete Research*, 25(2), 332-338.

[98] Song S., Jennings H.M. (1999), ñPore solution chemistry of alkali-activated ground granulated blast furnace slagò, *Cement and Concrete Research*, 29, 159ï 170.

[99] Song S., Sohn D., Jennings H.M., Mason T.O. (2004), ñHydration of alkali-activated ground granulated blast furnace slagò, *Material Sciences*, 35, 249ï 257.

[100] Stade H. (1989) ñOn the reaction of CSH with alkali hydroxidesò, *Cement and Concrete Research*, 19, 802ï 810.

[101] Sugama T., Brothers L.E. (2004), ñSodium-silicate-activated slag for acid-resistant geothermal well cementsò, *Advances in Cement Research*, 16(2), 77ï 87.

[102] Talling B., Brandstetr J. (1981),ñPresent state and future of alkali ï activated slag concretes fly ash, silica fume, slag, and natural pozzolans in concreteò, *Proc 3rd Intern Conf Trondheim*, Norway, SP114-74: 519-45.

[103] Talling, B.(1989), ñEffect of curing conditions on alkali-activated Slagsò, *3rd International Conference on the Use of Fly Ash, Silica Fume, Slag & Natural Pozzolans in Concrete*, American concrete institute ACI SP-114, Trondheim, Norway, 2, 1989, 1485ï 1500.

[104] Tanyildizi, H. (2009), ñStatistical analysis for mechanical properties of polypropylene fiber reinforced lightweight concrete containing silica fume exposed to high temperatureò, *Material Design*, 30(8), 3252ï 3258.

[105] Taylor H.F.W. (1997) Cement Chemistry, 2nd ed. Thomas Telford.

[106] TimurCihana M, Güner A, Yüzer N. (2013), ñResponse surfaces for compressive strength of concreteò, *Construction and Building Materials,* 40, 763ï 74.

[107] Torres J. J., Palacios M., Hellouin M., Puertas F. (2009),ñAlkaline chemical activation of urban glass wastes to produce

cementiousmaterialsò, *1st Spanish National Conference on Advances in Materials Recycling and Eco–Energy Madrid*, S04-6,111-114.

[108] Wang S., Scrivener K. L., Pratt, P. L. (1994),ñFactors affecting the strength of alkali-activated slagò, *Cement and Concrete Research*, 24(6), 1033ï 1043.

[109] Wang S. D., Scrivener K. (1995), ñHydration products of alkali activated slag cementò, Cement *and Concrete Research,* 25,561ï 571.

[110] Weast R.C.(1997) CRC Handbook of chemistry and physics, 59th Edition CRC press Inc, Boca Raton Florida (1979)

[111] Wu X., Jiang W., Roy D.M. (1990),ñEarly activation and properties of slag cementò, *Cement and Concrete Research,* 20(6): 961-74.

[112] Yazici H. (2007), ñThe effect of curing conditions on compressive strength of ultra-high strength concrete with high volume mineral admixturesò, *Building and Environment*, 42, 2083ï 2089.

[113] Yazic H., Yigiter H., Karabulut A.S., Baradan B. (2008),ñUtilization of fly ash and ground granulatedblast furnace slag as an alternative silica source in reactive powder concreteò, *Fuel*, 8 (12), 2401-2407.

[114] Yazici H., Yardimci Y.M., Aydin S., Karabulut A.S.(2009),ñMechanical properties of reactive powder concrete containing mineral admixtures under different curing regimesò, *Construction and Building Materials*, 23, 1223ï 1231.

[115] Zhang D., Liu W., Hou H., He H. (2007), Strength, leachability and microstructure characterization of Na2SiO3-activated ground granulated

blast-furnace slag solidiýed MSWI þy ashò, *Waste Management and Research*, 25, 402ï 407.

[116] Zhihua P., Dongxu L., Jian Y., Nanry Y. (2002), ñHydration products of alkali-activated slag red mud cementitious materialò, *Cement and Concrete Research*, 32 , 357ï 362.

[117] Zhihua P., Dongxu L., Jian Y., Nanry Y. (2003),ñProperties and microstructure of the hardened alkali-activated red mud-slag cementitious materialò, *Cement and Concrete Research,* 33, 1437ï 1441.

[118] Zivica V. (1993), ñAlkaliï silicate admixture for cement composites incorporating pozzolan or blast furnace slagò, *Cement and Concrete Research*, 23(5), 1215ï 1222.

[119] ZivicaV. (2004), ñHigh effective silica fume alkali activatorò, *Building Material Sciences*, 27(2):179-182.

[120] Zivica V. (2006), ñEffectiveness of new silica fumes alkali activatedò, *Cement and Concrete Composite*, 28(1), 21-25.

[121] Technical report: The Federal Association of the German Ready-Mixed Concrete Industry, ñGround Granulated Blast Furnace Slag (GGBS) as a concrete additive-Current situation and scenarios for its use in Germany - 23.03.2007ò.

LIST OF PUBLICATIONS

International Journals

1 M. Murmu and S.P. Singh, Influence of mineral admixtures on strength and hydration products of lime-activated slag cement, Advances in Cement Research, 2014, 26(1), 1ï 10.

2 M. Murmu and S.P. Singh, Strength Characteristics of Lime Activated Slag Cement, Advances in Cement Research, DOI:http://dX.doi.org/10.1608/adcr.13. 00097.

3 M. Murmu and S.P. Singh, Hydration Products, Morphology and Microstructure of Activated Slag Cement, International Journal of Concrete Structures and Materials, 2014, 8(1) , 61-68

4 M. Murmu and S.P. Singh, Some Studies on Strength and Hydration of Cold Process Cement, *International Journal of Advances in Management, Technology& Engineering Sciences,* 2012, 1 (7), 84-88.

5 M. Murmu and S.P. Singh, Strength and hydration products of lime activated slag cement with silica fume as an admixture, International Journal of Concrete Structures and Materials, (Queries to Reviewers submitted).

6 M. Murmu and S.P. Singh, Strength and Hydration Products of Autoclaved Lime Activated Slag Cement Blended with Micro Silica and Fly Ash, Journal of Sustainable Cement-Based Materials(Queries to Reviewers submitted).

7 M. Murmu and S. P. Singh, Effects of Curing Temperature Strength of Lime Activated Slag Cement, International Journal of Civil Engineering (Under Review).

International Conferences

1 M. Murmuand S.P. Singh, Effect of Mineral Admixture on Strength of Alkali Activated Slag Cement, 1st Annual *International Conference on Architecture and Civil Enguneering2013.*18-19th March 2013. Singapore.

2 M. Murmuand S.P. Singh, Hydration Products in Alkali Activated Slag Cement Added With Mineral Admixtures, *International Conference on Advanced Materials for Energy Efficient Building Materials, AME2B-2013.* 13-15thFebruray 203 New Delhi.

3 M. Murmuand S.P. Singh, Strength Characteristics of Cold Process Cement with and without Admixtures, *International Conference on Advanced Materials for Energy Efficient Building Materials,AME2B-2013.*13-15thFebruray 203 New Delhi.

4 M. Murmu and S.P. Singh, Hydration Mechanism of Cold Process Cement, *International Conference on Sustainability Challenges and Advances in Concrete Technology SCACT 2012.pp441-447.*2-5th May 2012 Coimbatore.

5 M. Murmuand S.P. Singh, Effect of Accelerators on Strength and Hydration Products of Cold Process Cement,*2nd International Conference on Advances in Engineering and Technology (ICAET2012)ISBN 978-1-4675-2245-8 © 2012.*28-29th March 2012 Nagpattinum.

6 M. Murmuand S.P. Singh, Some studies on physical and mechanical properties of cold process cement, *RITS ICAEM-2012: RITS International Conference on Advancements in Engineering and Technology*. 28-29thFebrury 2012 Hydrabad.